Microscopic optical potentials
- recent achievements and applications -

Paolo Finelli

Theory and Phenomenology of Fundamental Interactions
UNIVERSITY AND INFN · BOLOGNA

13th Spring Seminar in Nuclear Physics

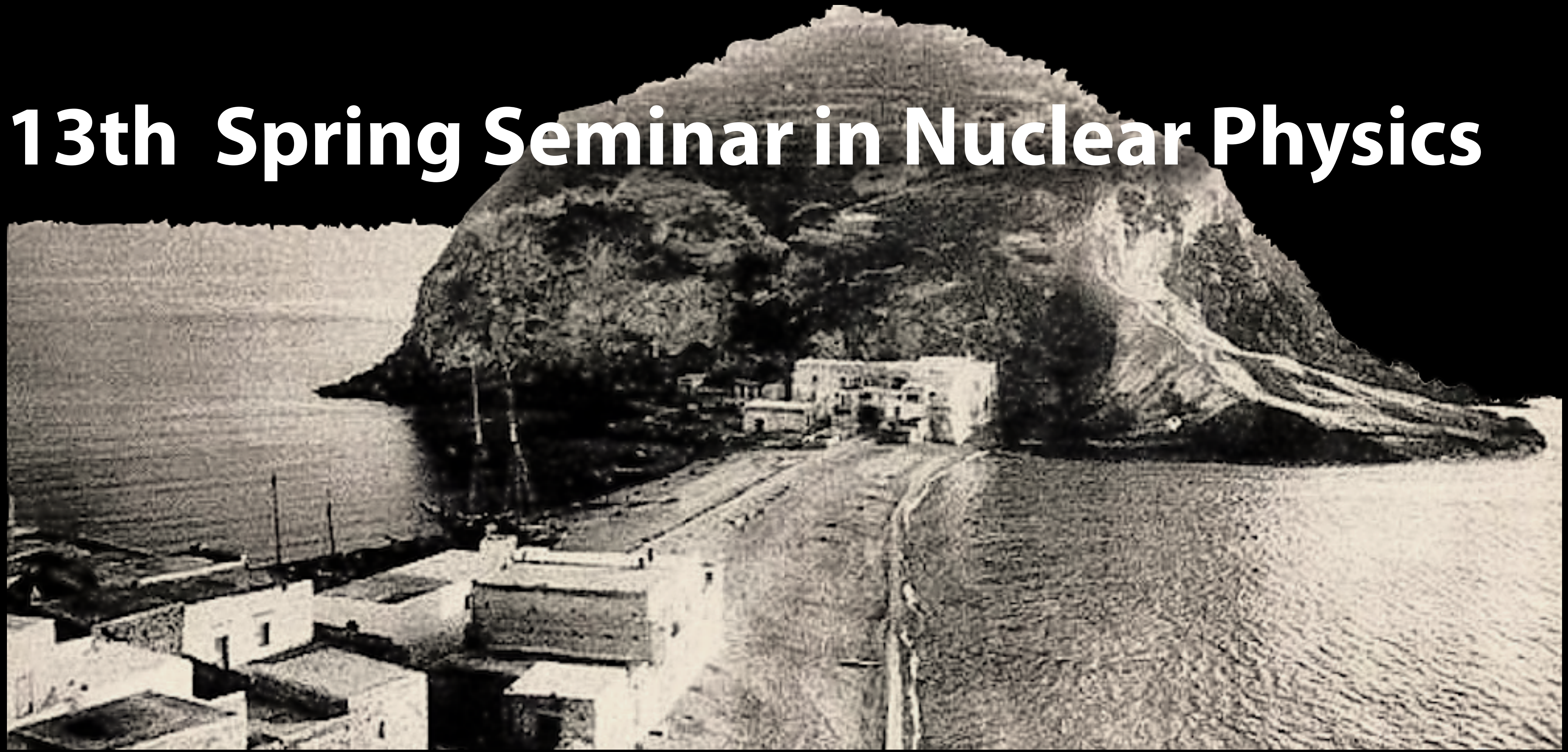

in collaboration with M. Vorabbi (BNL), C. Giusti (Pavia), P. Navratil and M. Gennari (TRIUMF), and R. Machleidt (Idaho)

Motivations

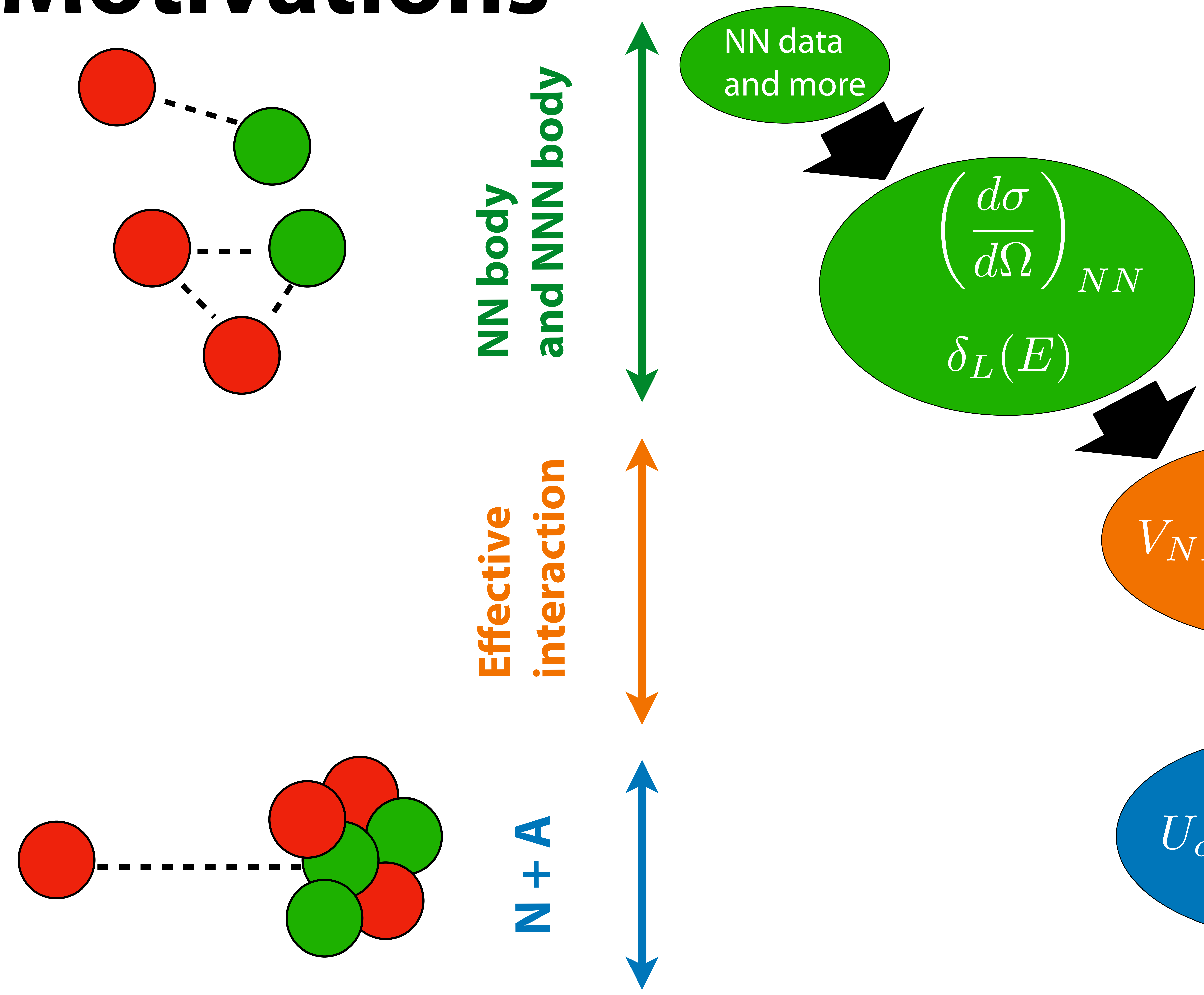

Nuclear reaction theory relies on reducing the many-body problem to a problem with few degrees of freedom: **optical potentials**.

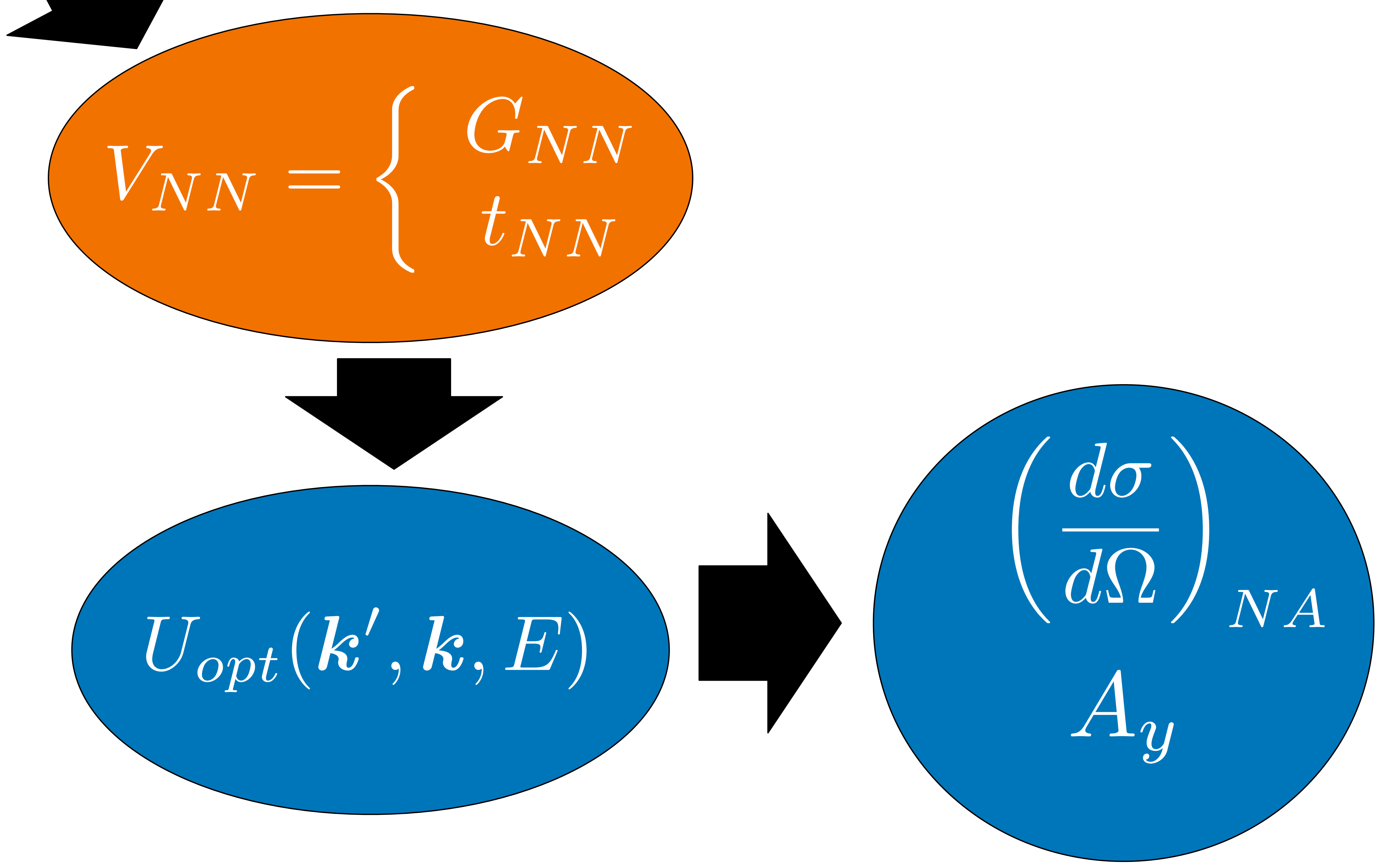

Motivations

- Increasing experimental efforts to develop the technologies necessary to study the elastic proton scattering in inverse kinematics
- Attempts to use such experiments to determine the matter distribution of nuclear systems at intermediate energies

Sakaguchi, Zenihiro, PPNP 97 (2017) 1

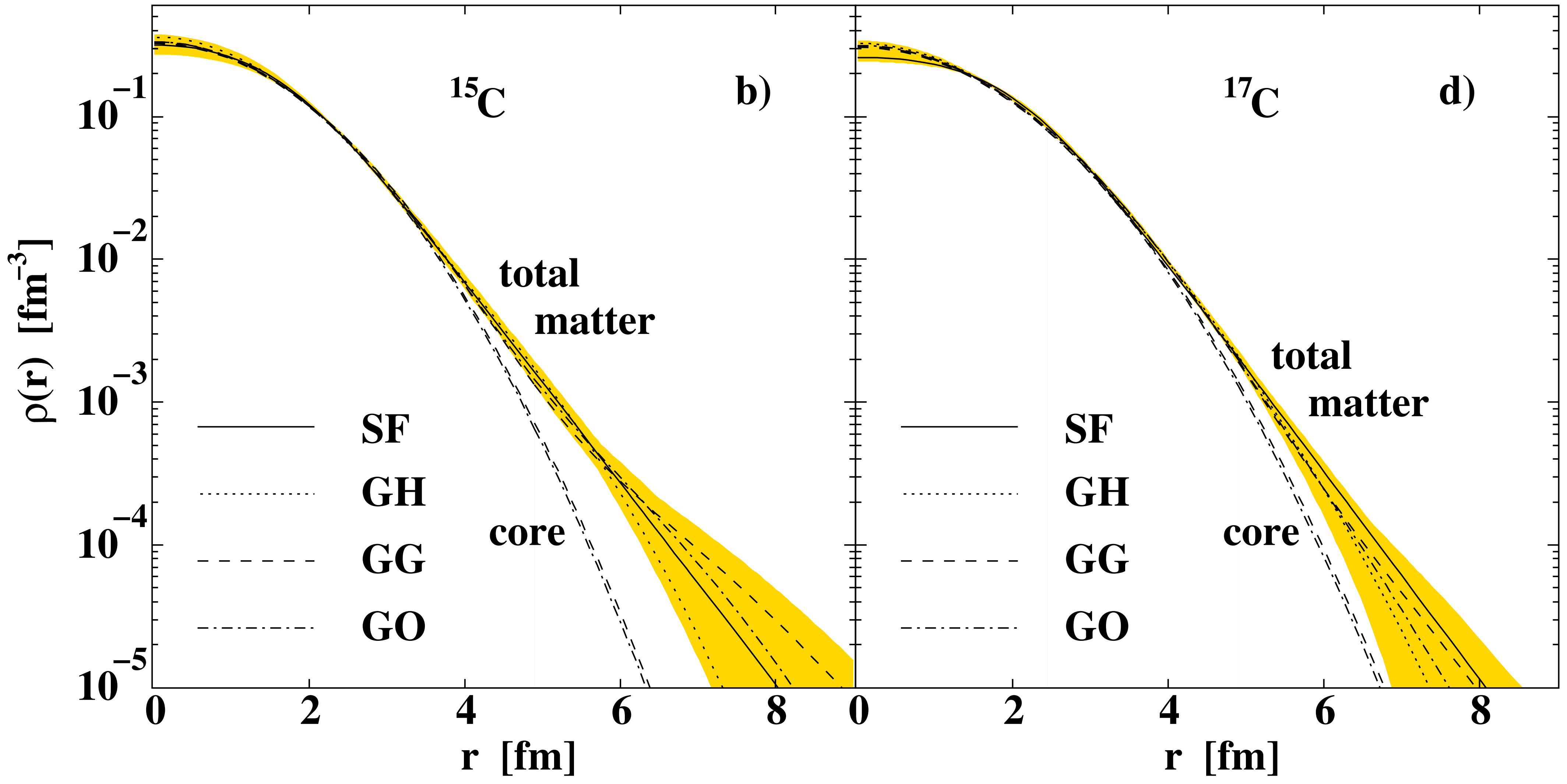

Dobrovolsky et al., NPA 1008 (2021) 122154

Measurements are not free from sizable uncertainties

- Glauber model is conventionally used to analyze the data
- An essential step in the data analysis is the subtraction of contributions from the inelastic scattering

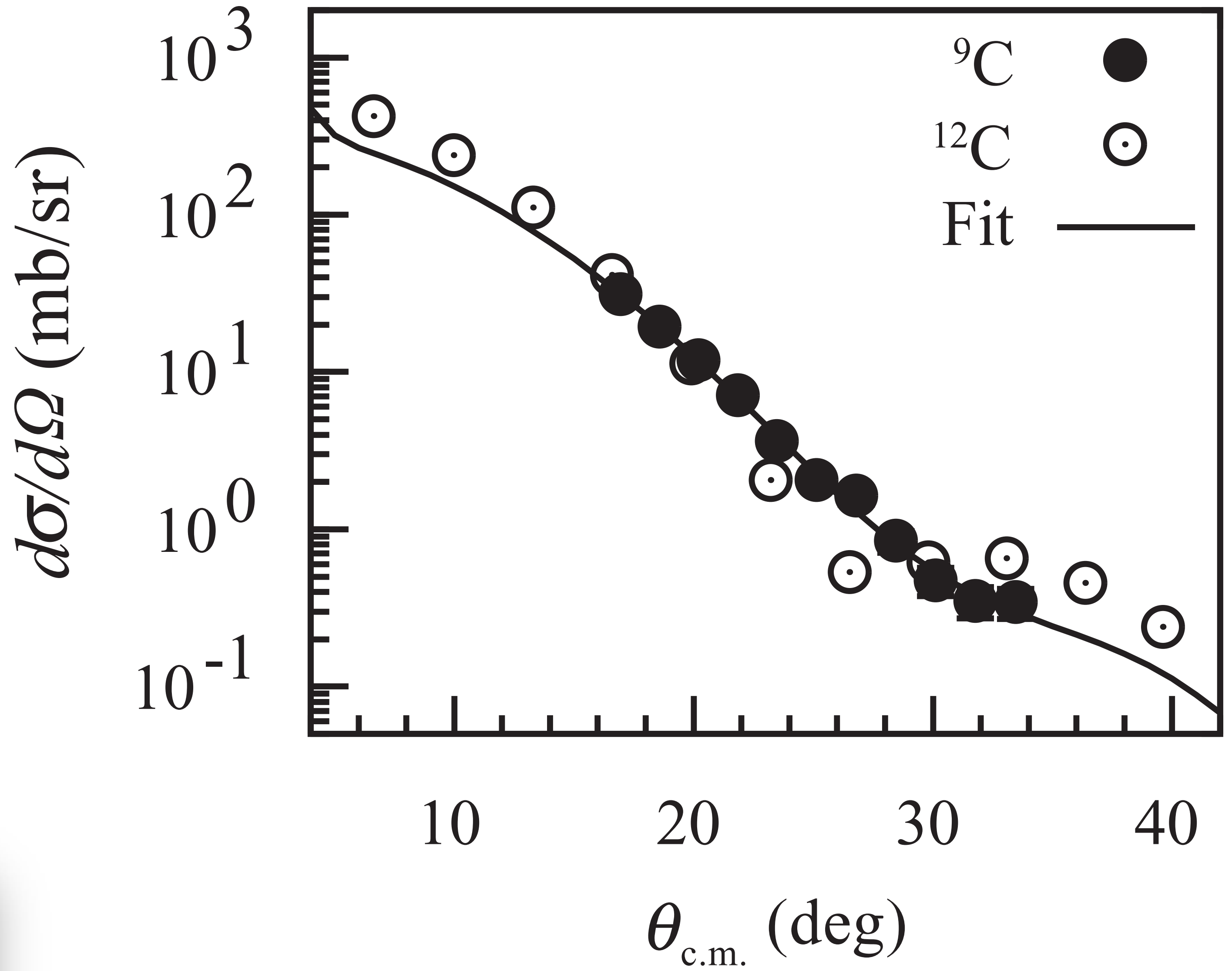

Matsuda et al., PRC **87** (2013) 034614

Develop a microscopic approach to make reliable predictions for elastic and inelastic scattering

Optical potential

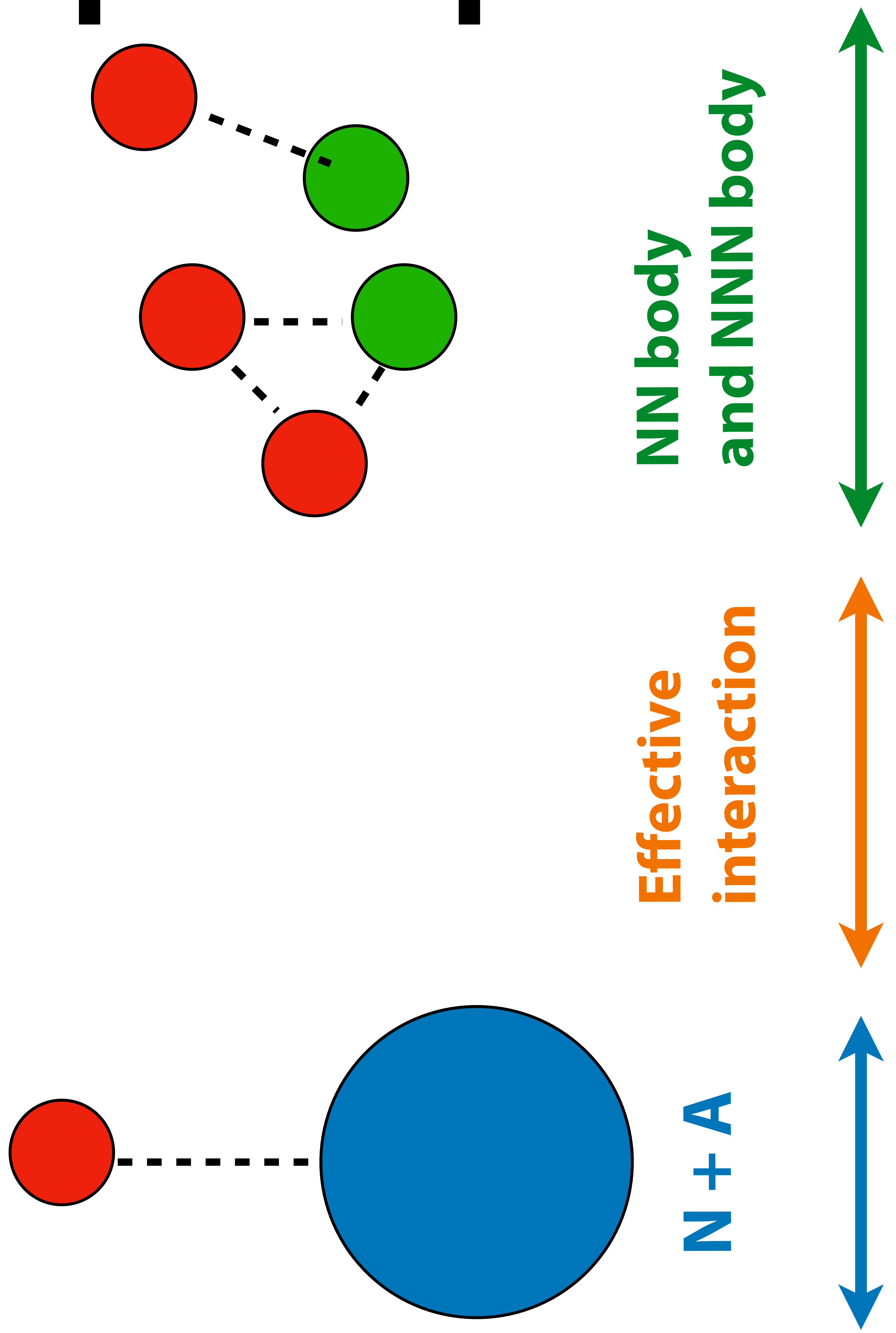

"In the center-of-mass system the motion of the particle is given by the Schroedinger equation

$$\nabla^2\Psi + \frac{2\mu}{\hbar^2}(E - V)\Psi = 0$$

where μ is the reduced mass. This approximation is referred to as the optical model because it is in many ways analogous to the index of refraction approximation which is employed to describe the propagation of light in a medium."

H. Feshbach, ***Nuclear Reactions***

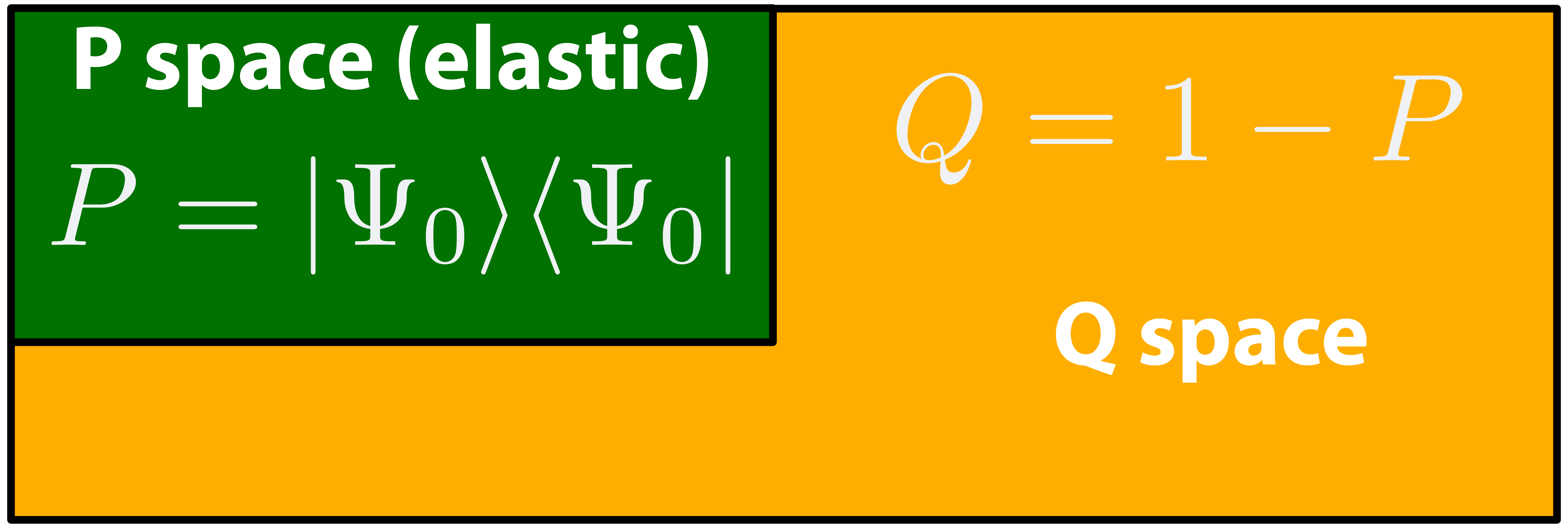

$$\left\{E - T_0 - \langle\Psi_0|V|\Psi_0\rangle - \langle\Psi_0|VQ\frac{1}{E - QHQ}QV|\Psi_0\rangle\right\}\Phi_0 = 0$$

expansion

The effective potential

Optical potential

Phenomenological

Unfortunately, currently used optical potentials for low-energy reactions are phenomenological, primarily constrained by elastic scattering data.
Unreliable when extrapolated beyond their fitted range in energy and nuclei

Microscopical

Existing microscopic optical potentials are *usually* developed in an high-energy regime (≥ 100 MeV) and not calibrated to any reaction data. Calculations are more difficult.

No fit to exp. data

$$
\begin{aligned}
V(r) &= -V_R f_R(r) - iW_V f_V(r) \\
&+ 4a_{VD}V_D \frac{d}{dr} f_{VD}(r) + 4ia_{WD}\frac{d}{dr} f_{WD}(r) \\
&+ \frac{\lambda_\pi^2}{r}\left[V_{SO}\frac{d}{dr} f_{VSO}(r) + iW_{SO}\frac{d}{dr} f_{WSO}(r)\right]\vec{\sigma}\cdot\vec{l}
\end{aligned}
$$

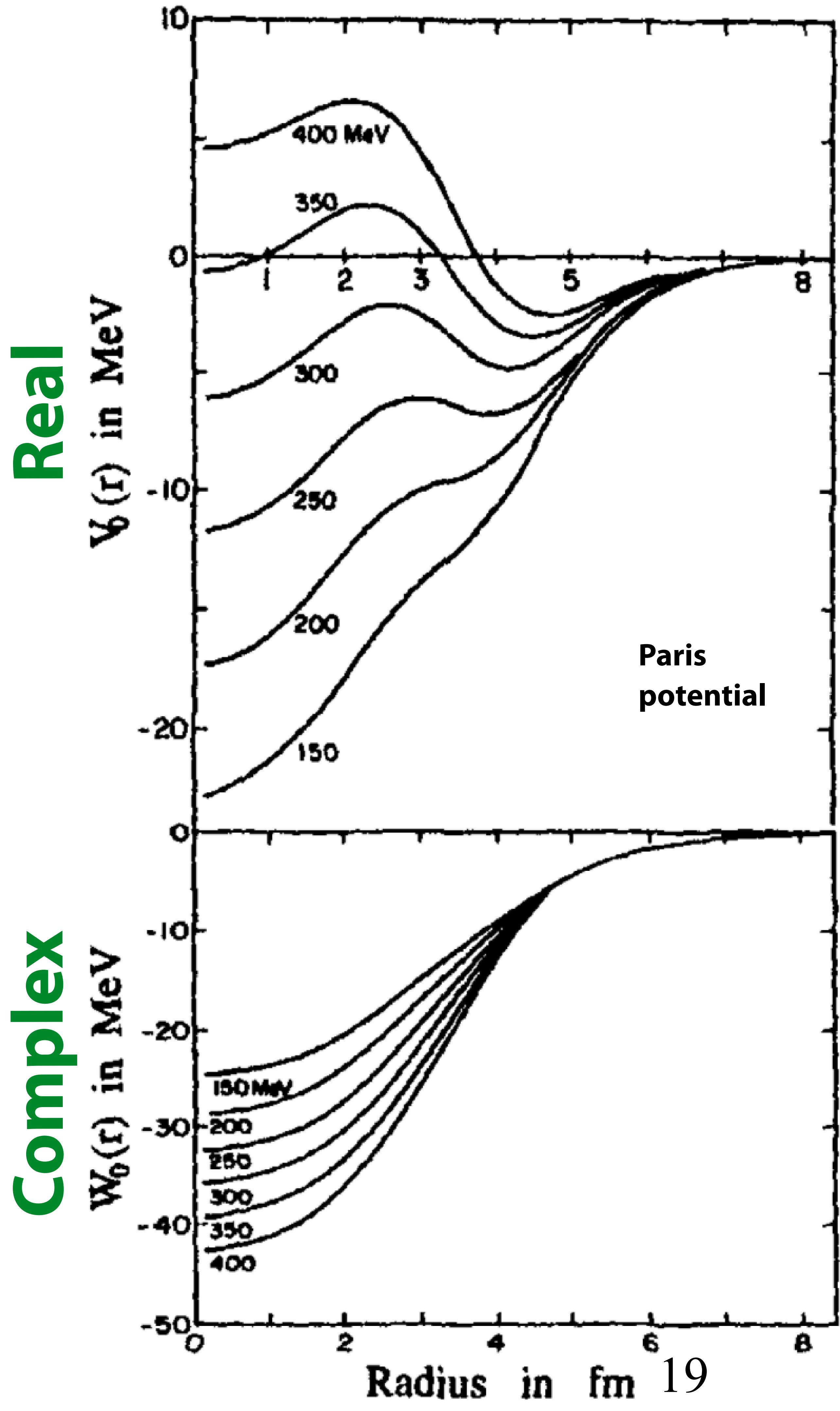

Theoretical framework

The general goal when solving the scattering problem of a nucleon from a nucleus is to solve the corresponding **Lippmann-Schwinger equation** for the many-body transition amplitude T

$$T = V + VG_0(E)T$$

<u>all two nucleon interactions</u>

$$V = \sum_{i=1}^{A} v_{0i}$$

<u>Green Function propagator</u>

$$G_0(E) = \frac{1}{E - H_0 + i\epsilon}$$

where

$$H_0 = h_0 + H_A$$

$H_A \left|\Phi_A\right\rangle = E_A \left|\Phi_A\right\rangle$ **target Hamiltonian**

h_0 **kinetic term of the projectile**

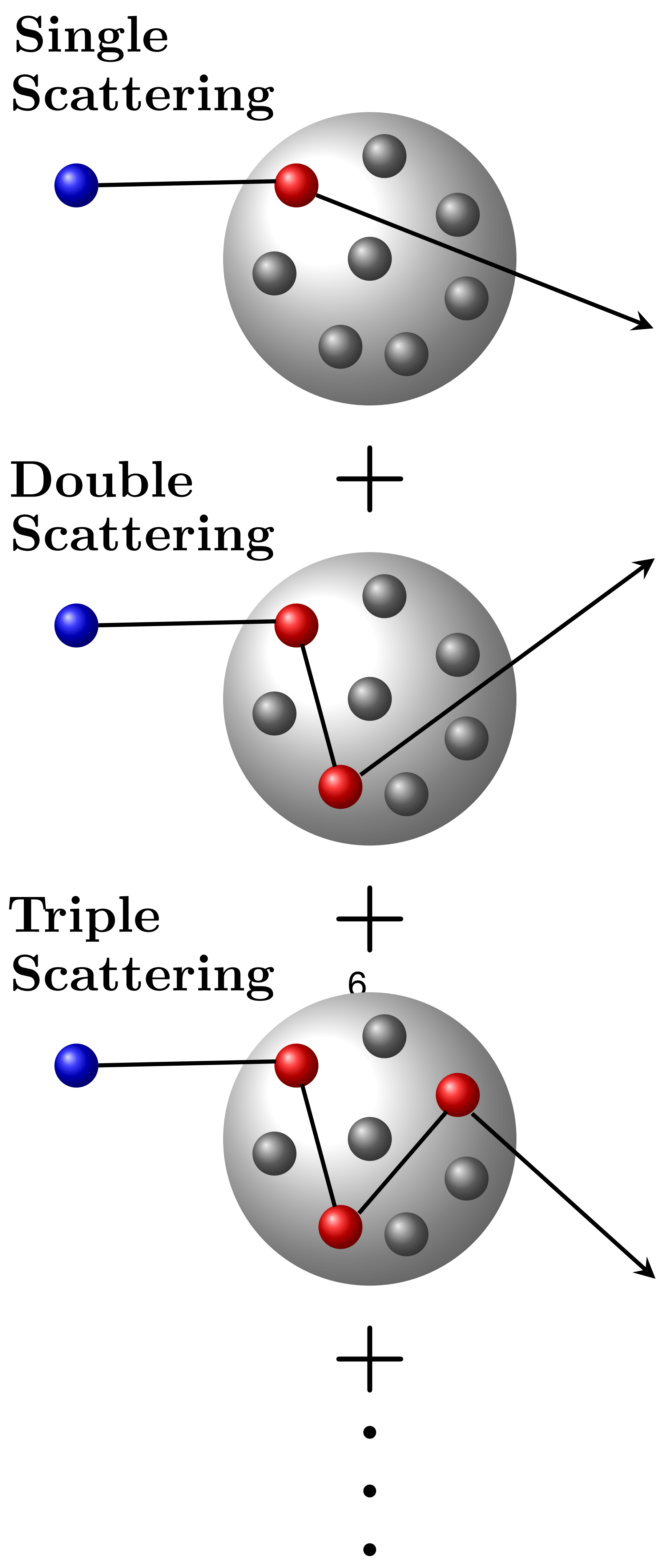

Theoretical framework

The general goal when solving the scattering problem of a nucleon from a nucleus is to solve the corresponding **Lippmann-Schwinger equation** for the many-body transition amplitude T

$$T = V + VG_0(E)T$$

two nucleon interaction dominates the scattering process $\quad T = \sum_{i=1} T_{0i}$

$$\begin{aligned}
T_{0i} &= v_{0i} + v_{0i}G_0(E)\sum_j T_{0j} \\
&= v_{0i} + v_{0i}G_0(E)T_{0i} + v_{0i}G_0(E)\sum_{j\neq i} T_{0j} \\
(1 - v_{0i}G_0(E))T_{0i} &= v_{0i} + v_{0i}G_0(E)\sum_{j\neq i} T_{0j}
\end{aligned}$$

$$\boxed{T_{0i} = t_{0i} + t_{0i}G_0(E)\sum_{j\neq i} T_{0j}.}$$

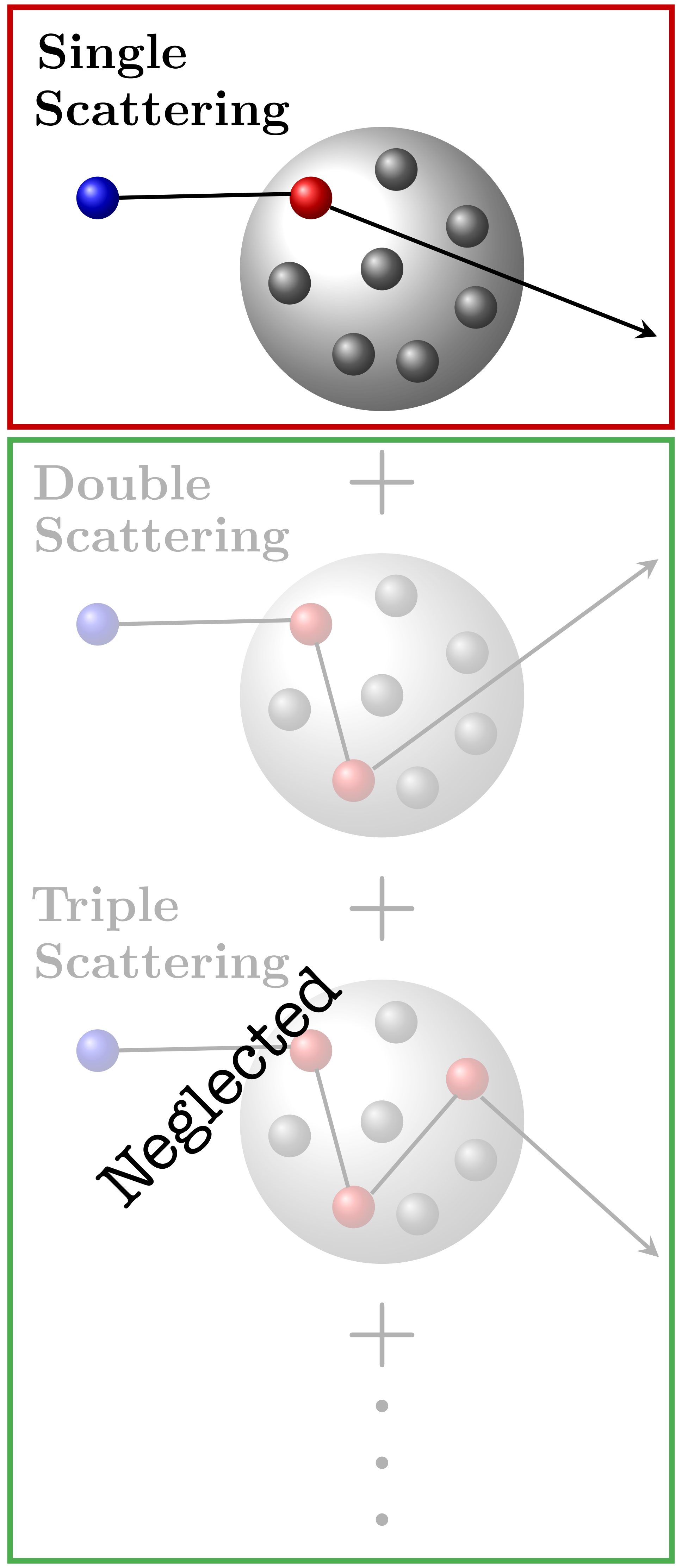

Theoretical framework

The general goal when solving the scattering problem of a nucleon from a nucleus is to solve the corresponding **Lippmann-Schwinger equation** for the many-body transition amplitude T

$$T = V + VG_0(E)T$$

Let's introduce the **optical potential U**

$$T = U + UG_0(E)PT$$

$$P + Q = 1$$

$$[G_0, P] = 0$$

In the case of elastic scattering,

P projects onto the elastic channel

$$U = V + VG_0(E)QU$$

$$P = \frac{|\Phi_A\rangle \langle\Phi_A|}{\langle\Phi_A|\Phi_A\rangle}$$

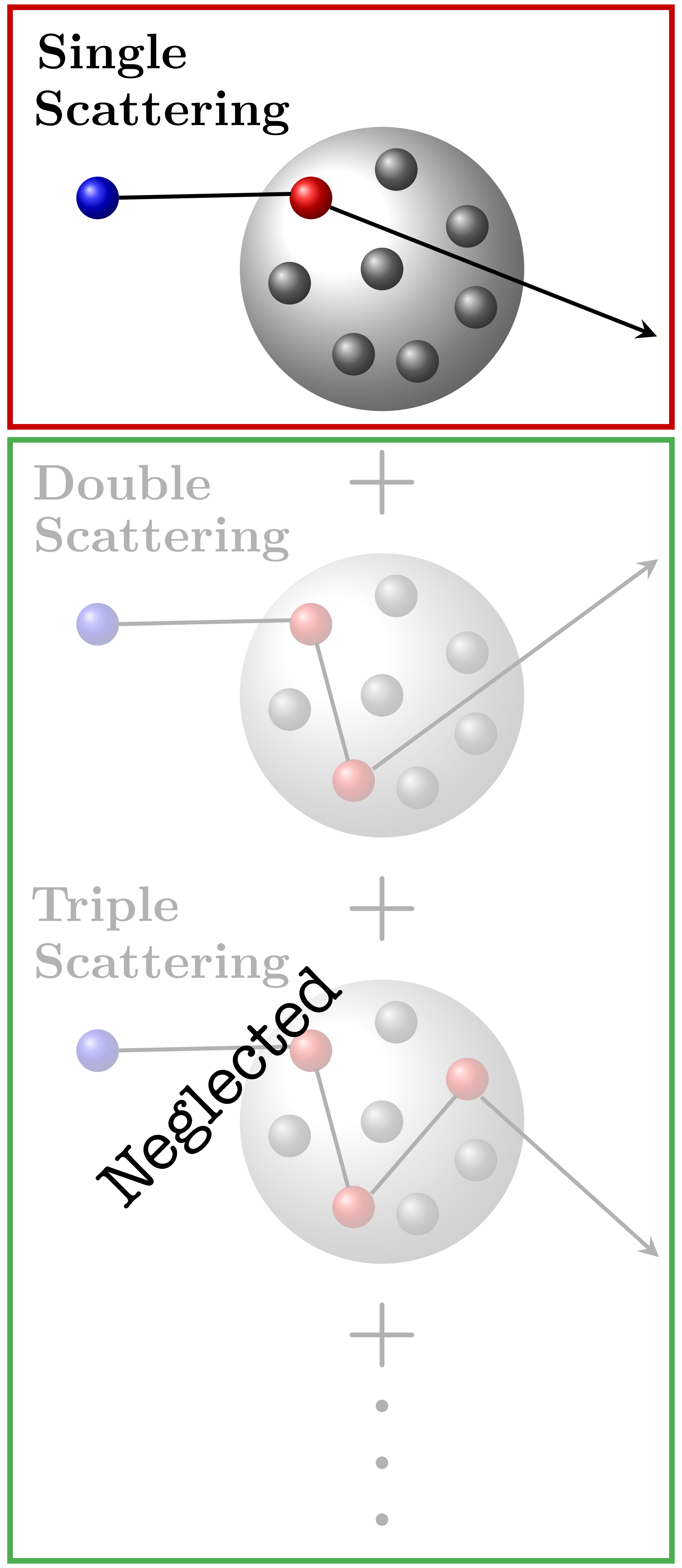

Theoretical framework

Transition amplitude for elastic scattering

$$T_{\rm el} \equiv PTP = PUP + PUPG_0(E)T_{\rm el}$$

The spectator expansion

Chinn, Elster, Thaler, Weppner, PRC **52 (1995)** 1992

$$U = \sum_{i=1}^{A} \tau_{0i} + \sum_{i,j\neq i}^{A} \tau_{0ij} + \sum_{i,j\neq i,k\neq i,j}^{A} \tau_{0ijk} + \dots$$

$$U \simeq \sum_{i=1}^{A} \tau_{0i} \xrightarrow{\text{Impulse approximation}} \tau_{0i} \approx t_{0i}$$

We neglect the coupling of the struck target nucleon with the residual nucleus!!!

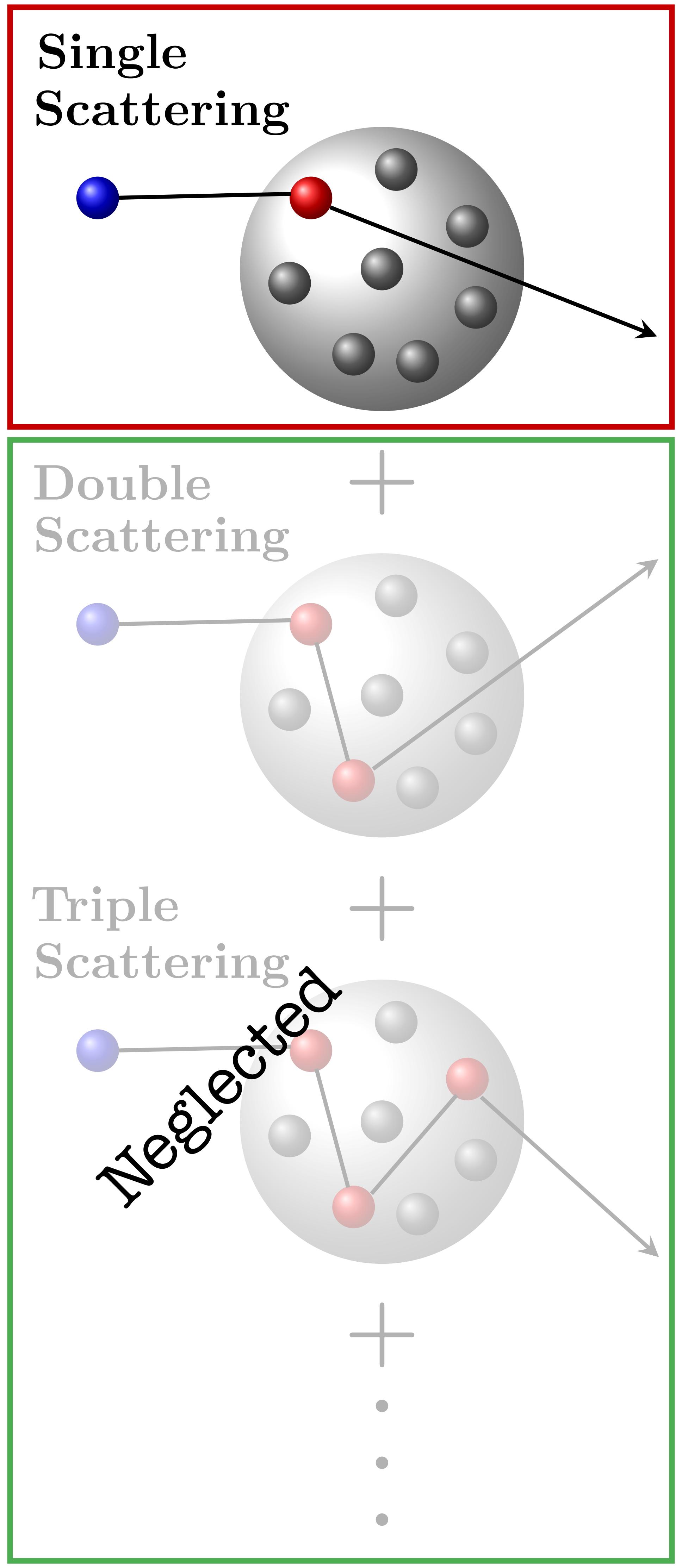

Theoretical framework - first order expansion

$$\boxed{\hat{U}(\boldsymbol{k}', \boldsymbol{k}; \omega) = (A-1)\, \langle \boldsymbol{k}', \Phi_A | t(\omega) | \boldsymbol{k}, \Phi_A \rangle}$$

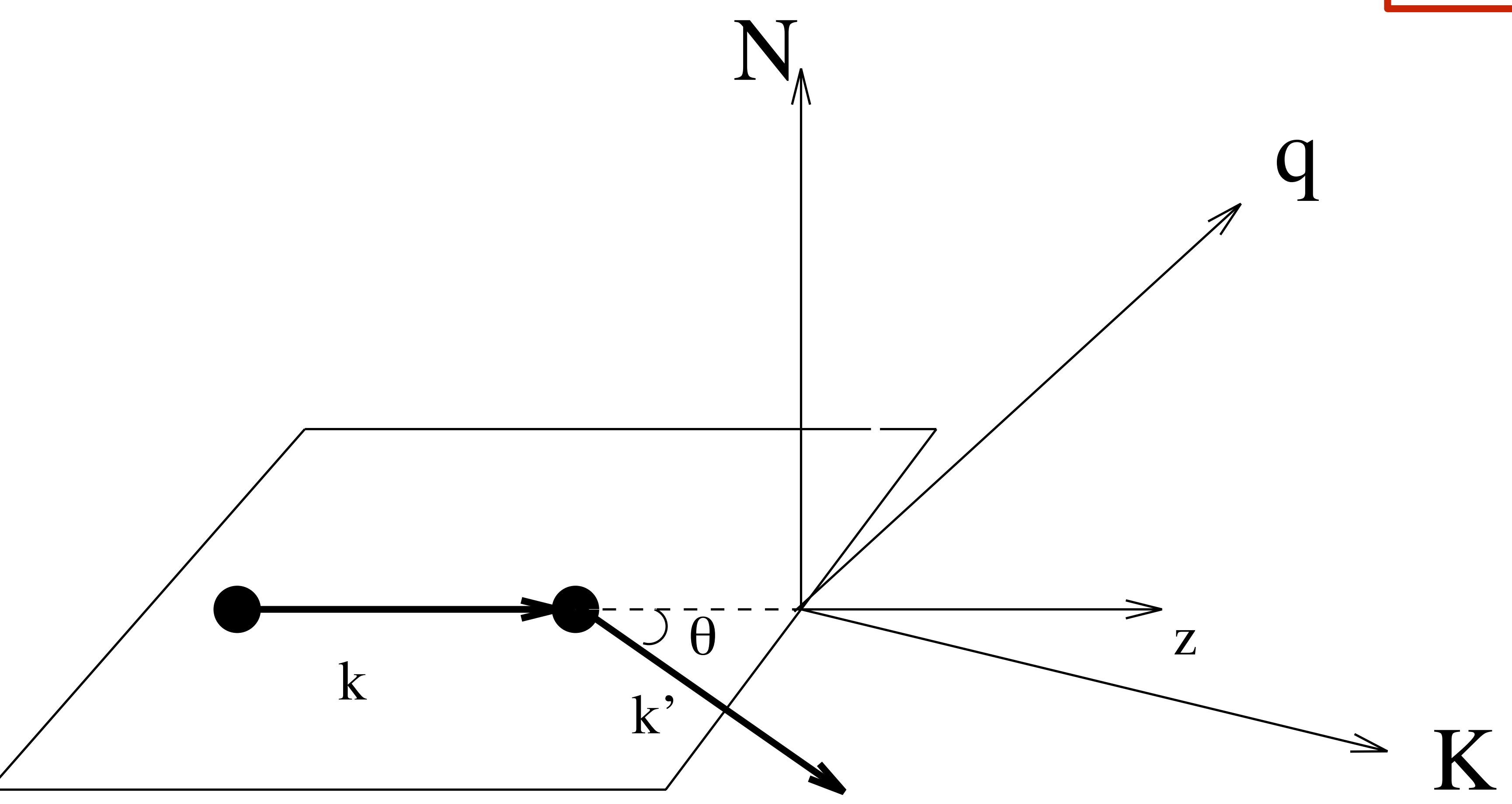

$$\boldsymbol{q} \equiv \boldsymbol{k}' - \boldsymbol{k}\,, \qquad \boldsymbol{K} \equiv \frac{1}{2}(\boldsymbol{k}' + \boldsymbol{k})$$

$$\hat{U}(\boldsymbol{q}, \boldsymbol{K}; \omega) = \frac{A-1}{A}\, \eta(\boldsymbol{q}, \boldsymbol{K}) \times \sum_{N=n,p} t_{pN}\left[\boldsymbol{q}, \frac{A+1}{A}\boldsymbol{K}; \omega\right] \rho_N(q)$$

Free two-body scattering matrix

$$t_{0i} = v_{0i} + v_{0i}\, g_{0i}\, t_{0i}$$

$$g_{0i} = (E - h_0 - h_i + i\epsilon)^{-1}$$

- Simple one-body equation
- Can be solved easily
- Only **NN** interaction

Kerman, McManus and Thaler, Ann. Phys. **8** (1959) 551 and many others

Theoretical framework - first order expansion

$$\boxed{\hat{U}(\boldsymbol{k}',\boldsymbol{k};\omega) = (A-1)\,\langle \boldsymbol{k}',\Phi_A|t(\omega)|\boldsymbol{k},\Phi_A\rangle}$$

$$\boldsymbol{q} \equiv \boldsymbol{k}' - \boldsymbol{k}\,, \qquad \boldsymbol{K} \equiv \frac{1}{2}(\boldsymbol{k}' + \boldsymbol{k})$$

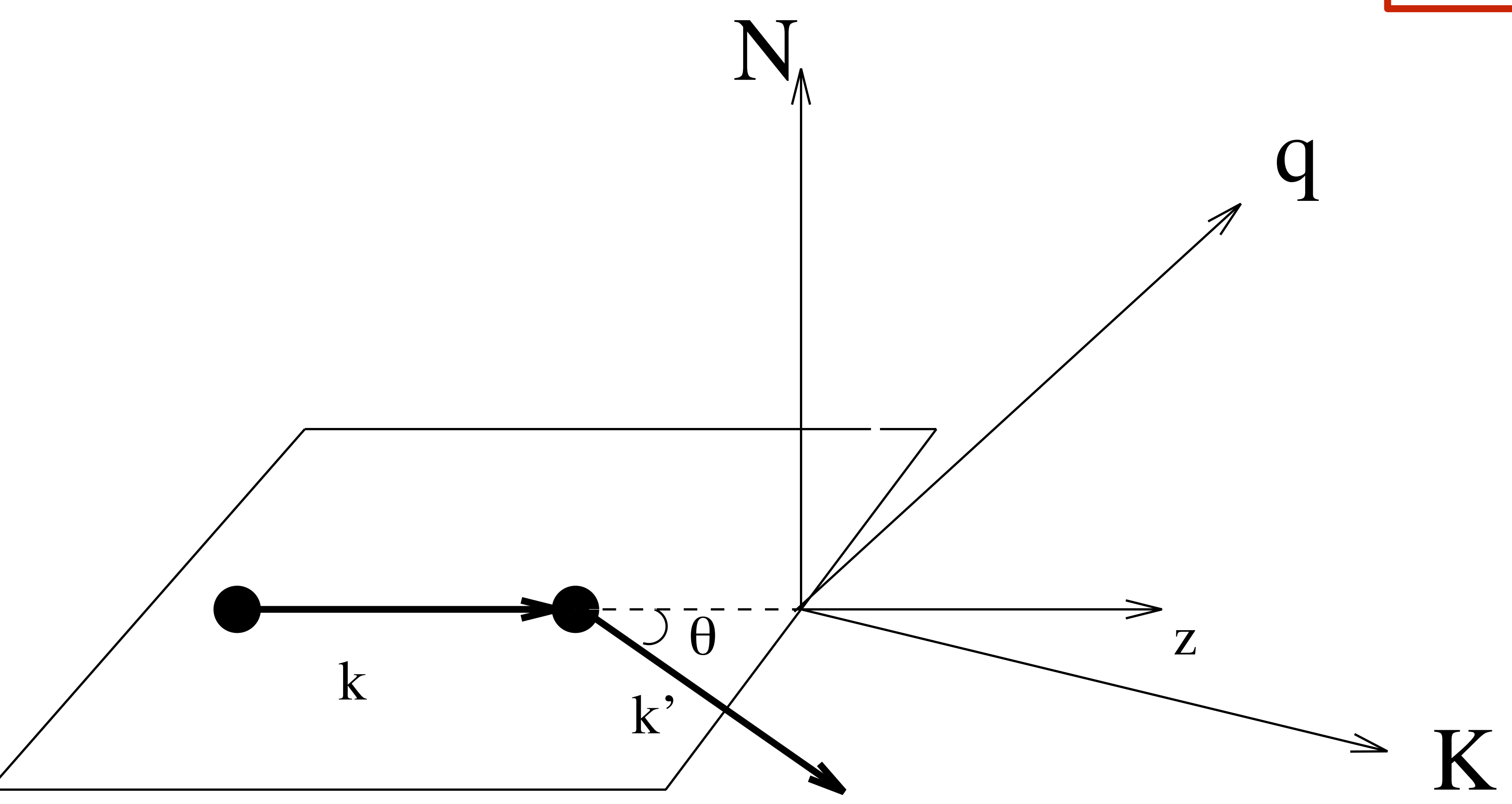

$$\hat{U}(\boldsymbol{q},\boldsymbol{K};\omega) = \frac{A-1}{A}\,\eta(\boldsymbol{q},\boldsymbol{K}) \times \sum_{N=n,p} t_{pN}\left[\boldsymbol{q},\frac{A+1}{A}\boldsymbol{K};\omega\right]\rho_N(q)$$

Free two-body scattering matrix

$$t_{0i} = v_{0i} + v_{0i}\,g_{0i}\,t_{0i}$$

$$g_{0i} = (E - h_0 - h_i + i\epsilon)^{-1}$$

- Simple one-body equation
- Can be solved easily
- Only **NN** interaction

Nonlocal one-body density

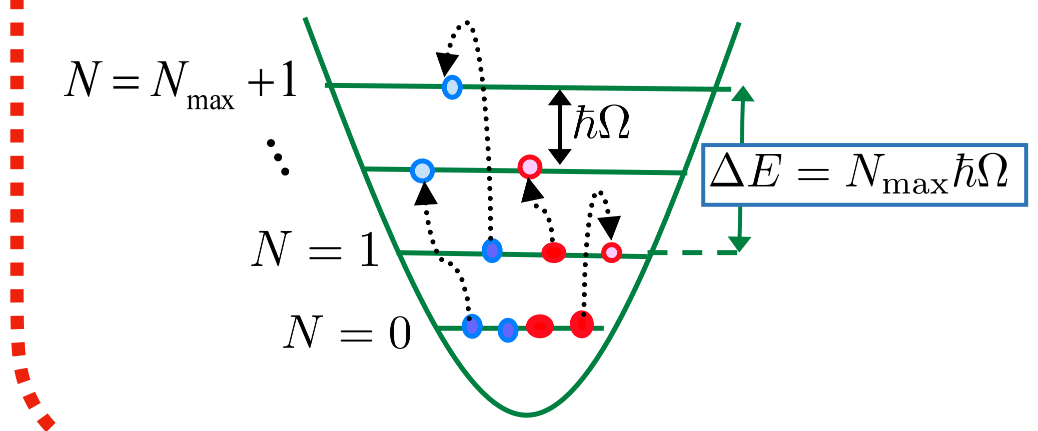

- Computationally expensive
- Obtained from the No-Core Shell Model
- Calculation performed with **NN** and **3N** interaction

Kerman, McManus and Thaler, Ann. Phys. **8** (1959) 551 and many others

Theoretical framework - first order expansion

$$\boxed{\hat{U}(\boldsymbol{k}', \boldsymbol{k}; \omega) = (A-1)\, \langle \boldsymbol{k}', \Phi_A | t(\omega) | \boldsymbol{k}, \Phi_A \rangle}$$

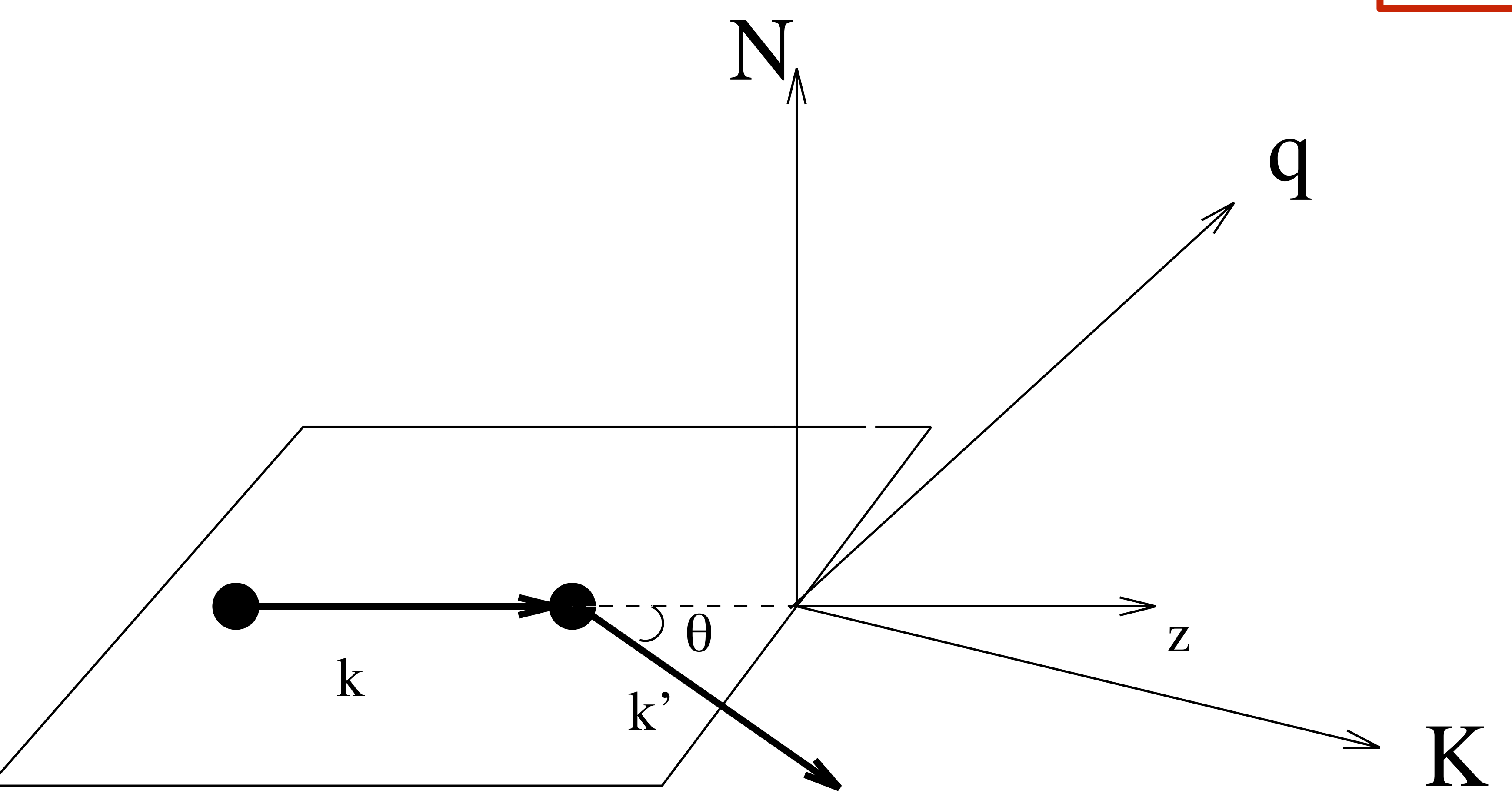

$$\boldsymbol{q} \equiv \boldsymbol{k}' - \boldsymbol{k}\,, \qquad \boldsymbol{K} \equiv \frac{1}{2}(\boldsymbol{k}' + \boldsymbol{k})$$

$$\hat{U}(\boldsymbol{q}, \boldsymbol{K}; \omega) = \frac{A-1}{A} \eta(\boldsymbol{q}, \boldsymbol{K})$$

$$\times \sum_{N=n,p} t_{pN}\left[\boldsymbol{q}, \frac{A+1}{A}\boldsymbol{K}; \omega\right] \rho_N(q)$$

$\eta(\boldsymbol{q}, \boldsymbol{K}) =$ **Møller factor**

$$\left[\frac{E_{\text{proj}}(\boldsymbol{\kappa}')\, E_{\text{proj}}(-\boldsymbol{\kappa}')\, E_{\text{proj}}(\boldsymbol{\kappa})\, E_{\text{proj}}(-\boldsymbol{\kappa})}{E_{\text{proj}}(\boldsymbol{k}')\, E_{\text{proj}}\left(-\frac{\boldsymbol{q}}{2} - \frac{\boldsymbol{K}}{A}\right)\, E_{\text{proj}}(\boldsymbol{k})\, E_{\text{proj}}\left(\frac{\boldsymbol{q}}{2} - \frac{\boldsymbol{K}}{A}\right)}\right]^{\frac{1}{2}}$$

Kerman, McManus and Thaler, Ann. Phys. **8** (1959) 551 and many others

Free two-body scattering matrix

$$t_{0i} = v_{0i} + v_{0i}\, g_{0i}\, t_{0i}$$

$$g_{0i} = (E - h_0 - h_i + i\epsilon)^{-1}$$

- Simple one-body equation
- Can be solved easily
- Only **NN** interaction

Nonlocal one-body density

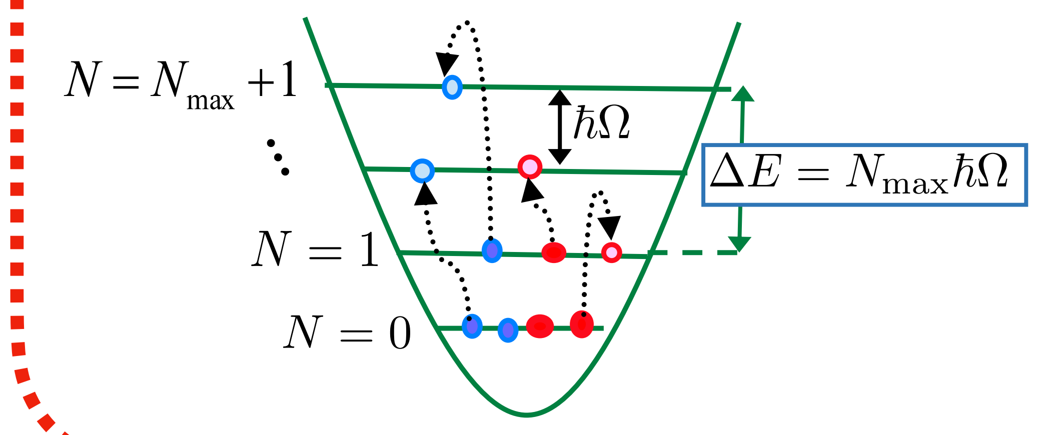

- Computationally expensive
- Obtained from the No-Core Shell Model
- Calculation performed with **NN** and **3N** interaction

Theoretical framework - first order expansion

$$\boxed{\hat{U}(\boldsymbol{k}', \boldsymbol{k}; \omega) = (A-1)\, \langle \boldsymbol{k}', \Phi_A | t(\omega) | \boldsymbol{k}, \Phi_A \rangle}$$

$$\boldsymbol{q} \equiv \boldsymbol{k}' - \boldsymbol{k}\,, \qquad \boldsymbol{K} \equiv \frac{1}{2}(\boldsymbol{k}' + \boldsymbol{k})$$

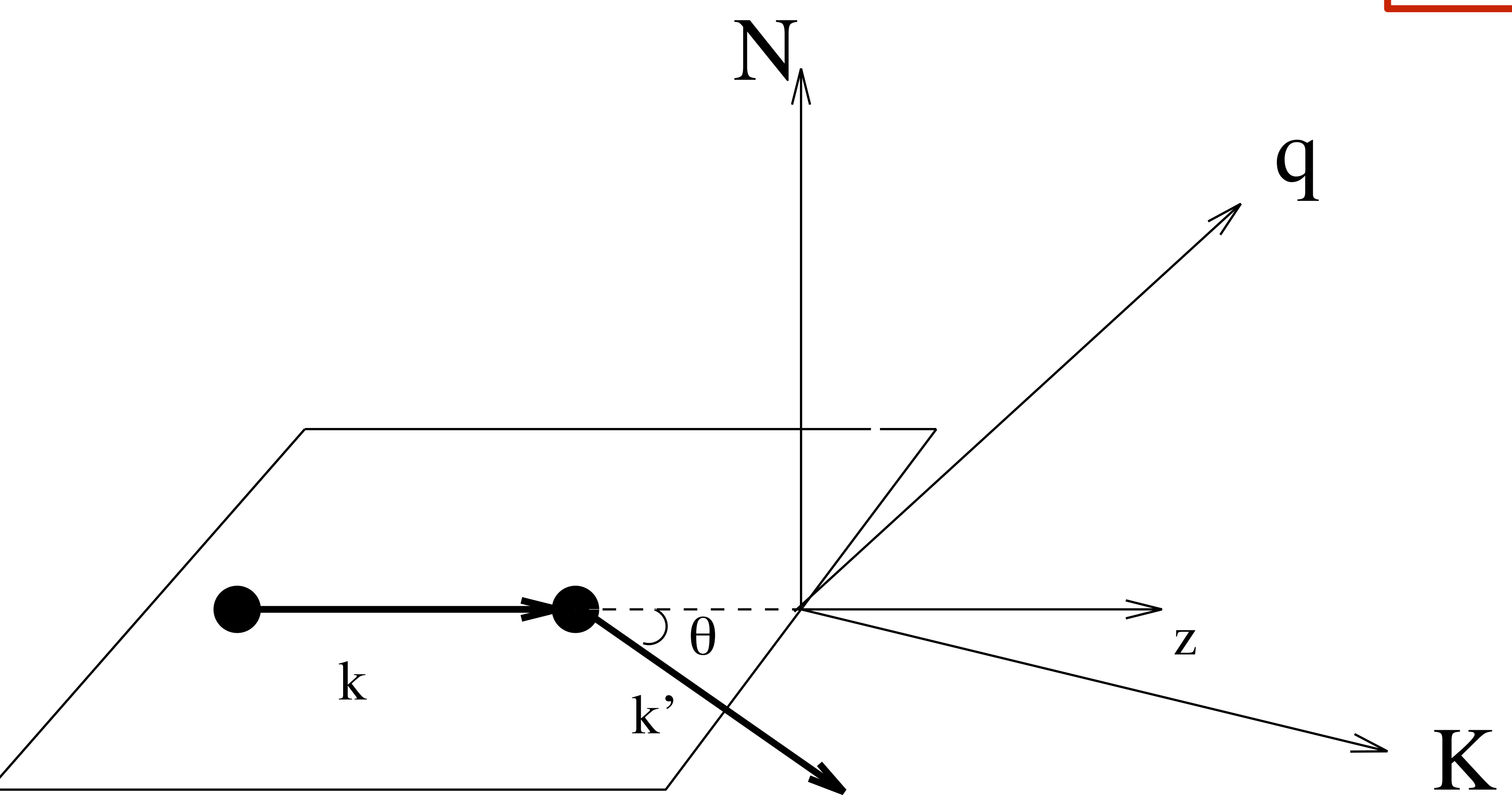

$$\hat{U}(\boldsymbol{q}, \boldsymbol{K}; \omega) = \frac{A-1}{A}\, \eta(\boldsymbol{q}, \boldsymbol{K}) \times \sum_{N=n,p} t_{pN} \left[\boldsymbol{q}, \frac{A+1}{A} \boldsymbol{K}; \omega \right] \rho_N(q)$$

$$\hat{U}(\boldsymbol{q}, \boldsymbol{K}; \omega) = \hat{U}^c(\boldsymbol{q}, \boldsymbol{K}; \omega) + \frac{i}{2} \boldsymbol{\sigma} \cdot \boldsymbol{q} \times \boldsymbol{K}\, \hat{U}^{ls}(\boldsymbol{q}, \boldsymbol{K}; \omega)$$

$$\hat{U}^c(\boldsymbol{q}, \boldsymbol{K}; \omega) = \frac{A-1}{A}\, \eta(\boldsymbol{q}, \boldsymbol{K}) \times \sum_{N=n,p} t^c_{pN} \left[\boldsymbol{q}, \frac{A+1}{A} \boldsymbol{K}; \omega \right] \rho_N(q)$$

Central component

$\eta(\boldsymbol{q}, \boldsymbol{K}) =$ **Møller factor**

$$\left[\frac{E_{\text{proj}}(\boldsymbol{\kappa}')\, E_{\text{proj}}(-\boldsymbol{\kappa}')\, E_{\text{proj}}(\boldsymbol{\kappa})\, E_{\text{proj}}(-\boldsymbol{\kappa})}{E_{\text{proj}}(\boldsymbol{k}')\, E_{\text{proj}}\left(-\frac{\boldsymbol{q}}{2} - \frac{\boldsymbol{K}}{A}\right)\, E_{\text{proj}}(\boldsymbol{k})\, E_{\text{proj}}\left(\frac{\boldsymbol{q}}{2} - \frac{\boldsymbol{K}}{A}\right)} \right]^{\frac{1}{2}}$$

Kerman, McManus and Thaler, Ann. Phys. **8** (1959) 551 and many others

Theoretical framework - first order expansion

$$\boxed{\hat{U}(\boldsymbol{k}', \boldsymbol{k}; \omega) = (A-1)\, \langle \boldsymbol{k}', \Phi_A | t(\omega) | \boldsymbol{k}, \Phi_A \rangle}$$

$$\boldsymbol{q} \equiv \boldsymbol{k}' - \boldsymbol{k}\,, \qquad \boldsymbol{K} \equiv \frac{1}{2}(\boldsymbol{k}' + \boldsymbol{k})$$

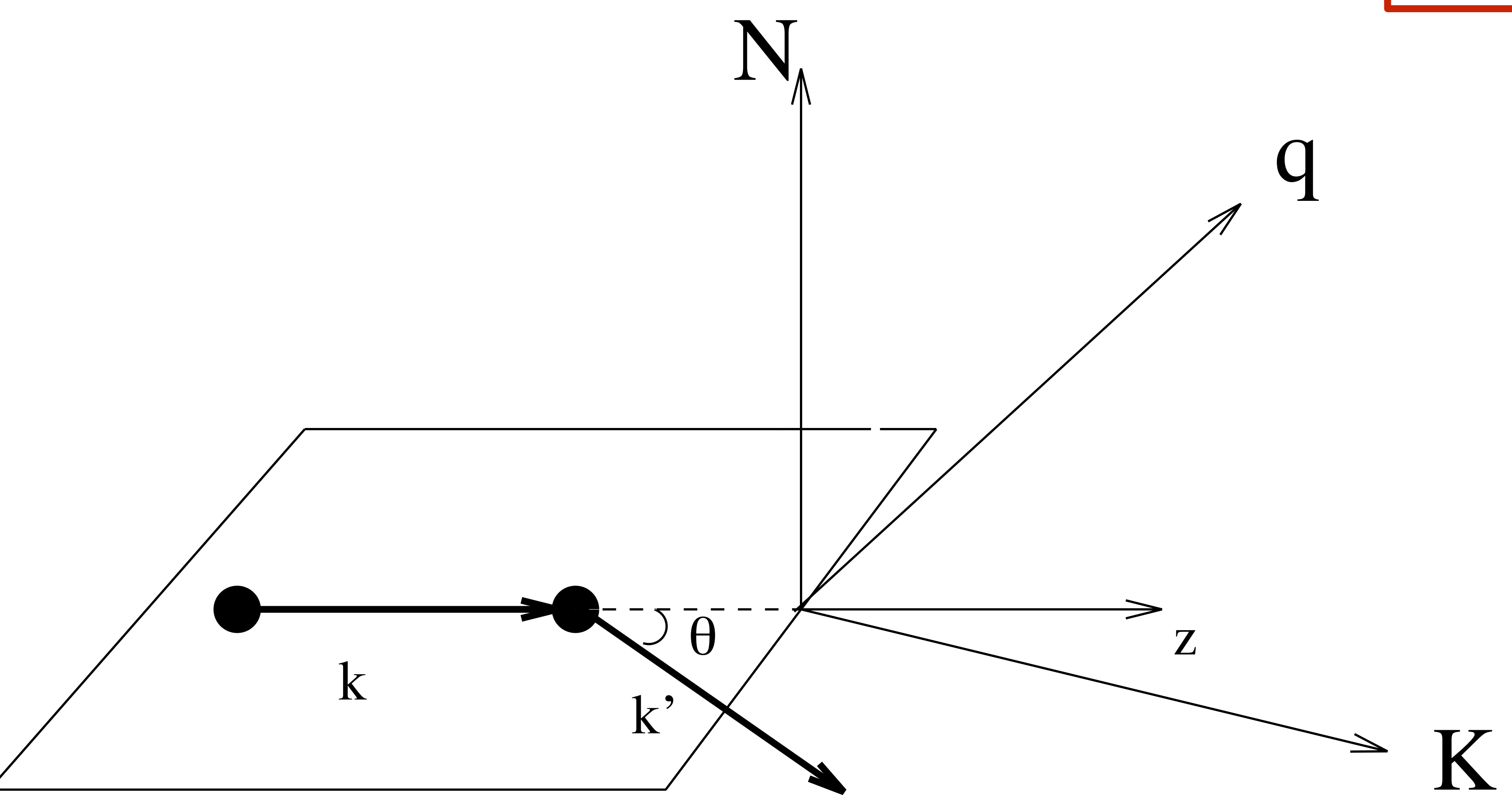

$$\hat{U}(\boldsymbol{q}, \boldsymbol{K}; \omega) = \frac{A-1}{A}\, \eta(\boldsymbol{q}, \boldsymbol{K}) \times \sum_{N=n,p} t_{pN} \left[\boldsymbol{q}, \frac{A+1}{A}\boldsymbol{K}; \omega \right] \rho_N(q)$$

$\eta(\boldsymbol{q}, \boldsymbol{K}) =$ **Møller factor**

$$\left[\frac{E_{\mathrm{proj}}(\boldsymbol{\kappa}')\, E_{\mathrm{proj}}(-\boldsymbol{\kappa}')\, E_{\mathrm{proj}}(\boldsymbol{\kappa})\, E_{\mathrm{proj}}(-\boldsymbol{\kappa})}{E_{\mathrm{proj}}(\boldsymbol{k}')\, E_{\mathrm{proj}}\left(-\frac{\boldsymbol{q}}{2} - \frac{\boldsymbol{K}}{A}\right)\, E_{\mathrm{proj}}(\boldsymbol{k})\, E_{\mathrm{proj}}\left(\frac{\boldsymbol{q}}{2} - \frac{\boldsymbol{K}}{A}\right)} \right]^{\frac{1}{2}}$$

$$\hat{U}(\boldsymbol{q}, \boldsymbol{K}; \omega) = \hat{U}^{c}(\boldsymbol{q}, \boldsymbol{K}; \omega) + \frac{i}{2}\boldsymbol{\sigma} \cdot \boldsymbol{q} \times \boldsymbol{K}\, \hat{U}^{ls}(\boldsymbol{q}, \boldsymbol{K}; \omega)$$

$$\hat{U}^{c}(\boldsymbol{q}, \boldsymbol{K}; \omega) = \frac{A-1}{A}\, \eta(\boldsymbol{q}, \boldsymbol{K}) \times \sum_{N=n,p} t^{c}_{pN} \left[\boldsymbol{q}, \frac{A+1}{A}\boldsymbol{K}; \omega \right] \rho_N(q)$$

Central component

$$\hat{U}^{ls}(\boldsymbol{q}, \boldsymbol{K}; \omega) = \frac{A-1}{A}\, \eta(\boldsymbol{q}, \boldsymbol{K}) \left(\frac{A+1}{2A} \right) \times \sum_{N=n,p} t^{ls}_{pN} \left[\boldsymbol{q}, \frac{A+1}{A}\boldsymbol{K}; \omega \right] \rho_N(q)$$

Spin-orbit component

Kerman, McManus and Thaler, Ann. Phys. **8** (1959) 551 and many others

Theoretical framework - Coulomb potential

Combine phase shifts from Coulomb and nuclear

$$\boxed{\sigma_L = \arg\Gamma\left[L + 1 + i\eta(k_0)\right]}$$

The central amplitude include a Coulomb component

$$A(k_0,\theta) = F^c_{pt}(k_0,\theta) + \frac{1}{2\pi^2}\sum_{L=0}^{\infty} e^{2i\sigma_L}\left[(L+1)\bar{F}^+_L(k_0) + L\bar{F}^-_L(k_0)\right]P_L(\cos\theta)$$

$$F^c_{pt}(k_0,\theta) = \frac{-\eta(k_0)\ \exp\left[2i\sigma_0 - i\eta(k_0)\ln(1-\cos\theta)\right]}{k_0(1-\cos\theta)}$$

Sommerfeld parameter

$$\eta(k) = \frac{\mu Z\alpha}{k}$$

$$u''_L(r) = \left[\frac{L(L+1)}{r^2} + \frac{2\mu}{\hbar^2}(V(r)-E)\right]u_L(r)$$

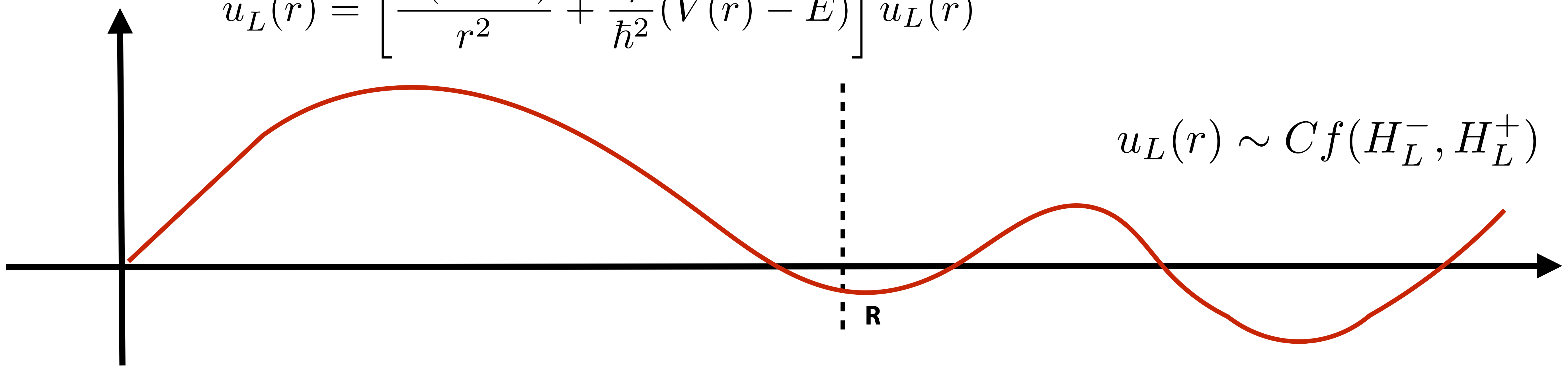

Do not add nuclear and Coulomb separately!

$$\bar{U}(\boldsymbol{k}',\boldsymbol{k};\omega) = \langle\boldsymbol{k}'|\bar{U}(\omega)|\boldsymbol{k}\rangle = \langle\psi^{(+)}_c(\boldsymbol{k}')|\hat{U}(\omega)|\psi^{(+)}_c(\boldsymbol{k})\rangle$$

Theoretical framework - observables

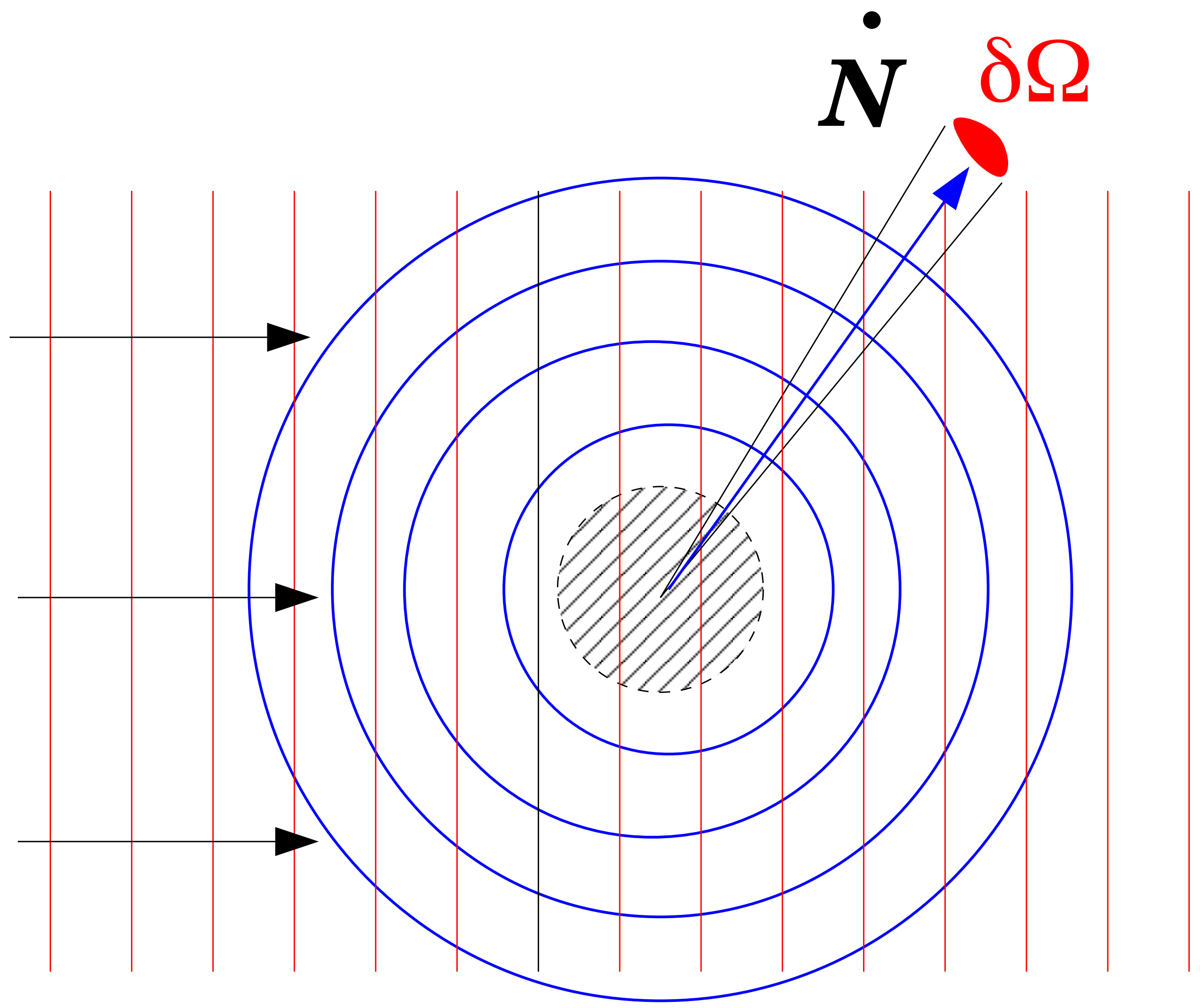

$$\dot{N} \sim \left\langle \frac{d\sigma}{d\Omega} \right\rangle \delta\Omega$$

$$M(k_0,\theta) = A(k_0,\theta) + \boldsymbol{\sigma}\cdot\hat{\mathbf{N}}\,\underline{C(k_0,\theta)}$$

Spin-flip amplitude

$$A(\theta) = \frac{1}{2\pi^2}\sum_{L=0}^{\infty}\left[(L+1)F_L^+(k_0) + LF_L^-(k_0)\right]P_L(\cos\theta)$$

$$F_{LJ}(k_0) = -\frac{A}{A-1}4\pi^2\mu(k_0)\hat{T}_{LJ}(k_0,k_0;E)$$

$$C(\theta) = \frac{i}{2\pi^2}\sum_{L=1}^{\infty}\left[F_L^+(k_0) - F_L^-(k_0)\right]P_L^1(\cos\theta)$$

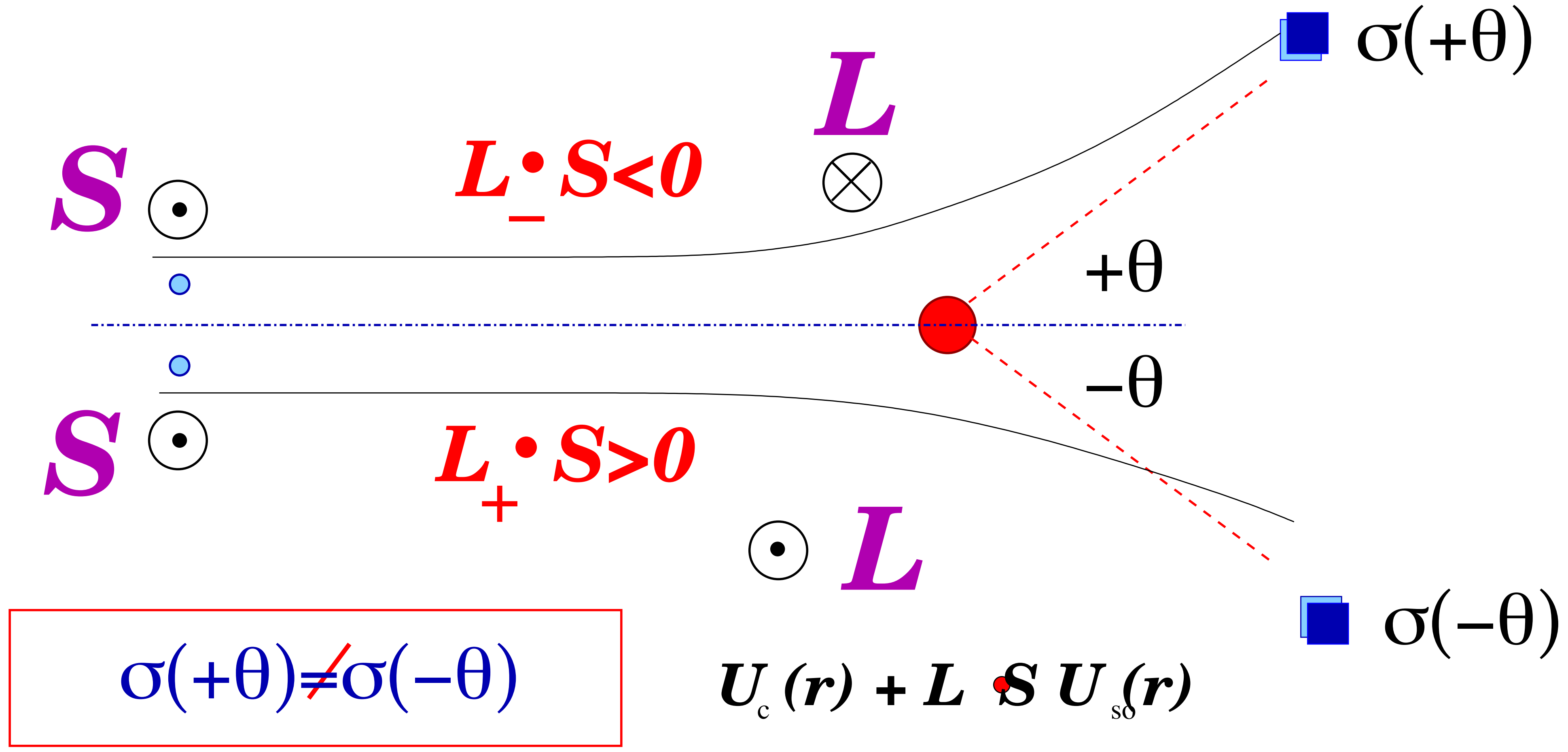

Differential cross section

$$\frac{d\sigma}{d\Omega}(\theta) = |A(\theta)|^2 + |C(\theta)|^2$$

Analyzing power

$$A_y(\theta) = \frac{2\mathrm{Re}[A^*(\theta)\,C(\theta)]}{|A(\theta)|^2 + |C(\theta)|^2}$$

Spin rotation

$$Q(\theta) = \frac{2\mathrm{Im}[A(\theta)\,C^*(\theta)]}{|A(\theta)|^2 + |C(\theta)|^2}$$

Rotation of the spin vector in the scattering plane, i.e. protons polarised along the ***+x*** axis have a finite probability of having the spin polarised along the **± *z*** axis after the collision

Theoretical inputs

NN (and also **NNN**) potentials to describe the interaction between the projectile and the target

Ab-initio (whenever is possible) description of the target
NCSM
SCGF

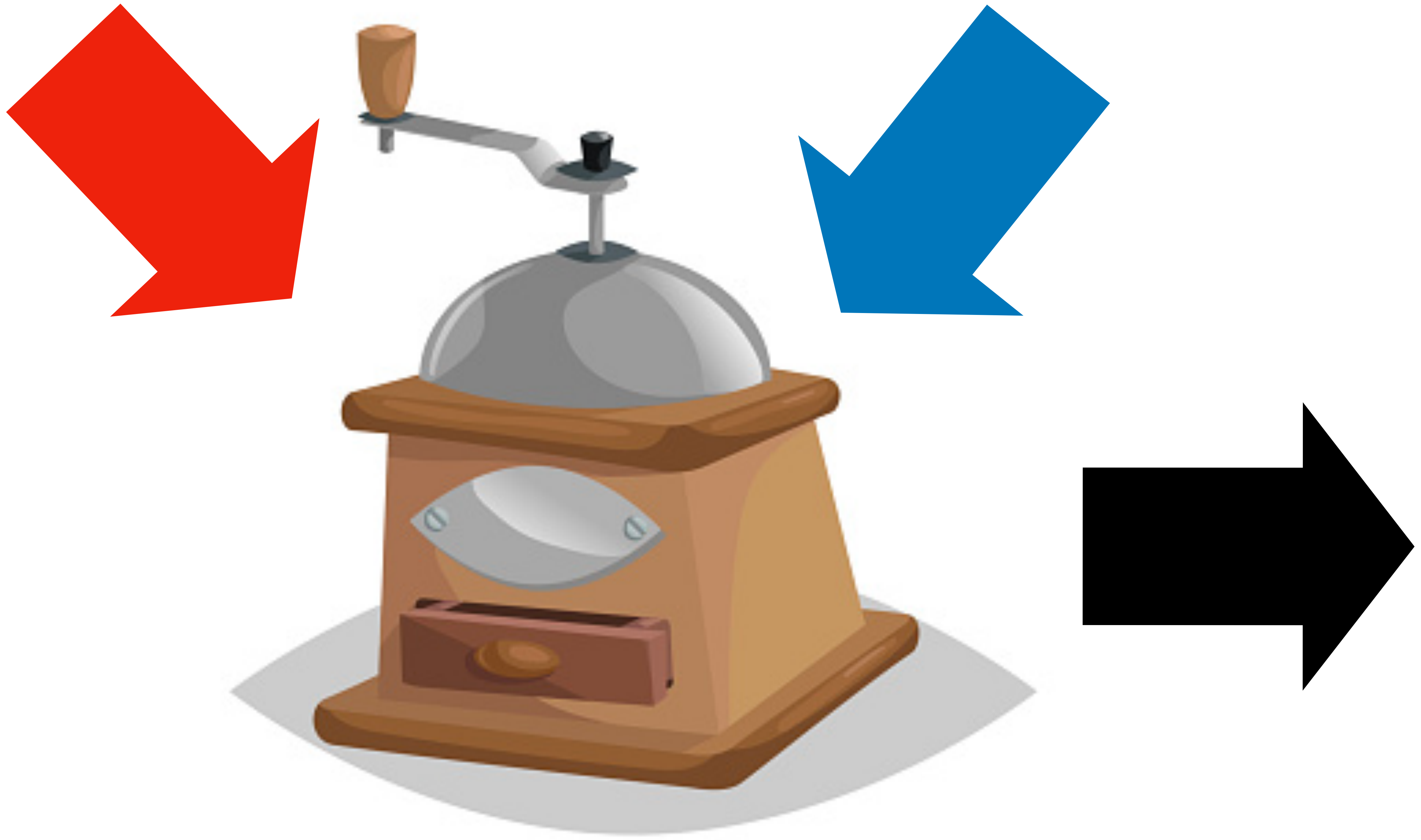

OBSERVABLES

*Our "**optical potential**" machinery*

Chiral NN potentials

Advantages

- QCD symmetries are consistently respected
- Systematic expansion (order by order you know exactly the terms to be included)
- Theoretical errors
- Two- and three-body forces belong to the same framework

Features

- Many-body data needed and many-body forces inevitable
- Exploit divergences (cutoff dependence as tool)
- Power counting determines diagrams and truncation error

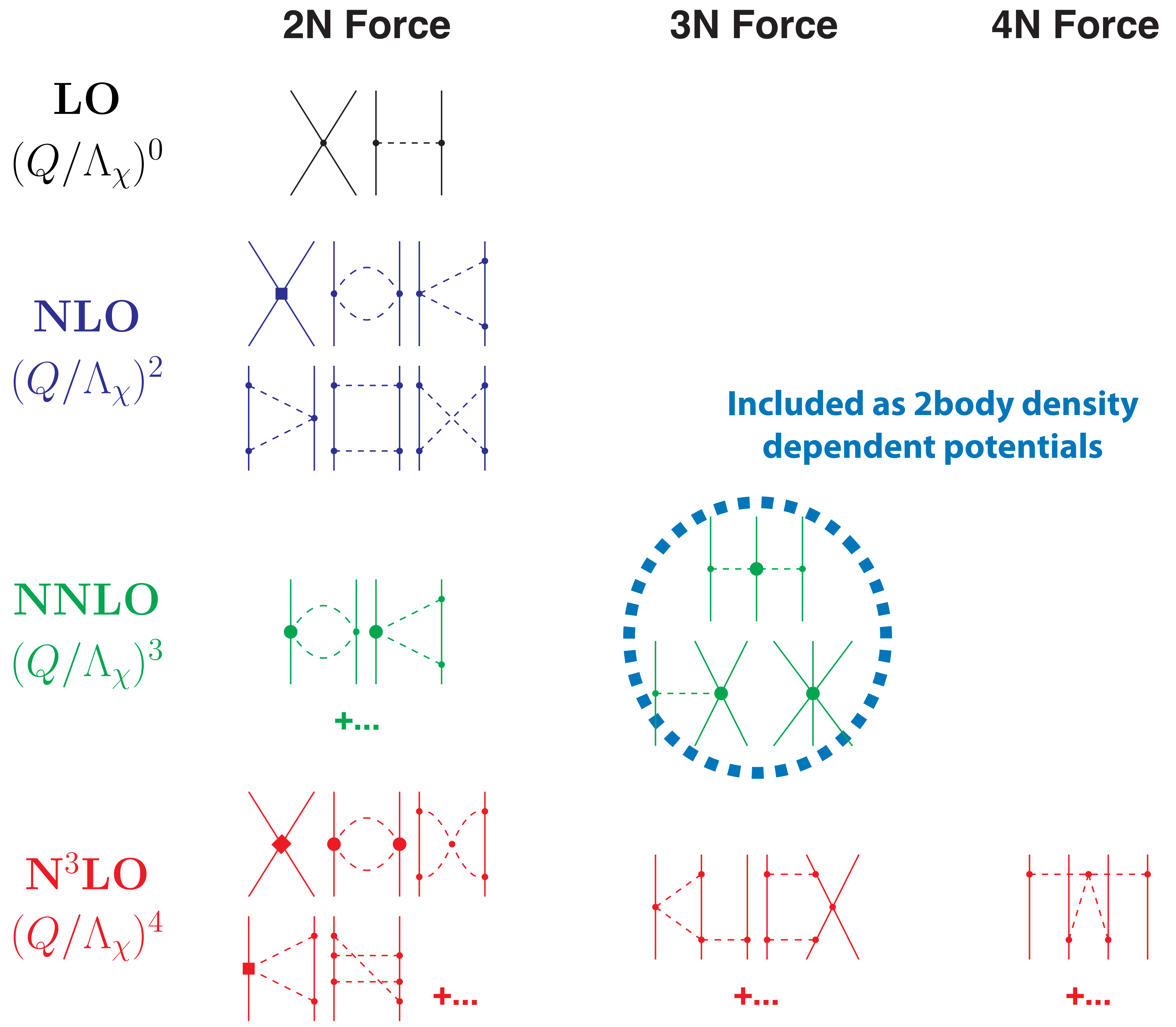

We employed both Machleidt and Epelbaum NN potentials at N3LO and N4LO order

Chiral effective field theory and nuclear forces, Phys. Rep. **503** (2011) 1-75

Modern Theory of Nuclear Forces, Rev. Mod. Phys. **81** (2009) 1773-1825

Chiral NN potentials

- **NN t matrix** computed with the addition of a density-dependent interaction

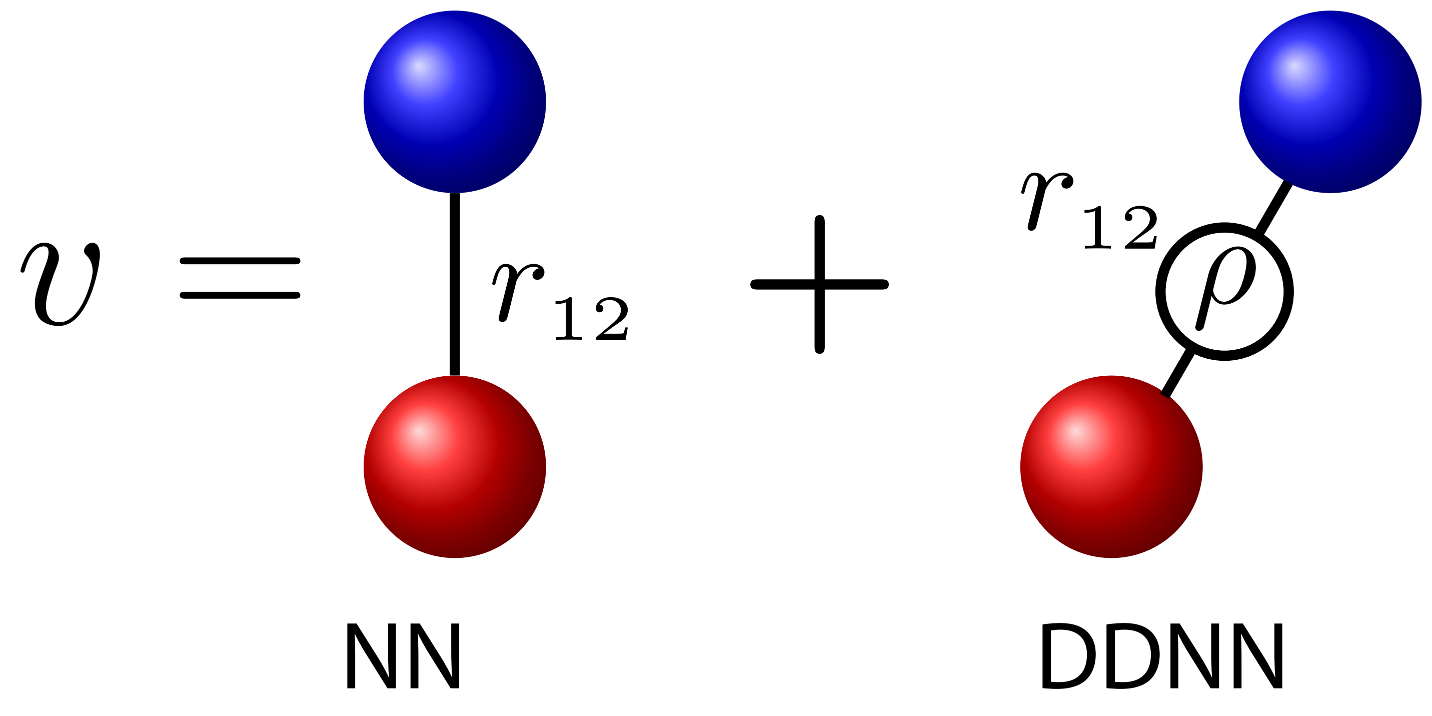

- **Nuclear density** computed with NN + 3N interaction

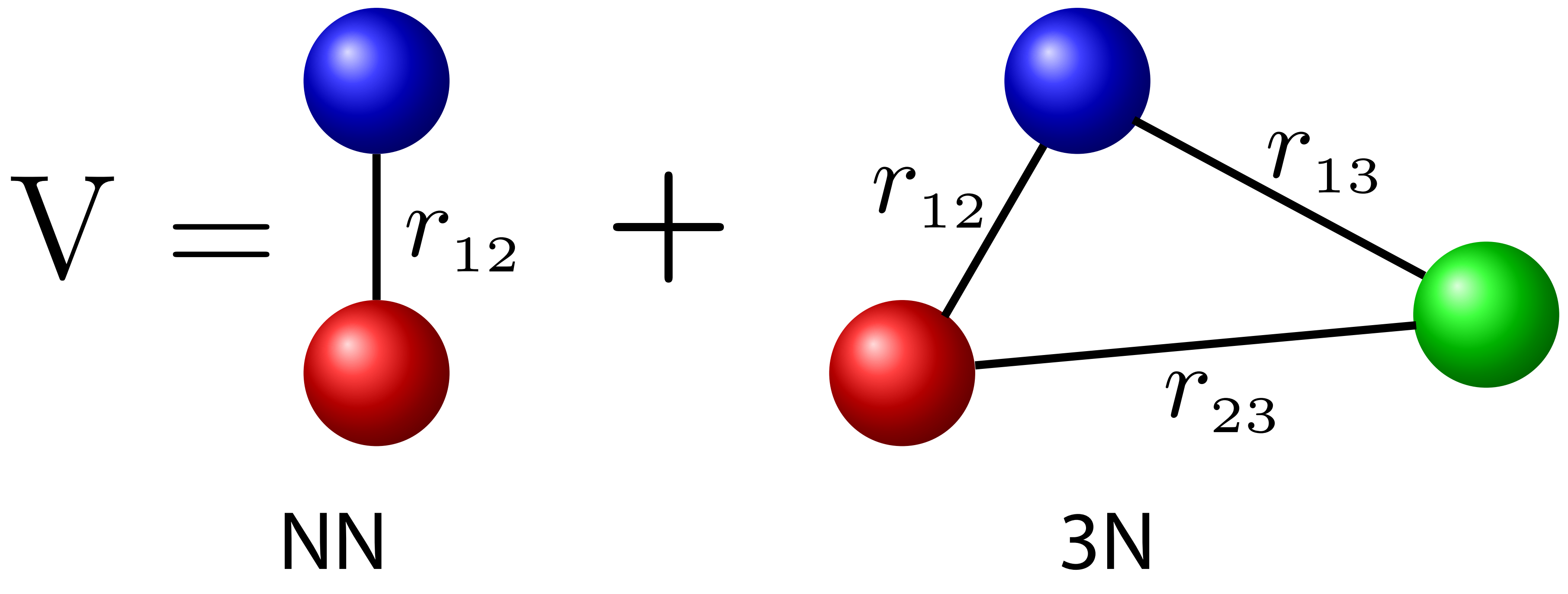

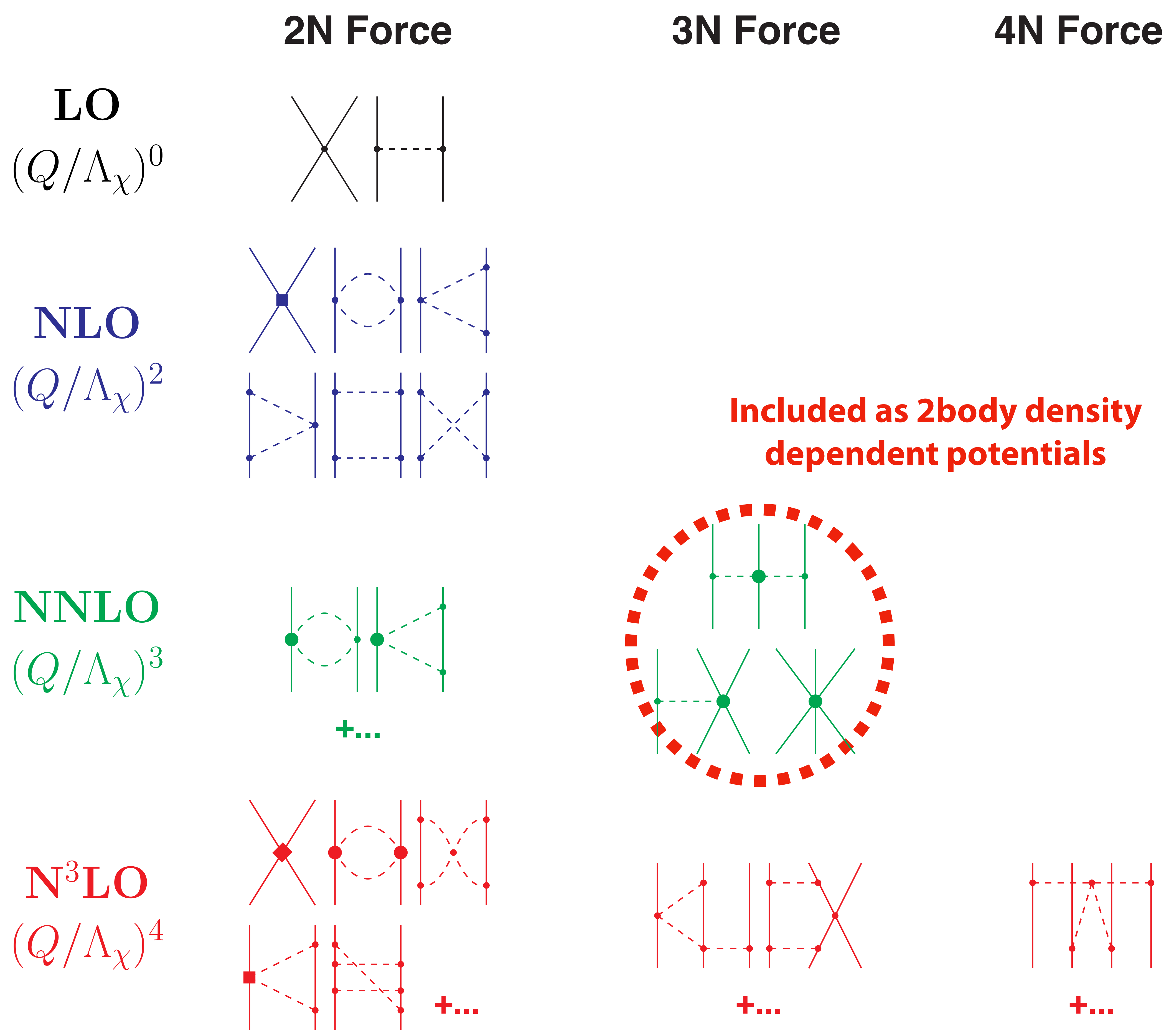

We employed both Machleidt and Epelbaum NN potentials at N3LO and N4LO order

Chiral effective field theory and nuclear forces, Phys. Rep. 503 (2011) 1-75

Modern Theory of Nuclear Forces, Rev. Mod. Phys. 81 (2009) 1773-1825

Target descriptions

No-Core Shell Model

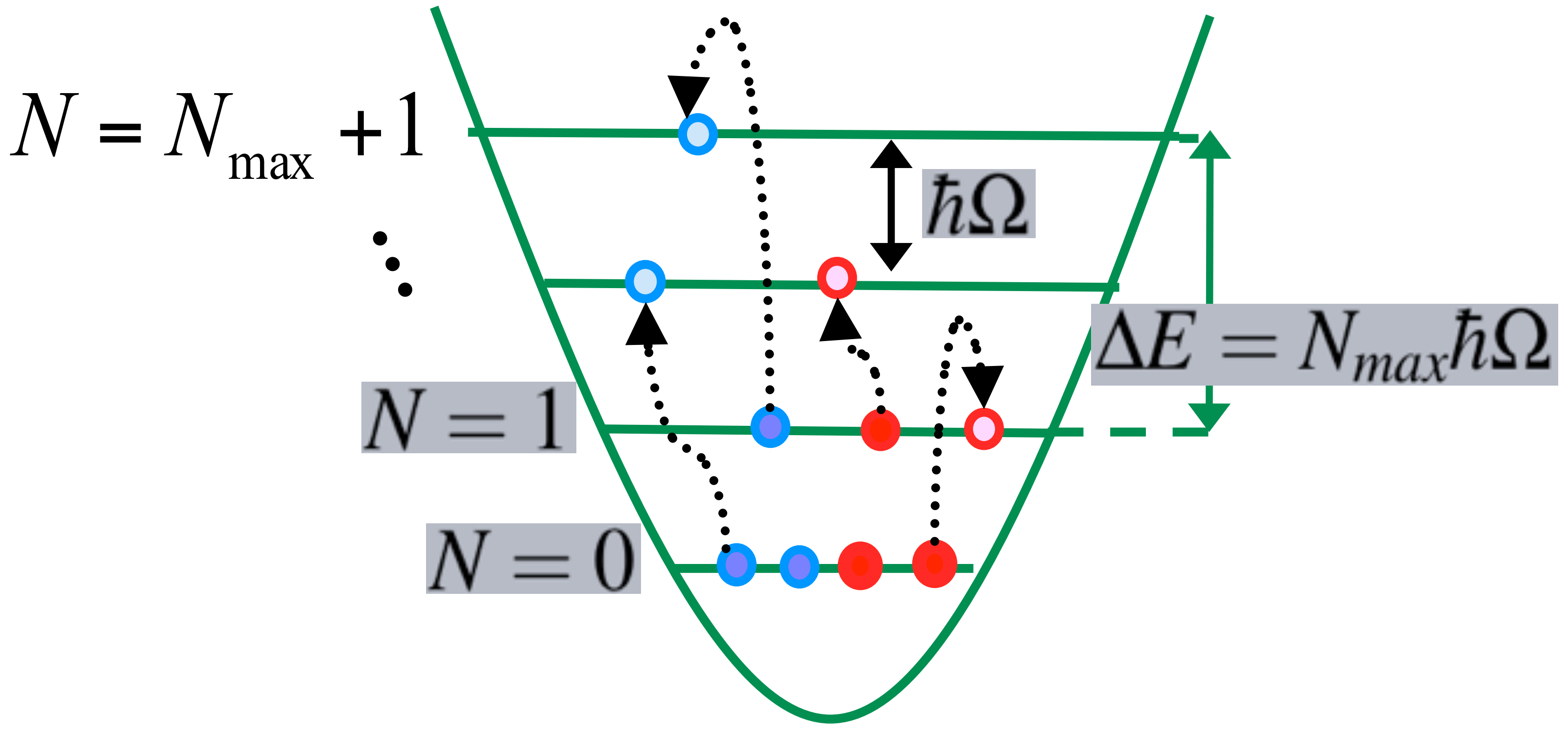

Harmonic oscillator basis

NCSM

in collaboration with P. Navratil and M. Gennari (TRIUMF)

Barrett et al., *Ab initio no core shell model*, PPNP **69** (2013) 131-181

- **NN-N⁴LO + 3NlnI (^{12}C, ^{16}O)**
  - **N⁴LO** Entem et al., Phys. Rev. C **96**, 024004 (2017)
  - **3NlnI** Navrátil, Few-Body Syst. **41**, 117 (2007)
  - **c_D & c_E** Kravvaris et al., Phys. Rev. C **102**, 024616 (2020)

- **NN-N³LO + 3NlnI (^{9,13}C, ^{6,7}Li, ^{10}B)**
  - **N³LO** E&M, Phys. Rev. C **68**, 041001(R) (2003)
  - **3NlnI** Navrátil, Few-Body Syst. **41**, 117 (2007)
  - **c_D & c_E** Somà et al., Phys. Rev. C **101**, 014318 (2020)

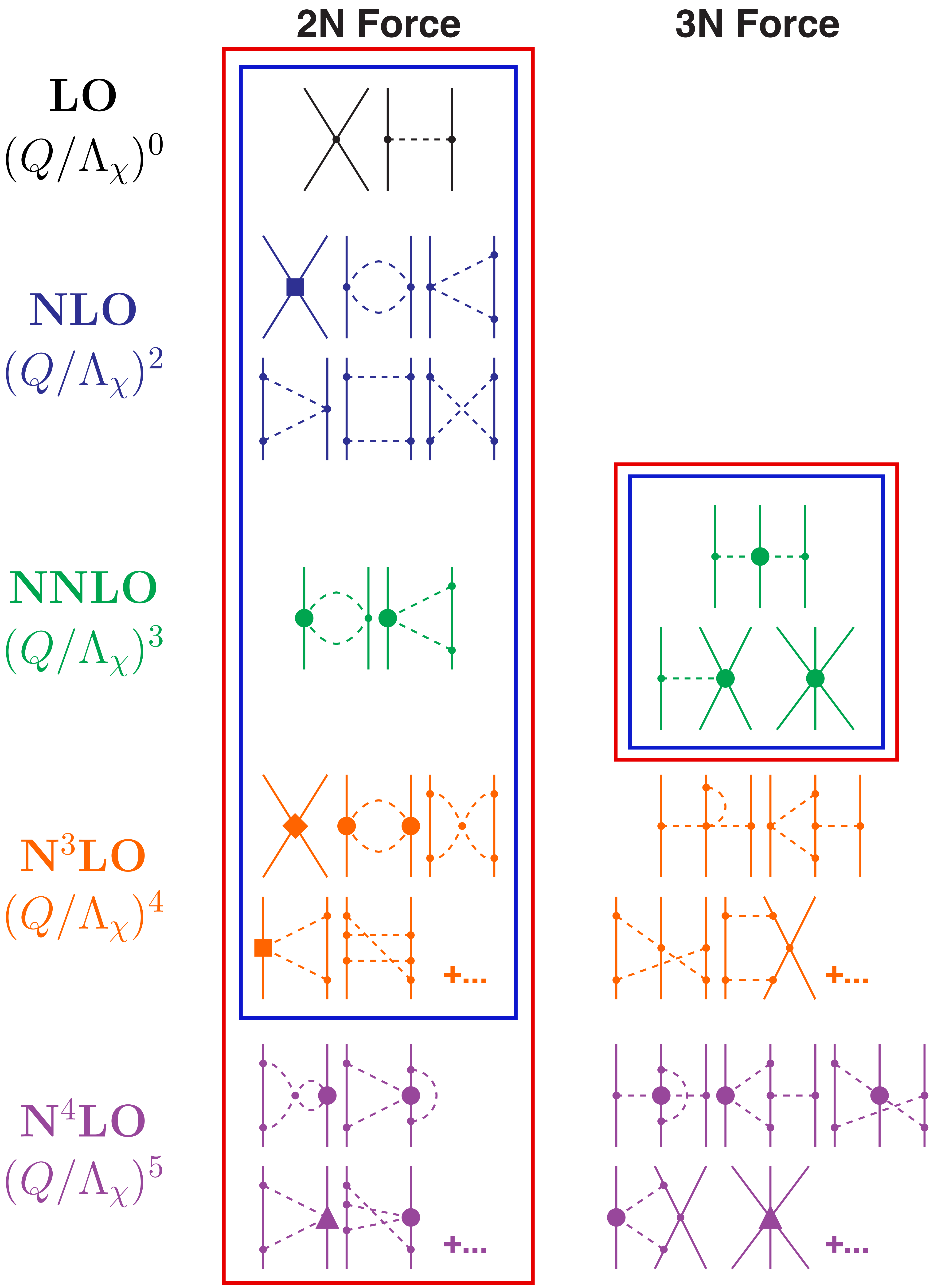

Target descriptions

No-Core Shell Model

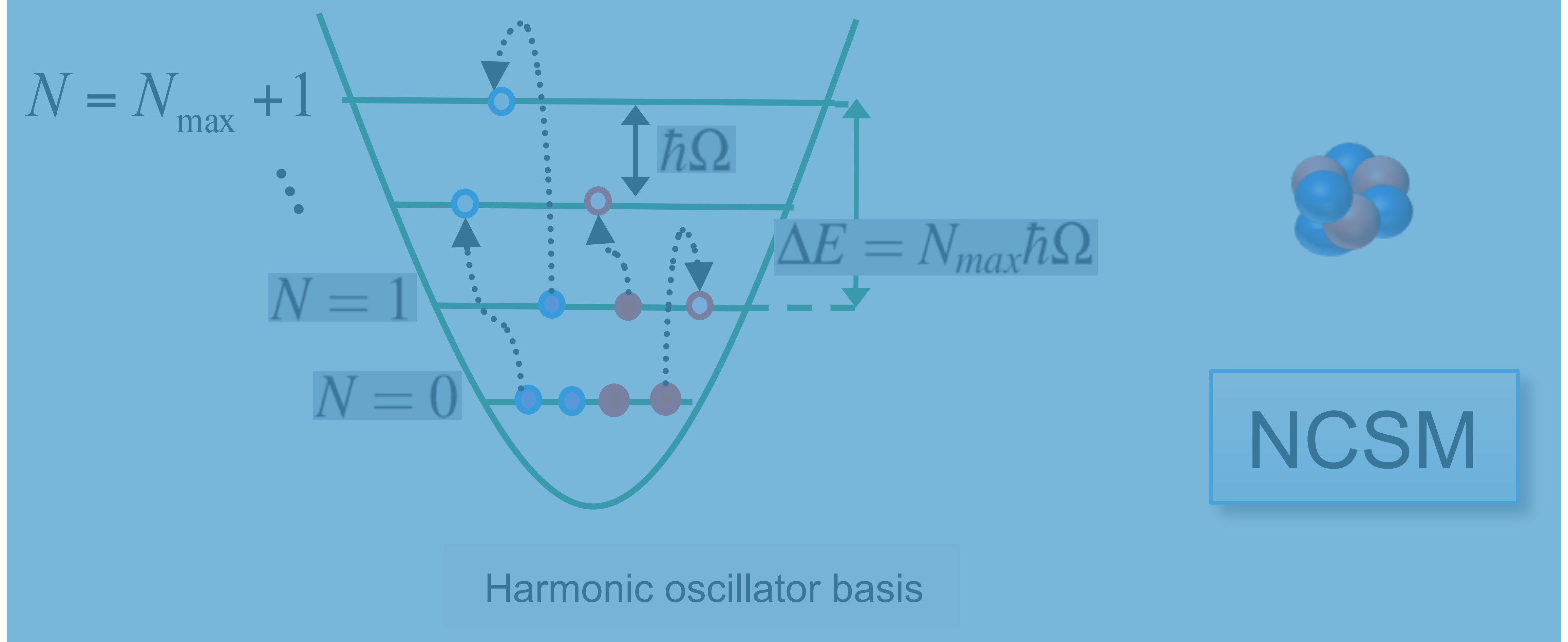

in collaboration with P. Navratil and M. Gennari (TRIUMF)

Barrett et al., *Ab initio no core shell model*, PPNP **69** (2013) 131-181

For heavier nuclei there are alternative approaches…

Self-consistent Green's functions

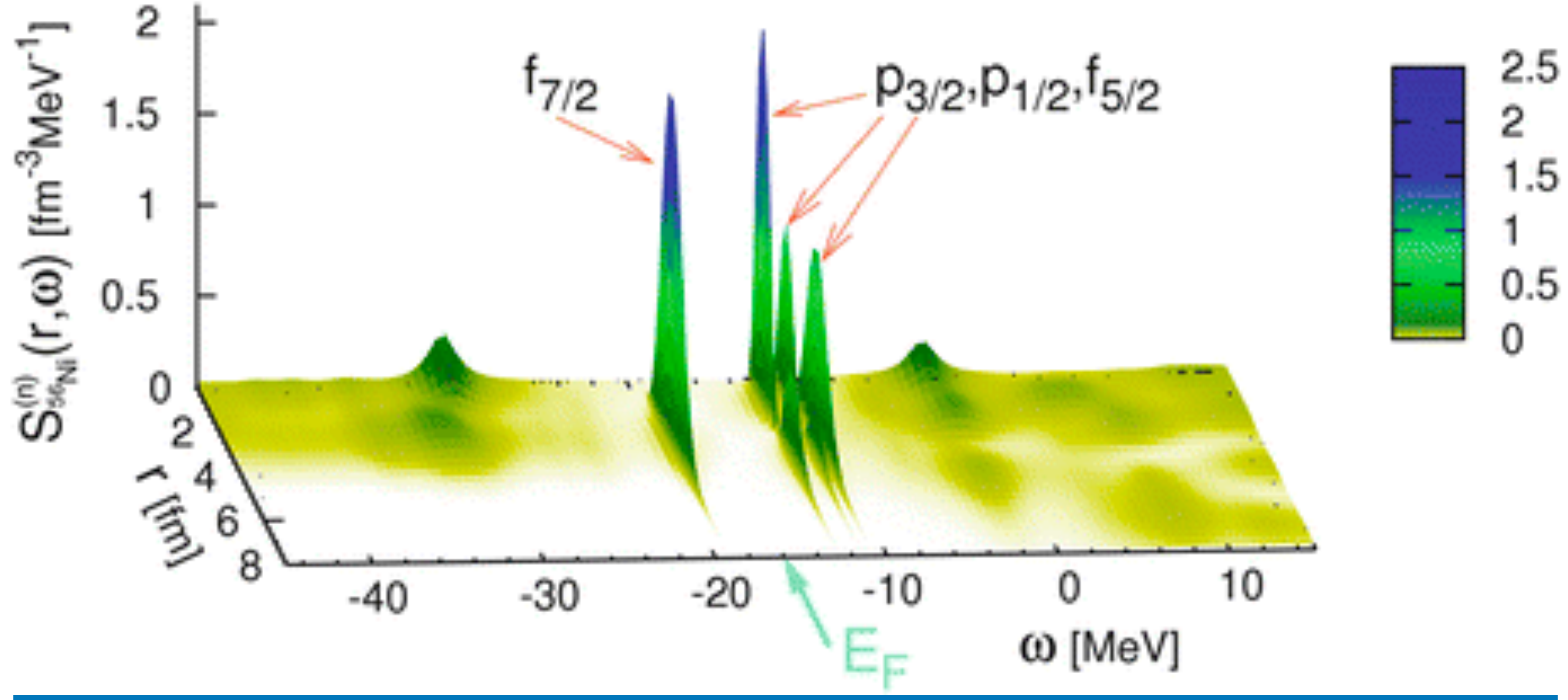

in collaboration with ***C. Barbieri*** *(Milano) and* ***V. Somà*** *(Paris)*

Somà, *SCGF Theory for Atomic Nuclei*, Frontiers **8** (2020) 340

Density functional theory

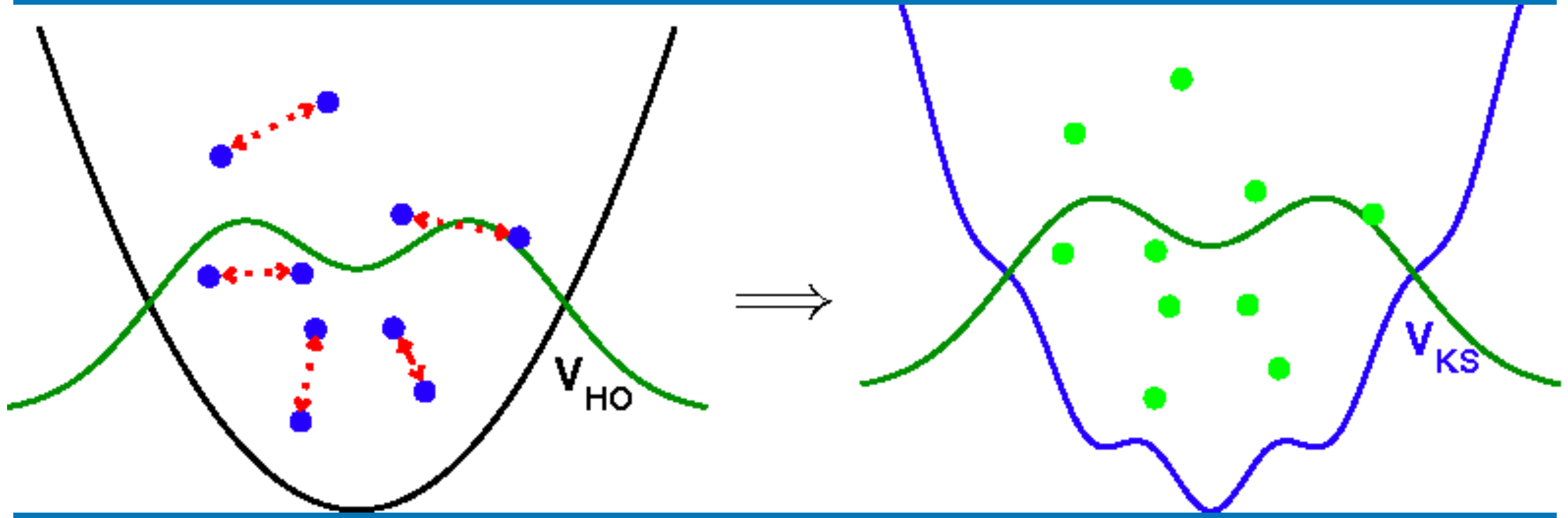

in collaboration with D. Vretenar and T. Niksic (Zagreb)

Theoretical predictions - closed shell nuclei

Theoretical optical potential derived from nucleon-nucleon chiral potentials

Matteo Vorabbi,[1] Paolo Finelli,[2] and Carlotta Giusti[1]

PHYSICAL REVIEW C **93**, 034619 (2016)

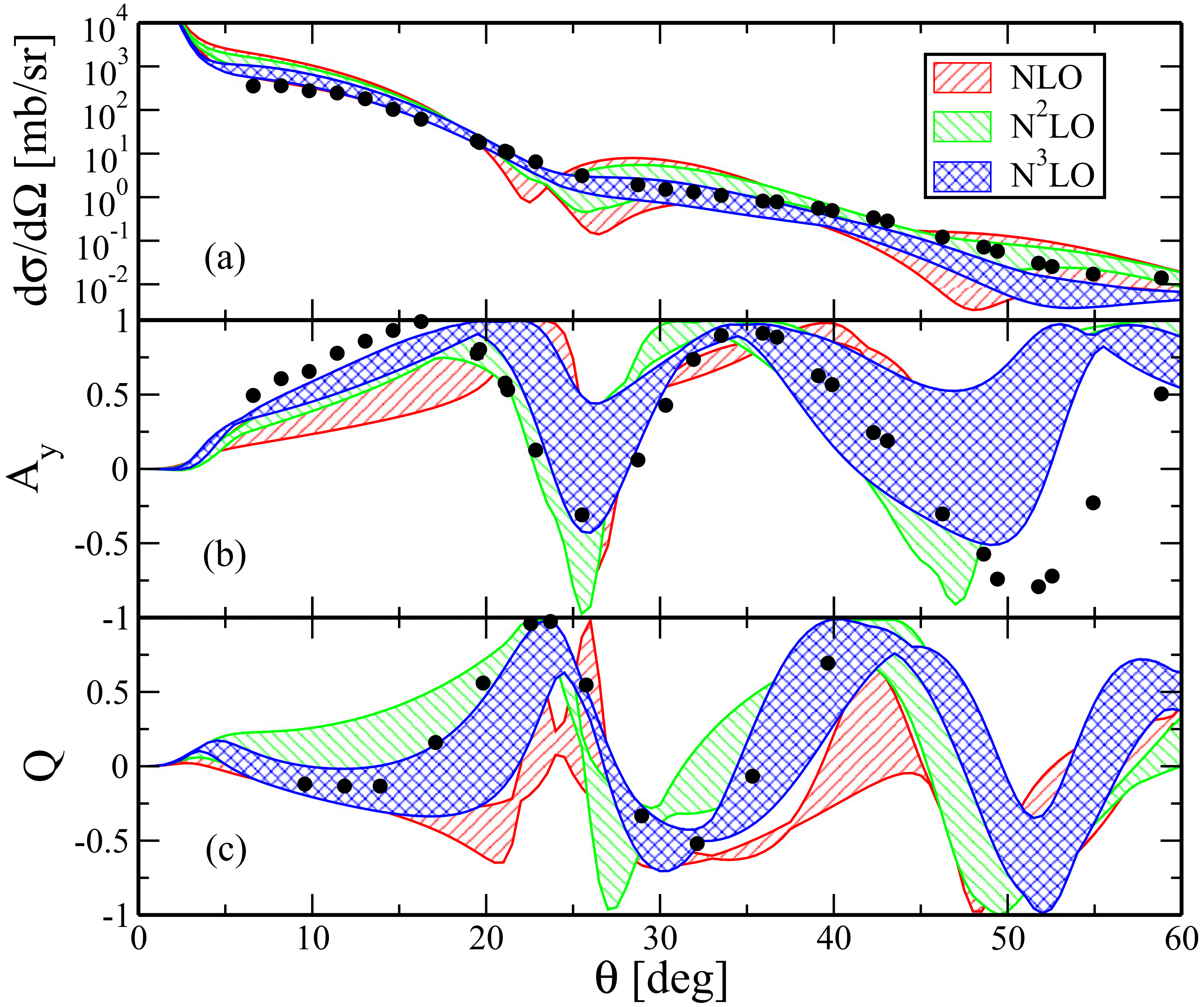

Scattering observables for ^{16}O computed at 200 MeV with the EGM potential at different orders: red bands are the NLO results, green and blue bands are respectively the N2LO and N3LO results.

^{16}O at 100 MeV

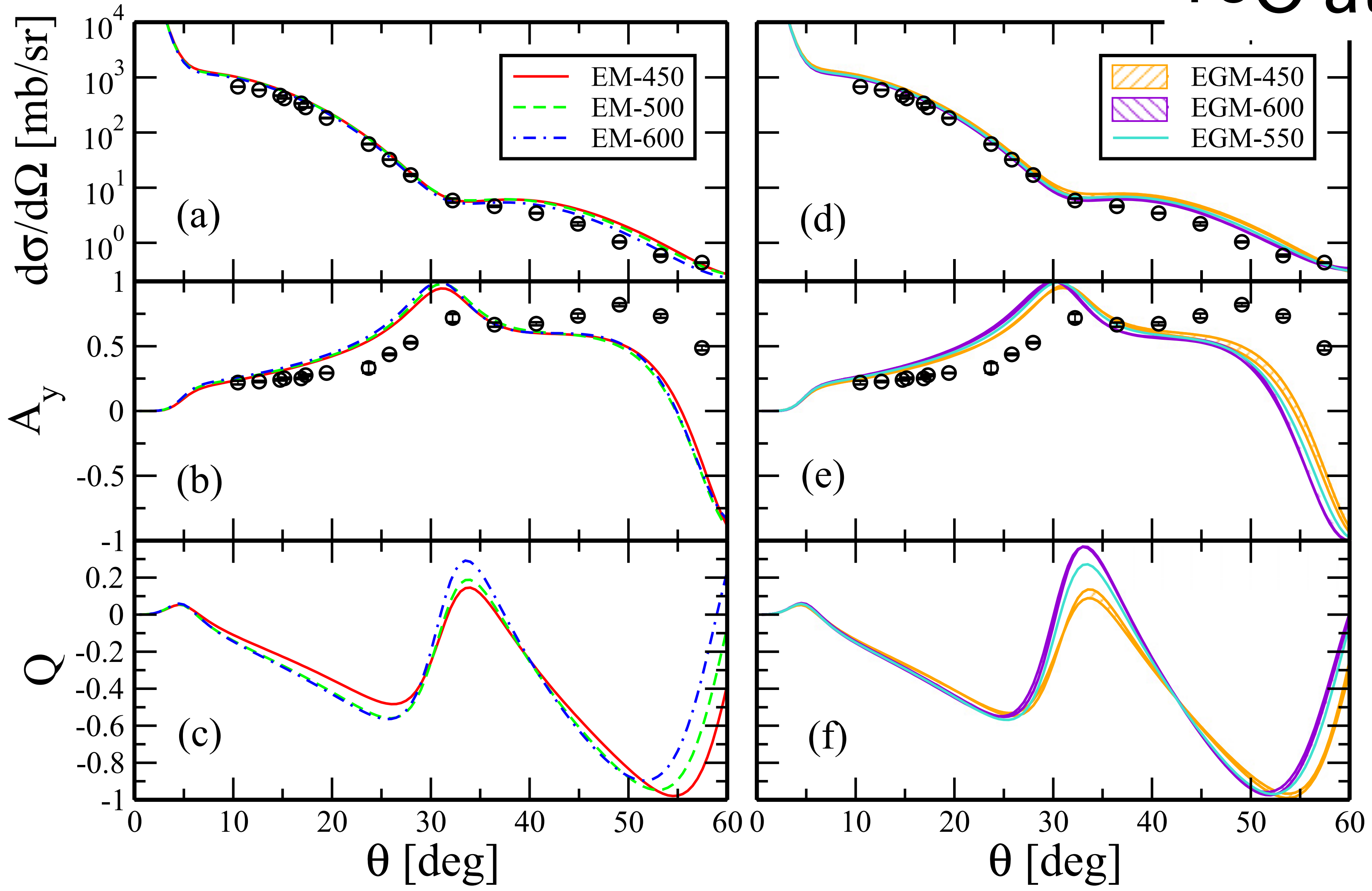

^{16}O at 200 MeV

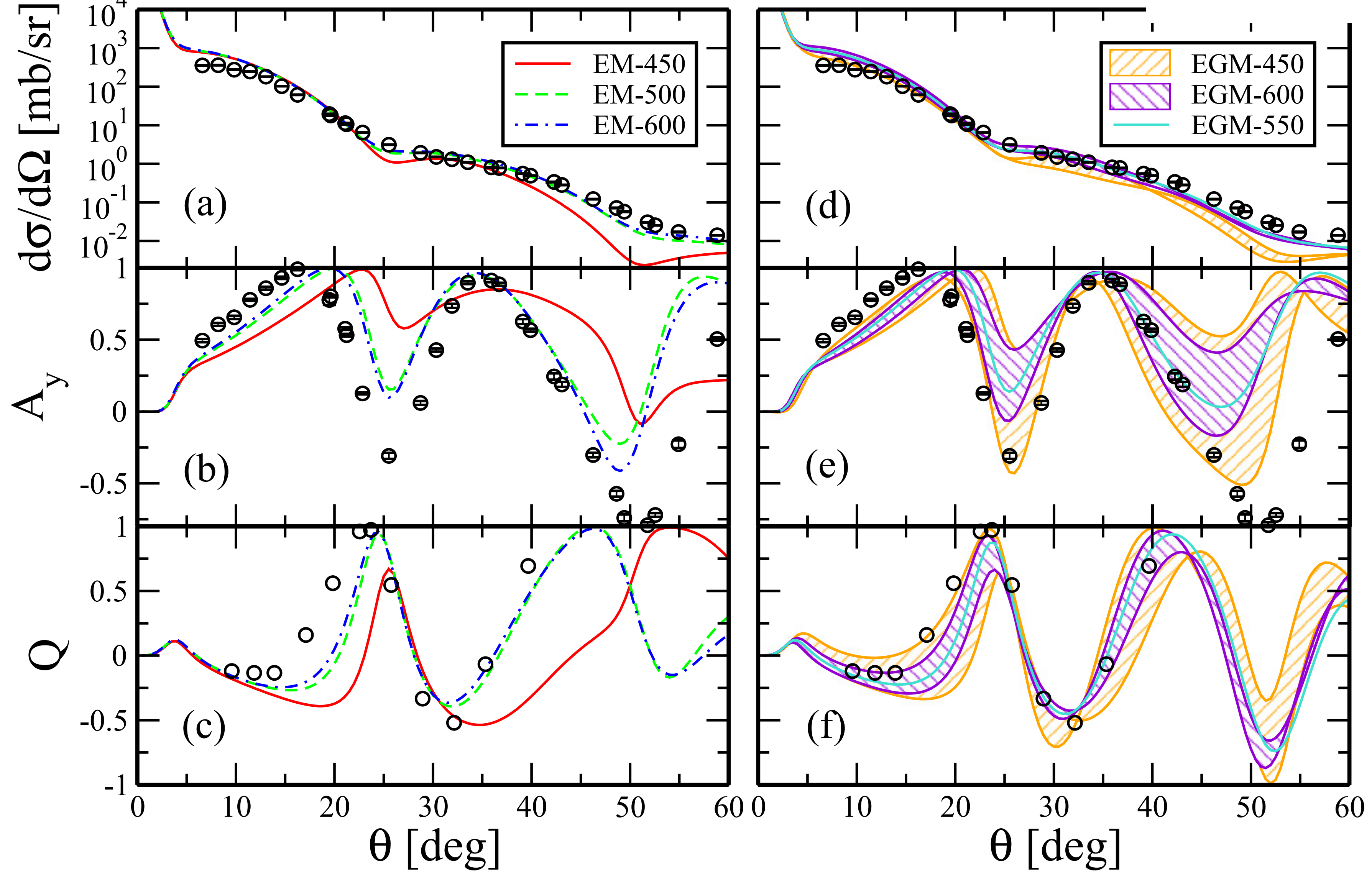

Theoretical predictions - convergence

Optical potentials derived from nucleon-nucleon chiral potentials at N^4LO

Matteo Vorabbi,[1] Paolo Finelli,[2] and Carlotta Giusti[3]

PHYSICAL REVIEW C **96**, 044001 (2017)

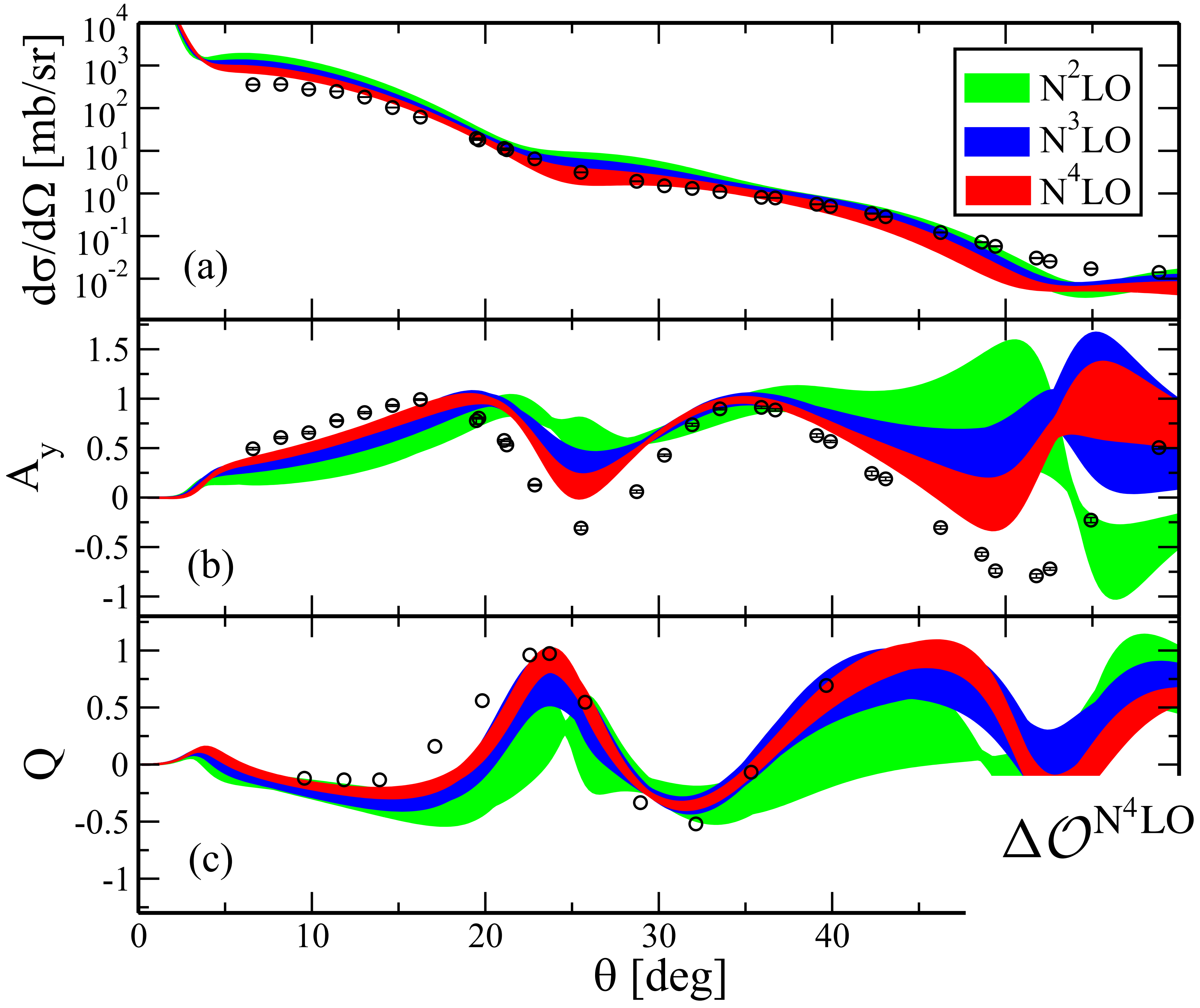

Scattering observables for ^{16}O computed at 200 MeV with the ***EKM*** *potential* at different orders: green bands are the **N2LO** results, and blue and red bands are the **N3LO** and **N4LO** results, respectively.

- The bands associated with the theoretical errors due to the truncation of the chiral expansion are small for the cross sections and larger for the polarization observables.
- The order-by-order convergence pattern is clear and we can conclude that <u>convergence has been reached</u> at N4LO and we do not expect large contributions from the higher-order extensions in the NN sector.

$$\begin{aligned}\Delta\mathcal{O}^{\mathrm{N^4LO}}(p) = \max\big(&Q^6 \times |\mathcal{O}^{\mathrm{LO}}(p)|,\\ &\times Q^4 \times |\mathcal{O}^{\mathrm{LO}}(p) - \mathcal{O}^{\mathrm{NLO}}(p)|,\\ &\times Q^3|\mathcal{O}^{\mathrm{NLO}}(p) - \mathcal{O}^{\mathrm{N^2LO}}(p)|,\\ &\times Q^2 \times |\mathcal{O}^{\mathrm{N^2LO}}(p) - \mathcal{O}^{\mathrm{N^3LO}}(p)|,\\ &\times Q|\mathcal{O}^{\mathrm{N^3LO}}(p) - \mathcal{O}^{\mathrm{N^4LO}}(p)|\big),\end{aligned}$$

$$Q = \max\left(\frac{p}{\Lambda_b}, \frac{M_\pi}{\Lambda_b}\right)$$

^{16}O at 200 MeV

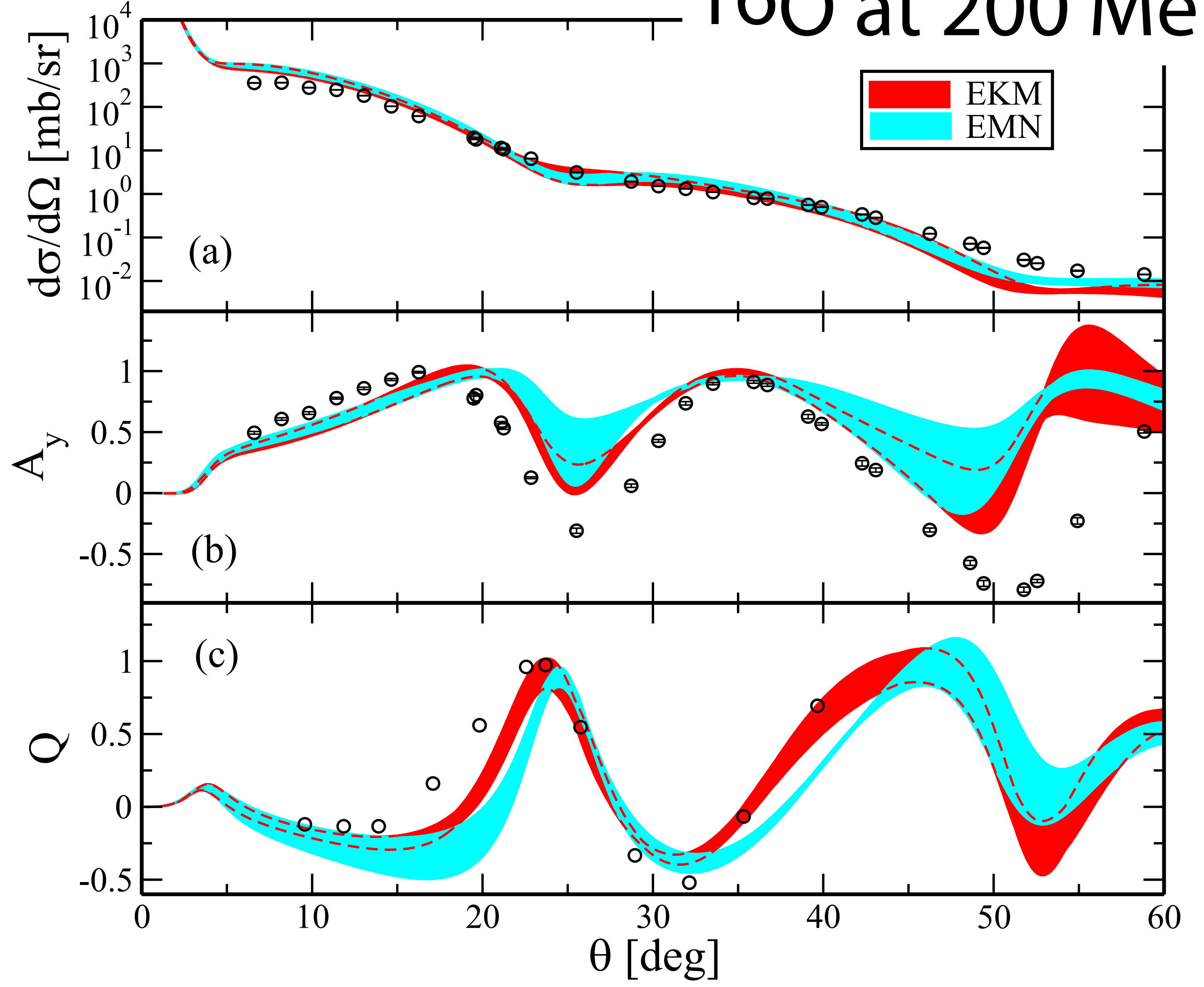

^{40}Ca at 200 MeV

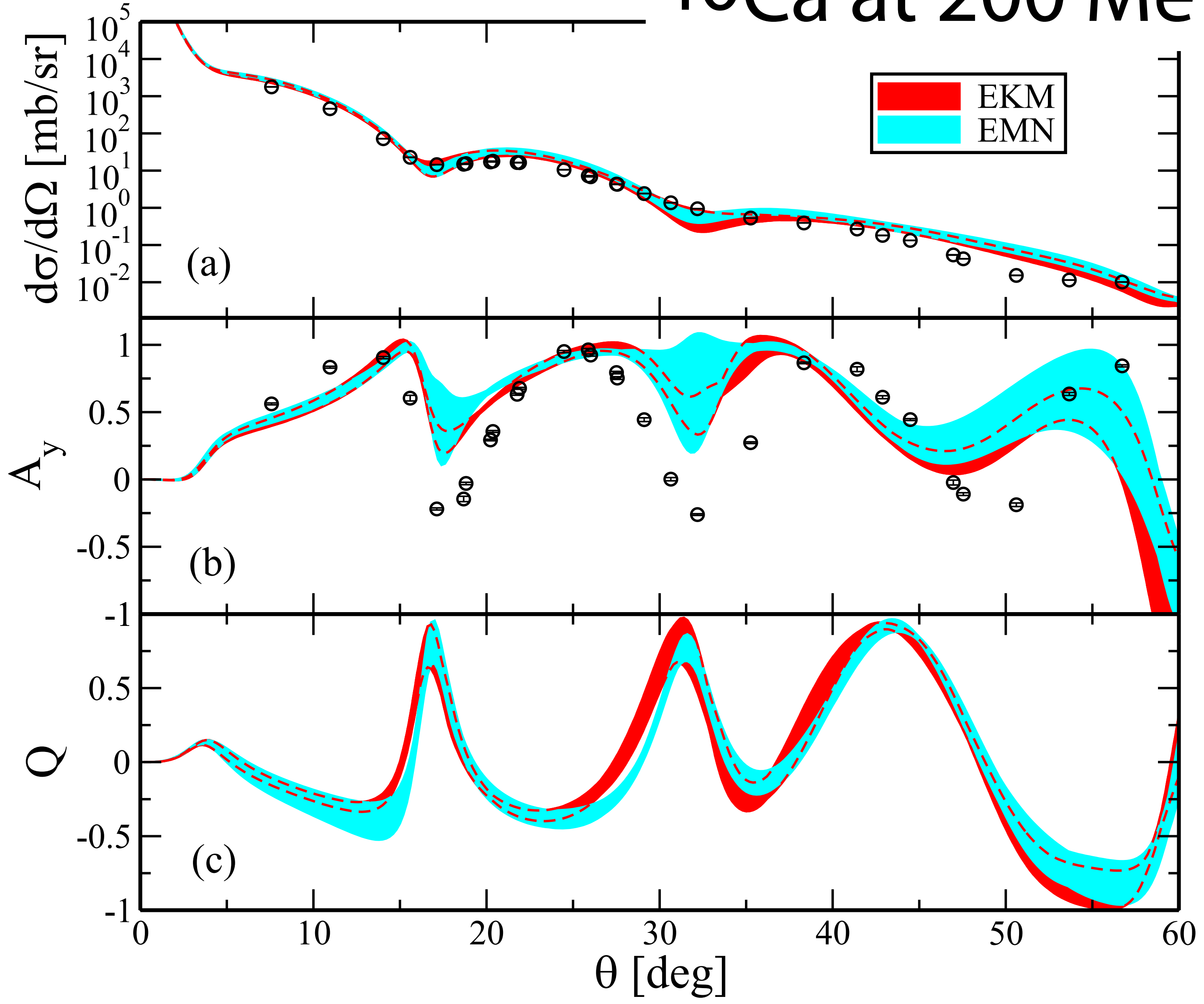

Theoretical predictions vs. Phenomenology

Proton-nucleus elastic scattering: Comparison between phenomenological and microscopic optical potentials

Matteo Vorabbi,[1] Paolo Finelli,[2] and Carlotta Giusti[3]

PHYSICAL REVIEW C **98**, 064602 (2018)

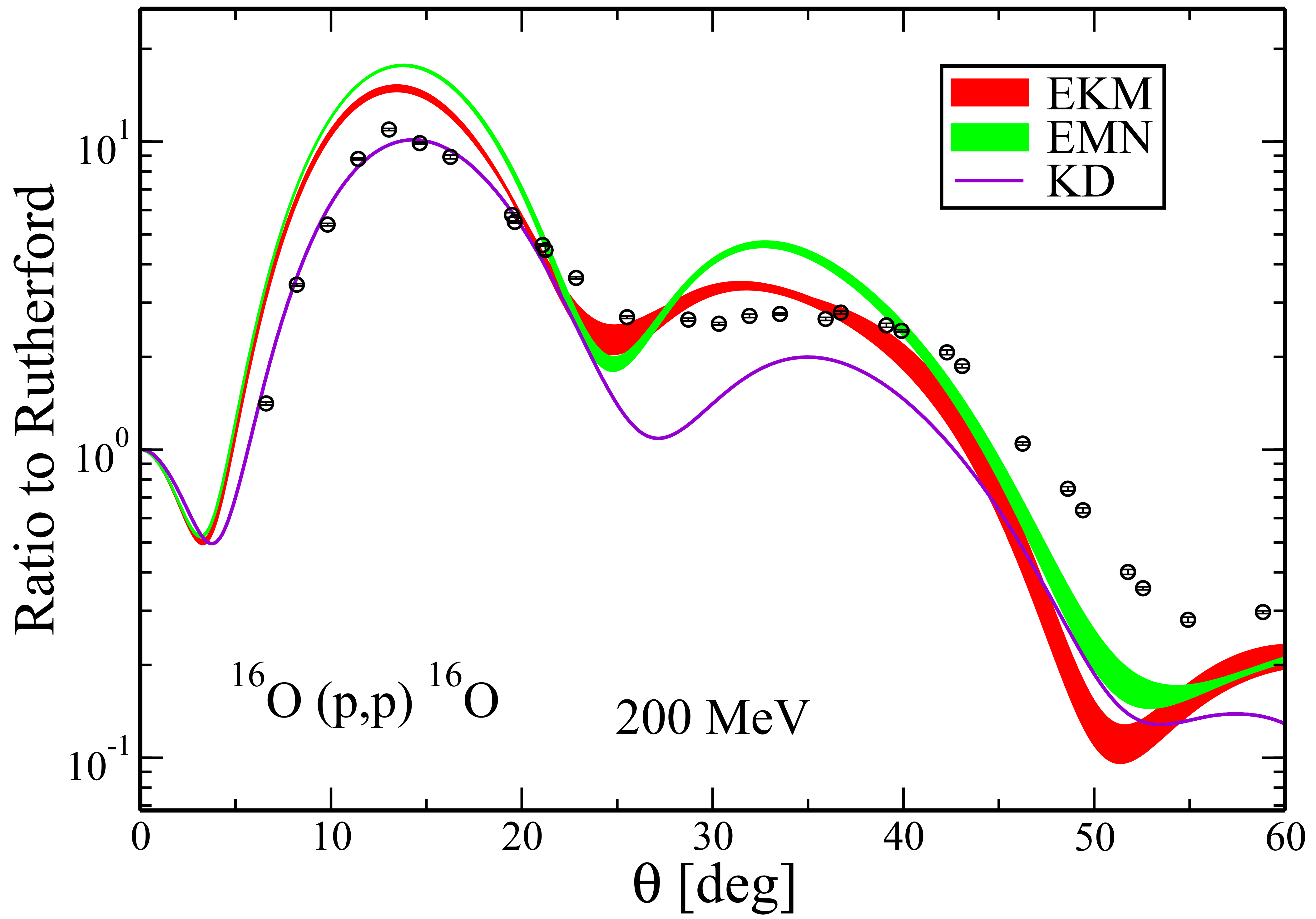

Calculations are performed at *E = 200 MeV* in comparison with the phenomenological global OP of Koning-Delaroche (TALYS code)

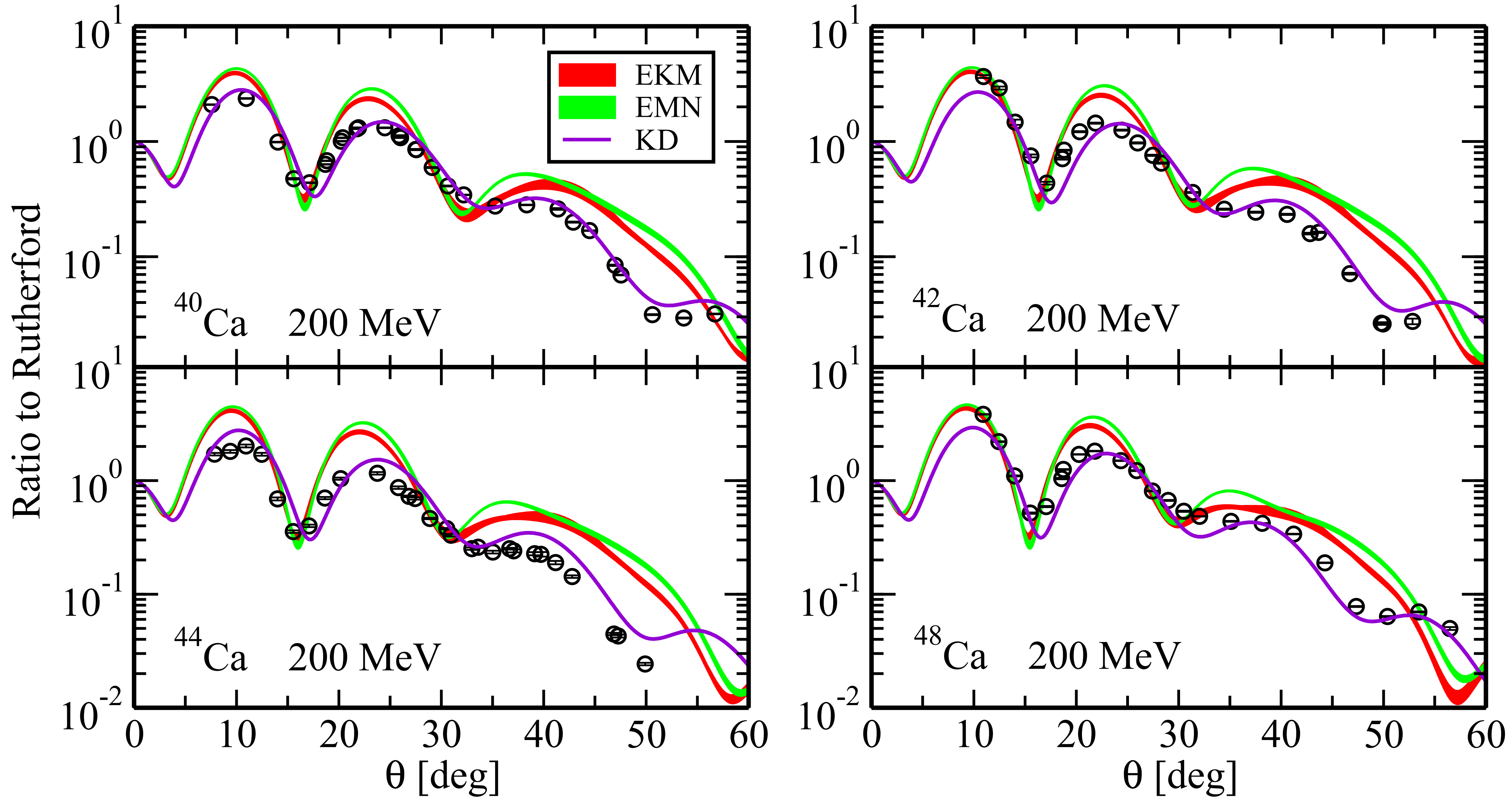

The agreement of our present results with empirical data is sometimes worse and sometimes better but overall comparable to the agreement given by the phenomenological OP, in particular for energies close to 200 MeV and above 200 MeV.

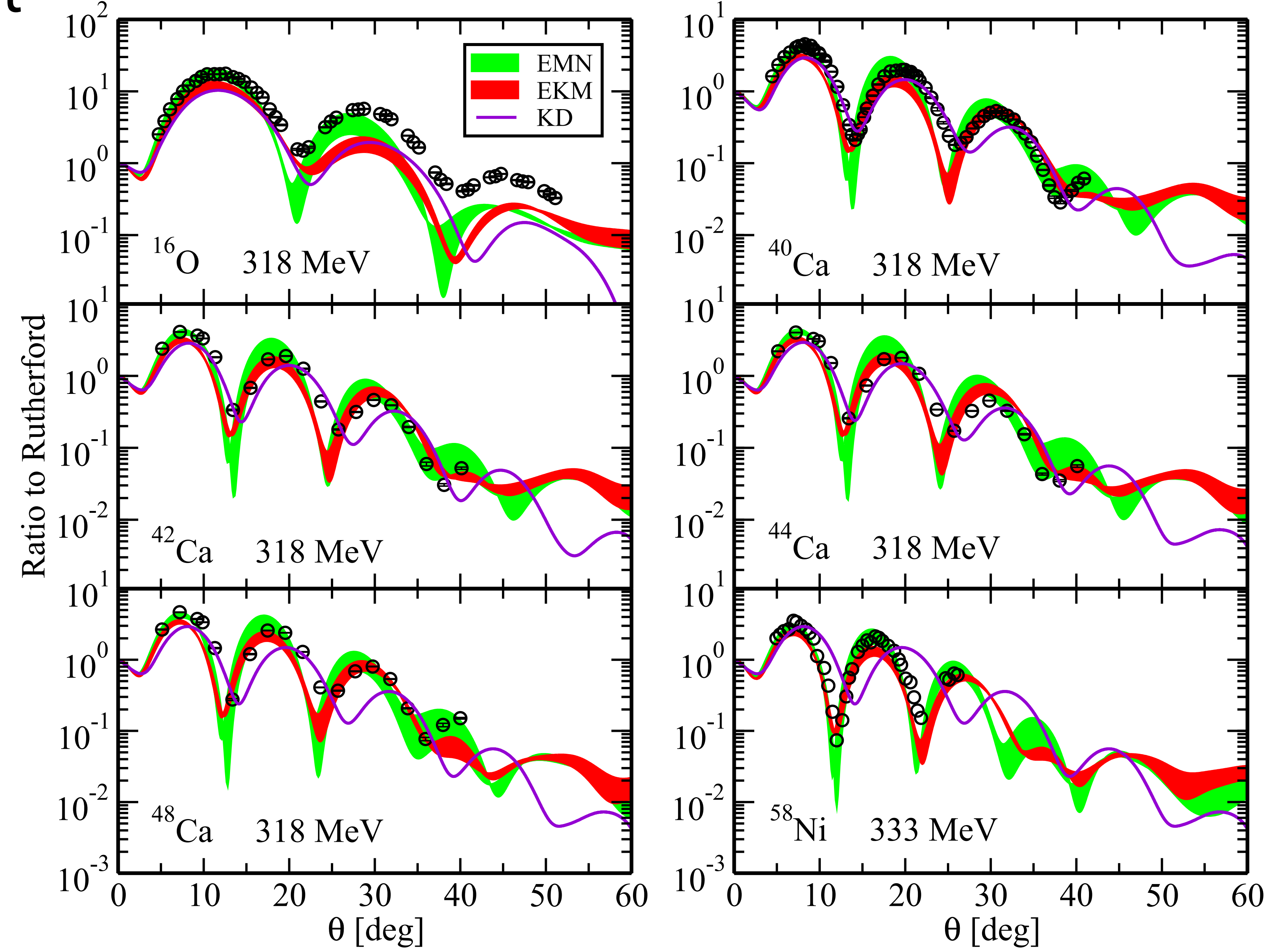

Theoretical predictions vs. Phenomenology

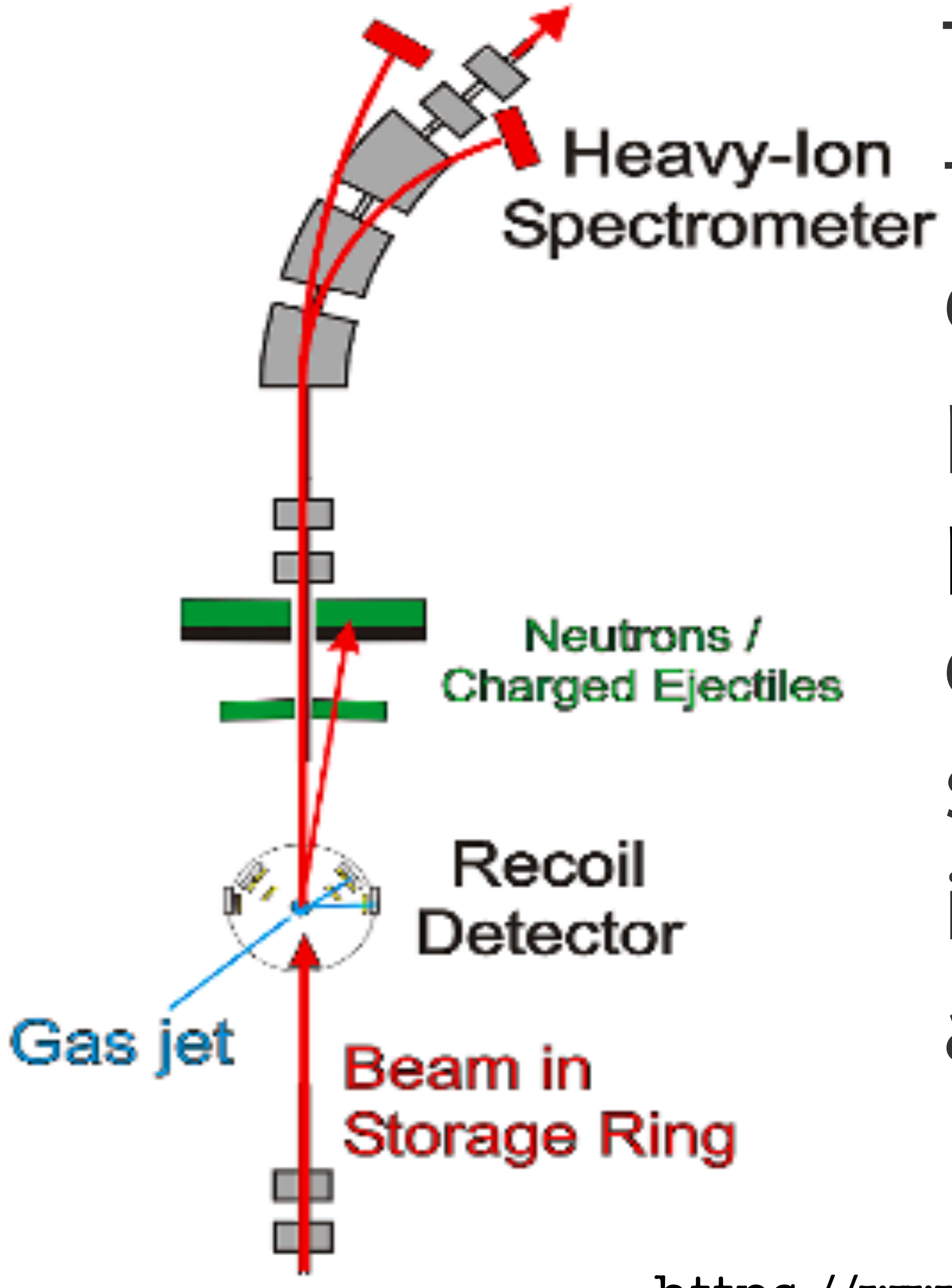

The experimental setup dedicated to studies of exotic nuclei with electromagnetic and ligh hadronic probes (EXL) is part of the FAIR project. The aim of the EXL experiment is to study the structure of unstable exotic nuclei in light-ion scattering experiments at intermediate energies.

https://www.rug.nl/kvi-cart/research/hnp/research/exl/

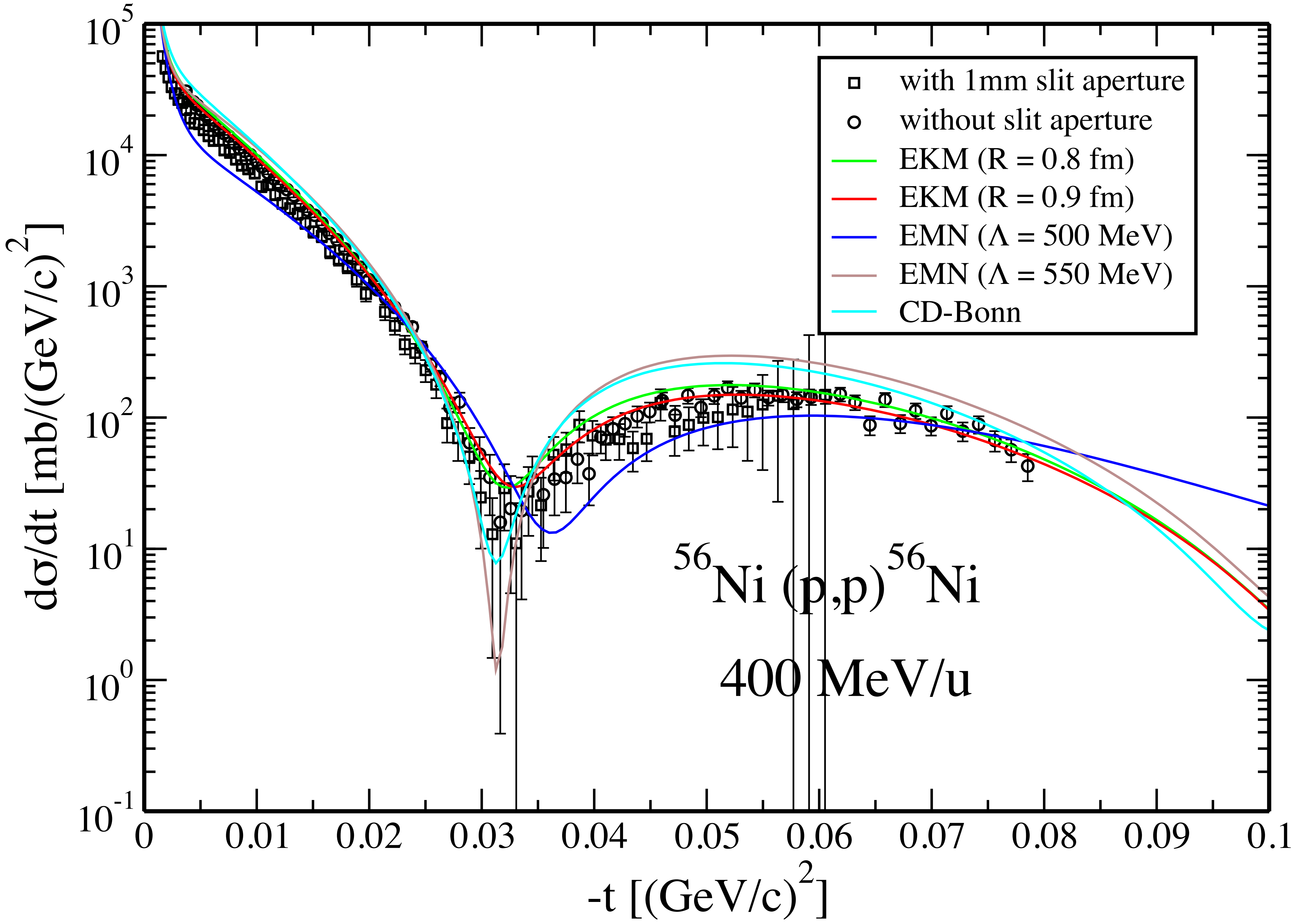

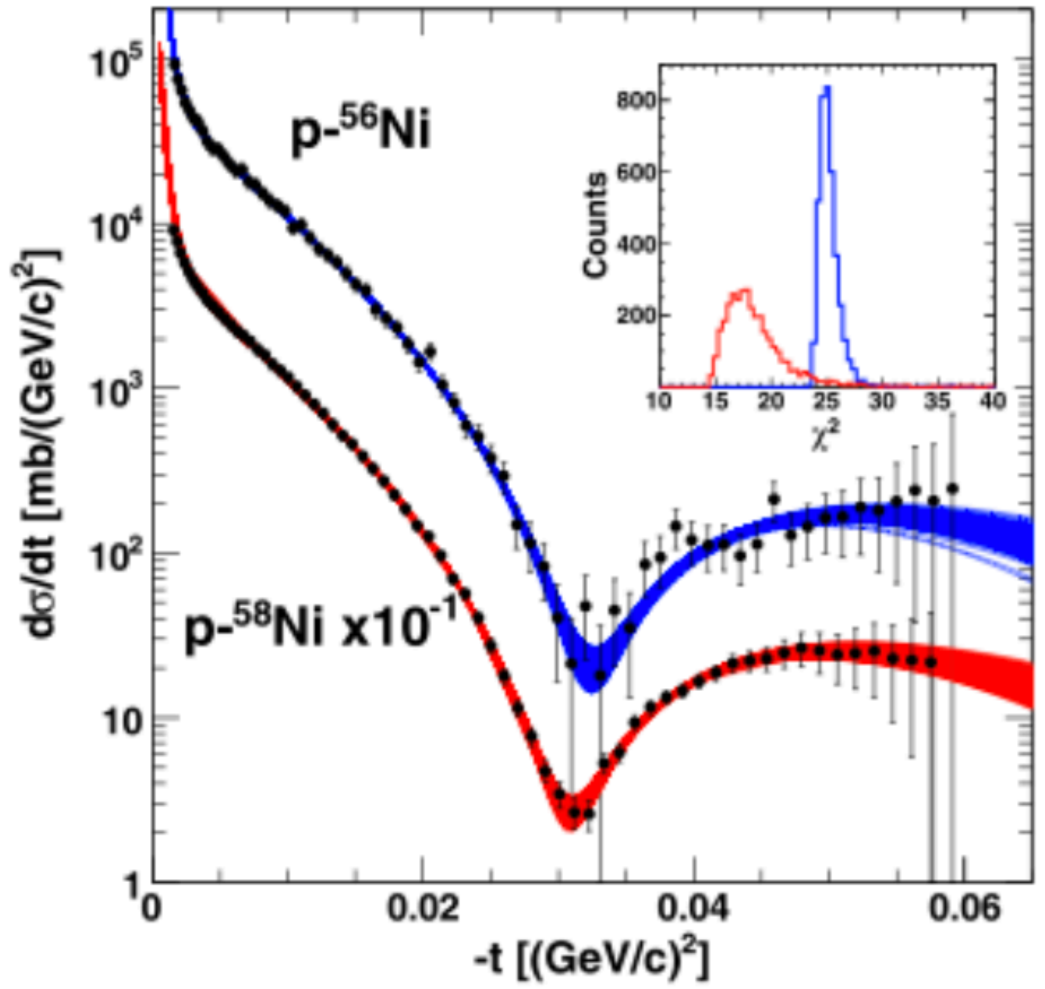

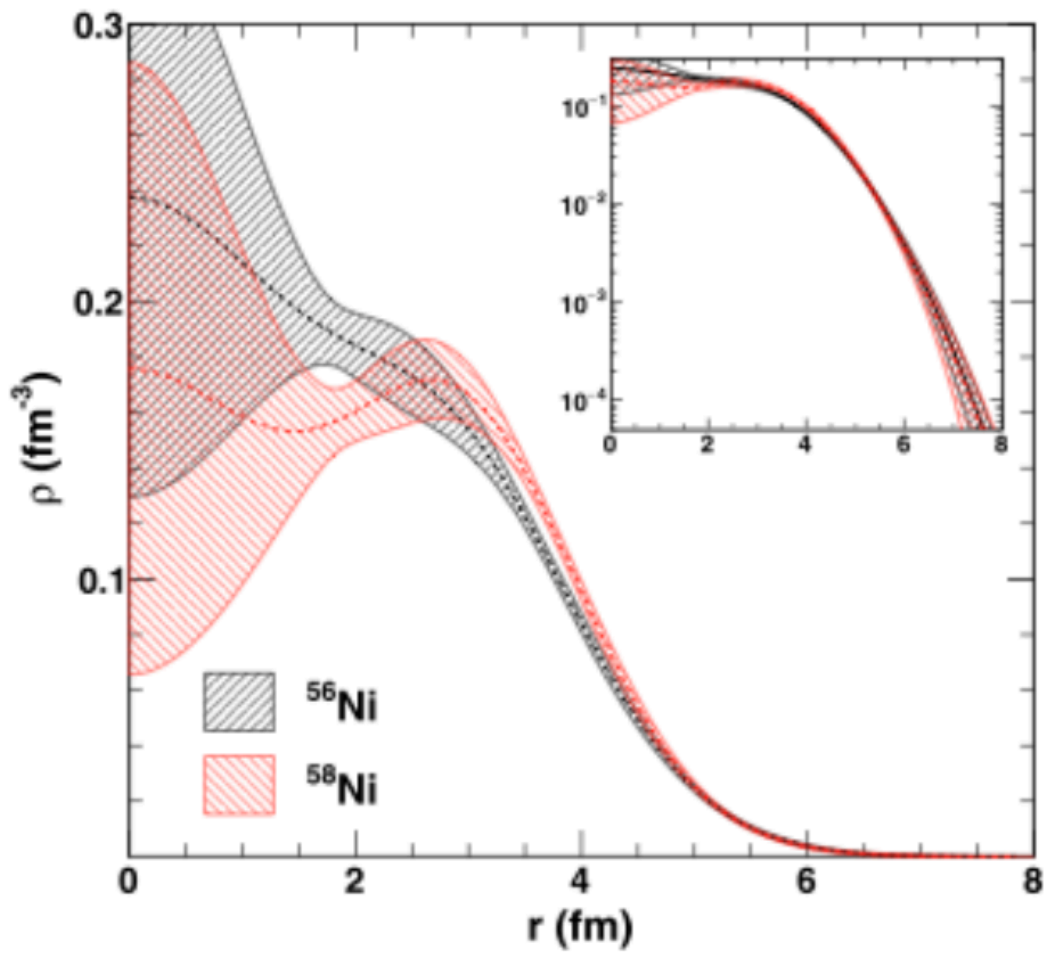

PLB 809 (2020) 135776

The example shown at 400 MeV suggests that, at this energy, the EKM potentials have not yet reached the limit after which the chiral expansion scheme breaks down.

Theoretical predictions - inclusion of 3body forces

Impact of three-body forces on elastic nucleon-nucleus scattering observables

Matteo Vorabbi[1], Michael Gennari,[2,3] Paolo Finelli[4], Carlotta Giusti[5], Petr Navrátil[3] and Ruprecht Machleidt[6]

PHYSICAL REVIEW C **103**, 024604 (2021)

3 body ➜ 2 body density dependent
Holt et al., [PRC **81** (2010) 024002]

$$U = (V_{NN} + V_{3N}) + (V_{NN} + \boxed{V_{3N}})G_0(E)QU$$

Treatment of the 3N force

$$\boxed{V_{3N}} = \frac{1}{2}\sum_{i=1}^{A}\sum_{\substack{j=1\\ j\neq i}}^{A} w_{0ij} \approx \sum_{i=1}^{A}\langle w_{0i}\rangle$$

Density dependent

Modification of the *t* matrix

$$t_{0i} = v_{0i}^{(1)} + v_{0i}^{(2)} g_{0i}\, t_{0i}$$

$$v_{0i}^{(1)} = v_{0i} + \frac{1}{2}\langle w_{0i}\rangle$$

$$v_{0i}^{(2)} = v_{0i} + \langle w_{0i}\rangle$$

In-medium NN interaction generated by the two-pion exchange component (**c_1,c_3,c_4**) of the chiral three-nucleon interaction.

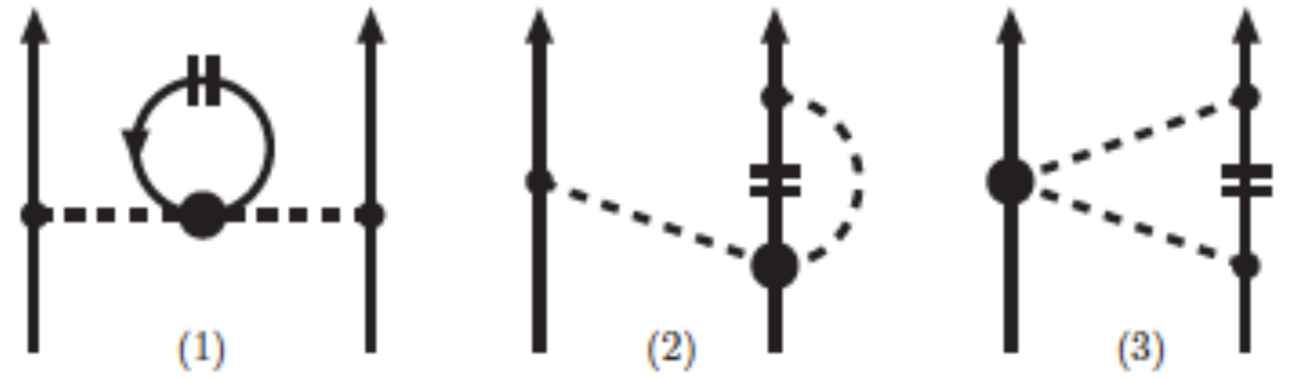

In-medium NN interaction generated by the one-pion exchange (**c_D**) and short-range component (**c_E**) of the chiral three-nucleon interaction.

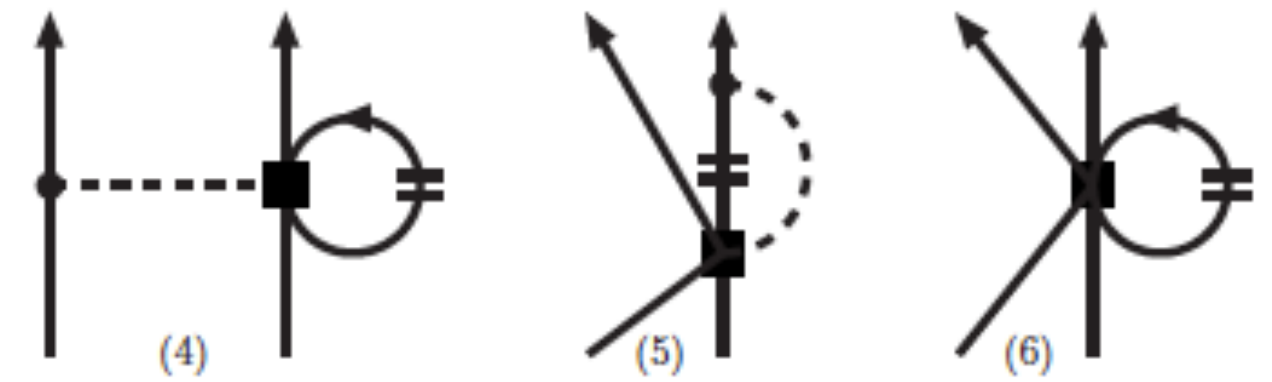

in-medium nucleon propagator

Theoretical predictions - inclusion of 3body forces

Impact of three-body forces on elastic nucleon-nucleus scattering observables

Matteo Vorabbi,[1] Michael Gennari,[2,3] Paolo Finelli,[4] Carlotta Giusti,[5] Petr Navrátil,[3] and Ruprecht Machleidt[6]

PHYSICAL REVIEW C **103**, 024604 (2021)

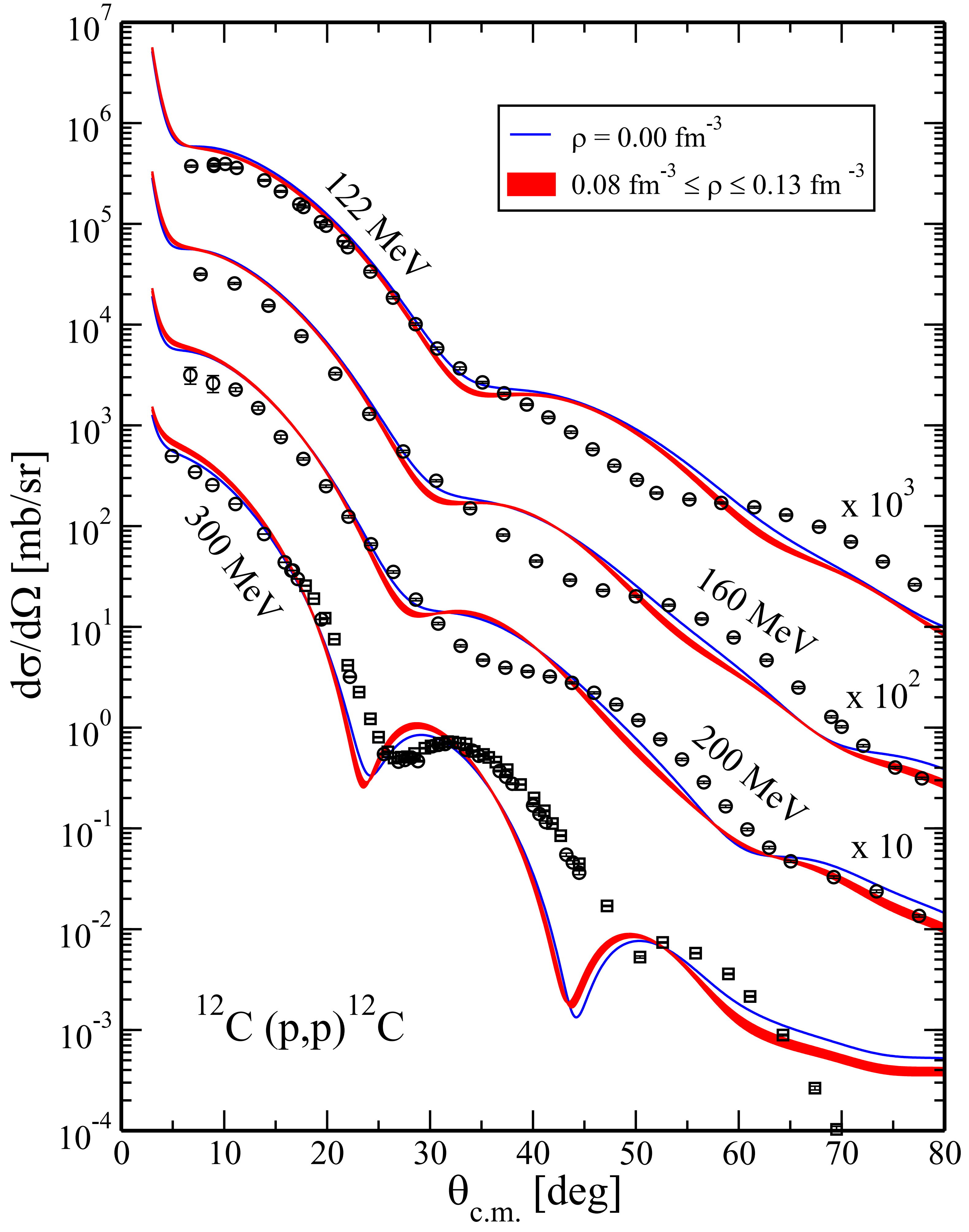

3 body ➜ 2 body density dependent
Holt et al., [PRC **81** (2010) 024002]

In-medium NN interaction generated by the two-pion exchange component (c_1,c_3,c_4) of the chiral three-nucleon interaction.

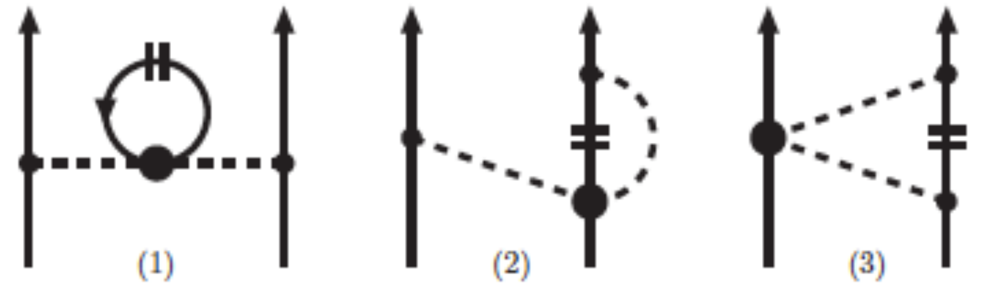

In-medium NN interaction generated by the one-pion exchange (c_D) and short-range component (c_E) of the chiral three-nucleon interaction.

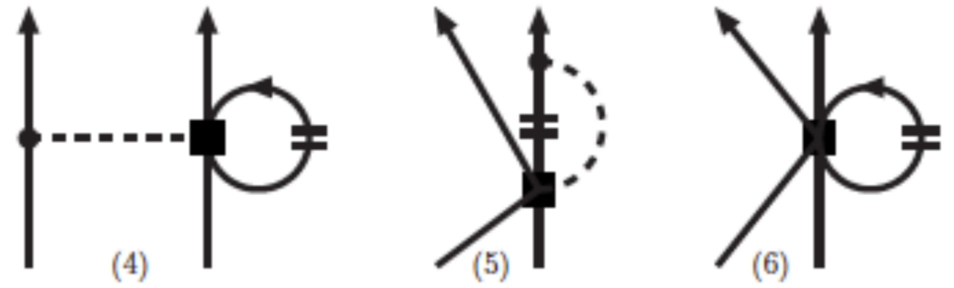

in-medium nucleon propagator

- We performed calculations for the *t* matrix varying the density parameter within reasonable values

$$0.08 \text{ fm}^{-3} \leqslant \rho \leqslant 0.13 \text{ fm}^{-3}$$

- The target density is computed with the NN and the full 3N interaction

- For all nuclei we found very small contributions to the differential cross section

- The contributions to the spin observables are larger and they seem to improve the agreement with the data

Theoretical predictions - inclusion of 3body forces

Impact of three-body forces on elastic nucleon-nucleus scattering observables

Matteo Vorabbi[1], Michael Gennari[2,3] Paolo Finelli[4], Carlotta Giusti[5], Petr Navrátil[3] and Ruprecht Machleidt[6]

PHYSICAL REVIEW C **103**, 024604 (2021)

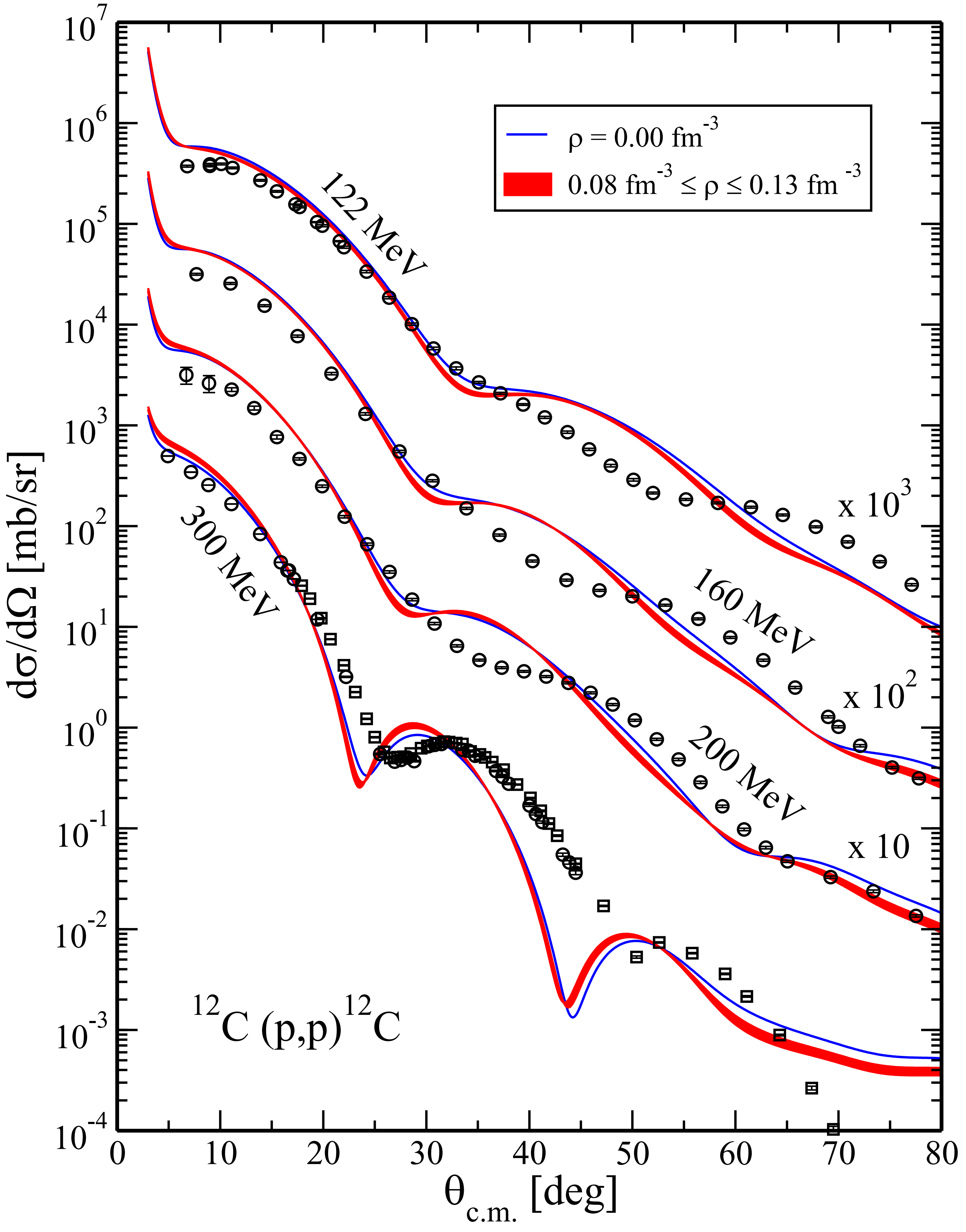

3 body ➜ 2 body density dependent
Holt et al., [PRC **81** (2010) 024002]

In-medium NN interaction generated by the two-pion exchange component (**c_1,c_3,c_4**) of the chiral three-nucleon interaction.

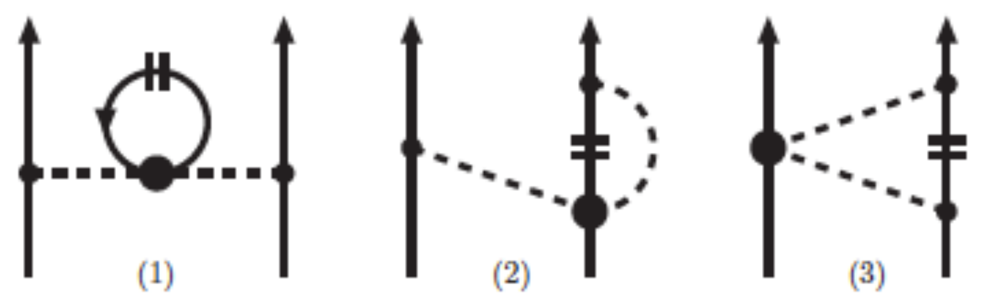

In-medium NN interaction generated by the one-pion exchange (**c_D**) and short-range component (**c_E**) of the chiral three-nucleon interaction.

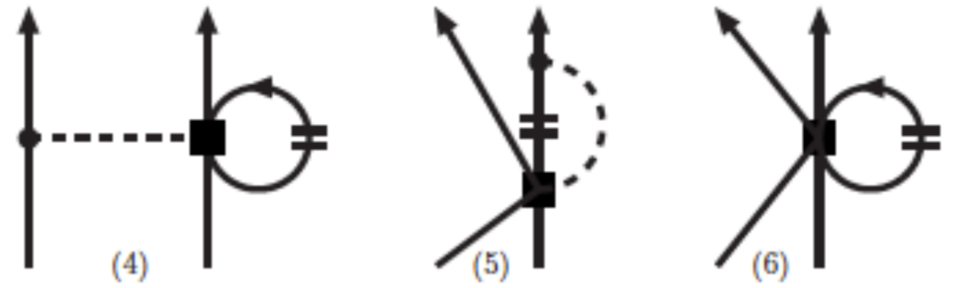

in-medium nucleon propagator

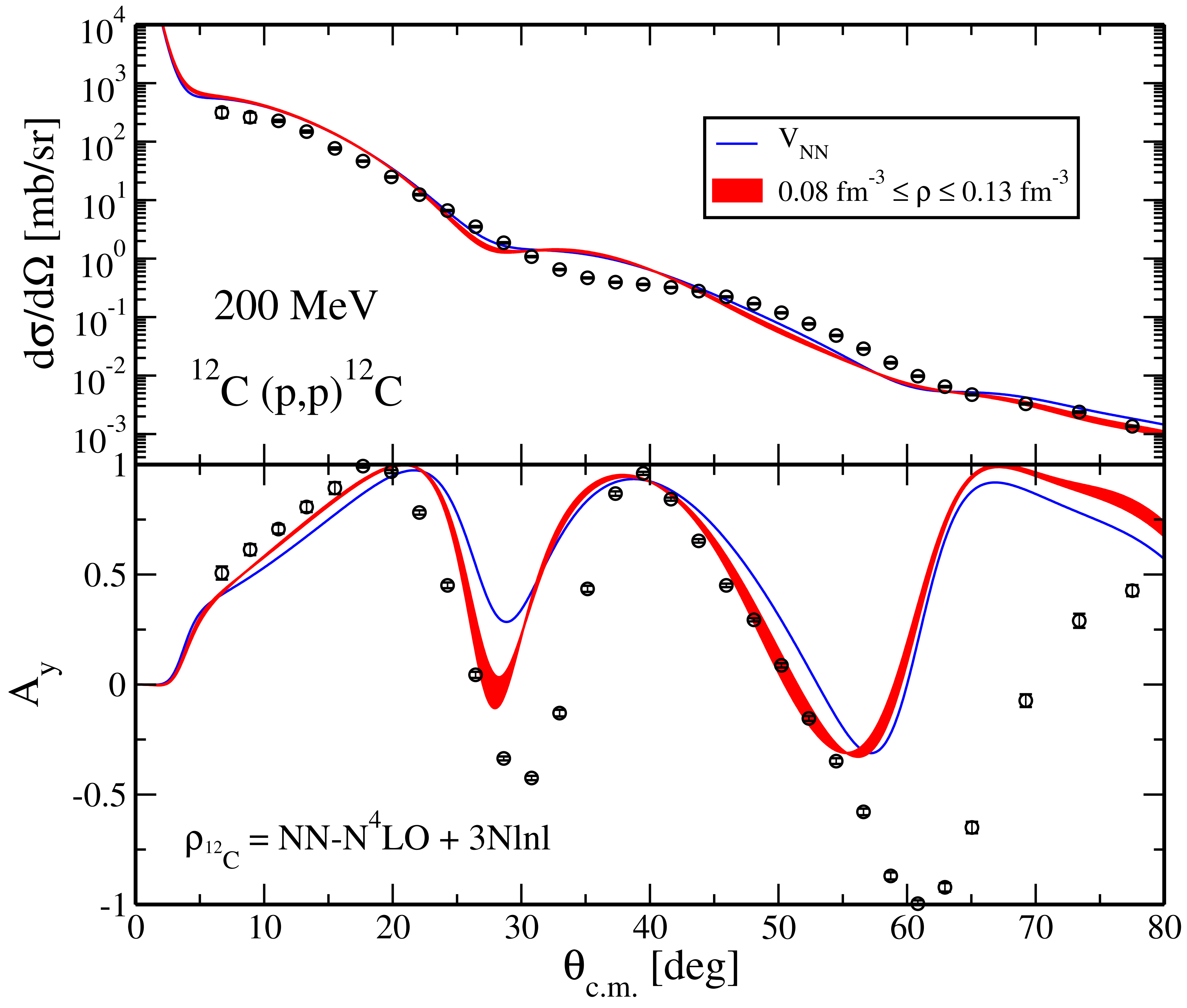

- The contributions to the spin observables are larger and they seem to improve the agreement with the data

Theoretical predictions - inclusion of 3body forces

Impact of three-body forces on elastic nucleon-nucleus scattering observables

Matteo Vorabbi,[1] Michael Gennari,[2,3] Paolo Finelli,[4] Carlotta Giusti,[5] Petr Navrátil,[3] and Ruprecht Machleidt[6]

PHYSICAL REVIEW C **103**, 024604 (2021)

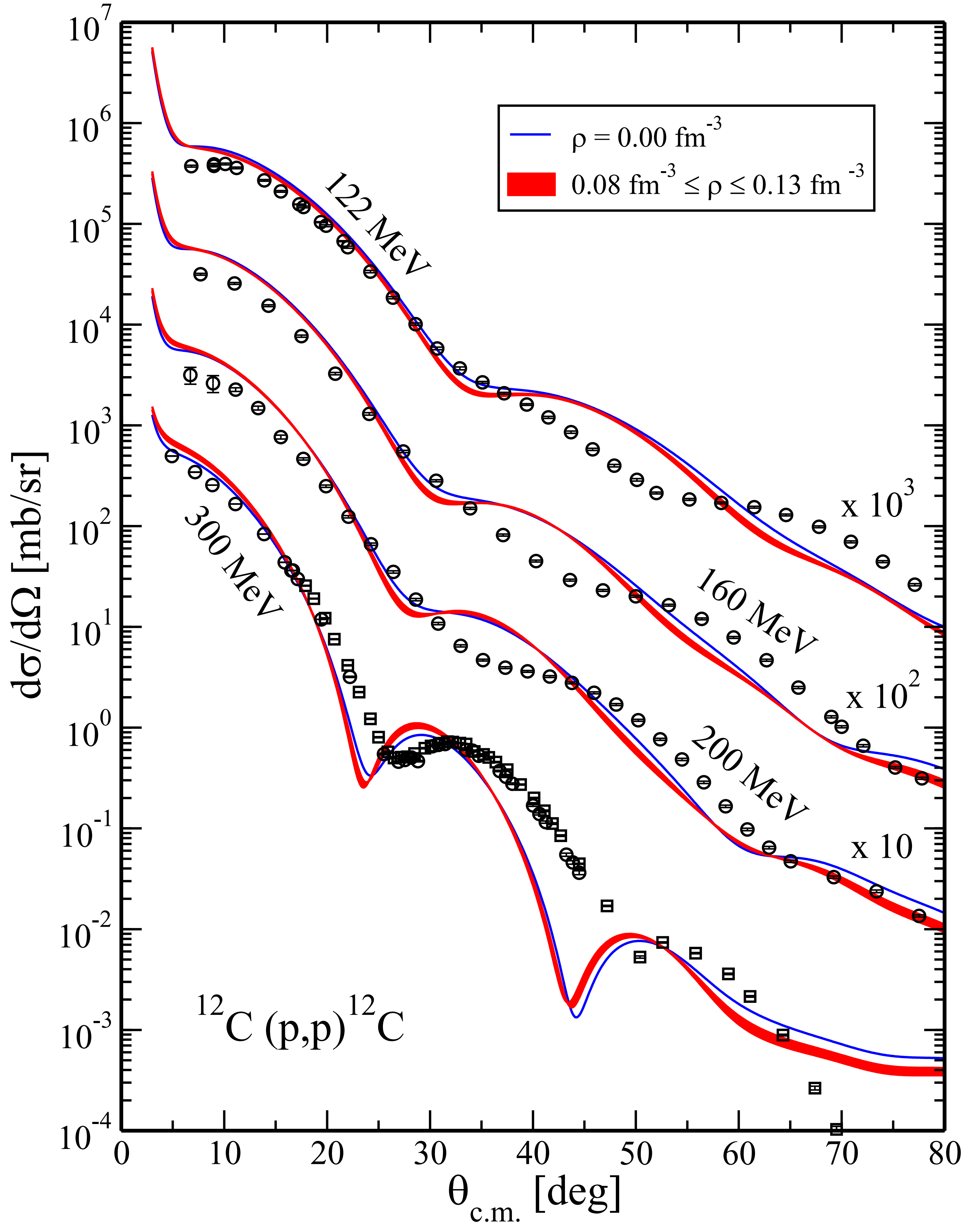

3 body ➜ 2 body density dependent
Holt et al., [PRC **81** (2010) 024002]

In-medium NN interaction generated by the two-pion exchange component (**c_1,c_3,c_4**) of the chiral three-nucleon interaction.

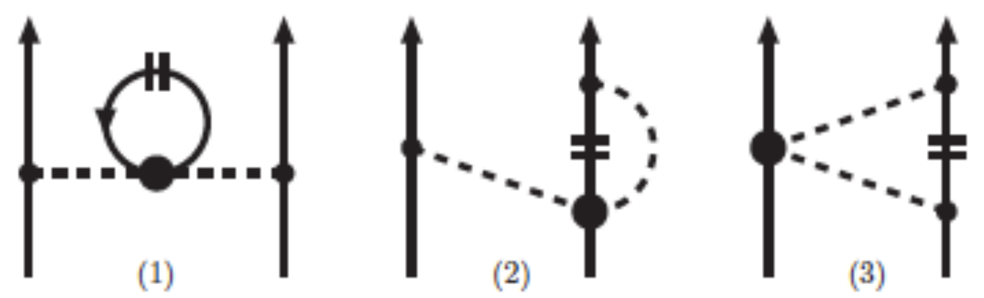

In-medium NN interaction generated by the one-pion exchange (**c_D**) and short-range component (**c_E**) of the chiral three-nucleon interaction.

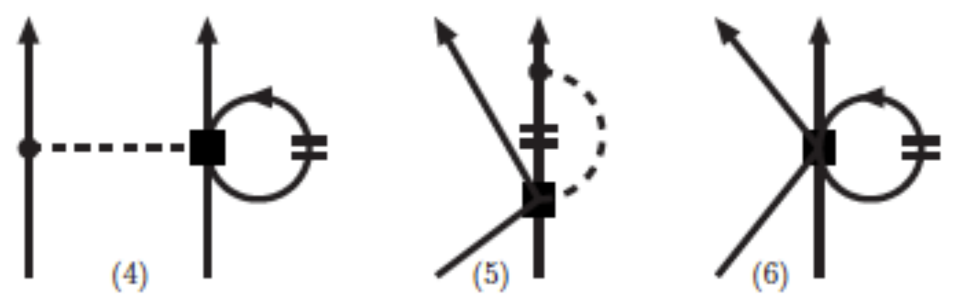

in-medium nucleon propagator

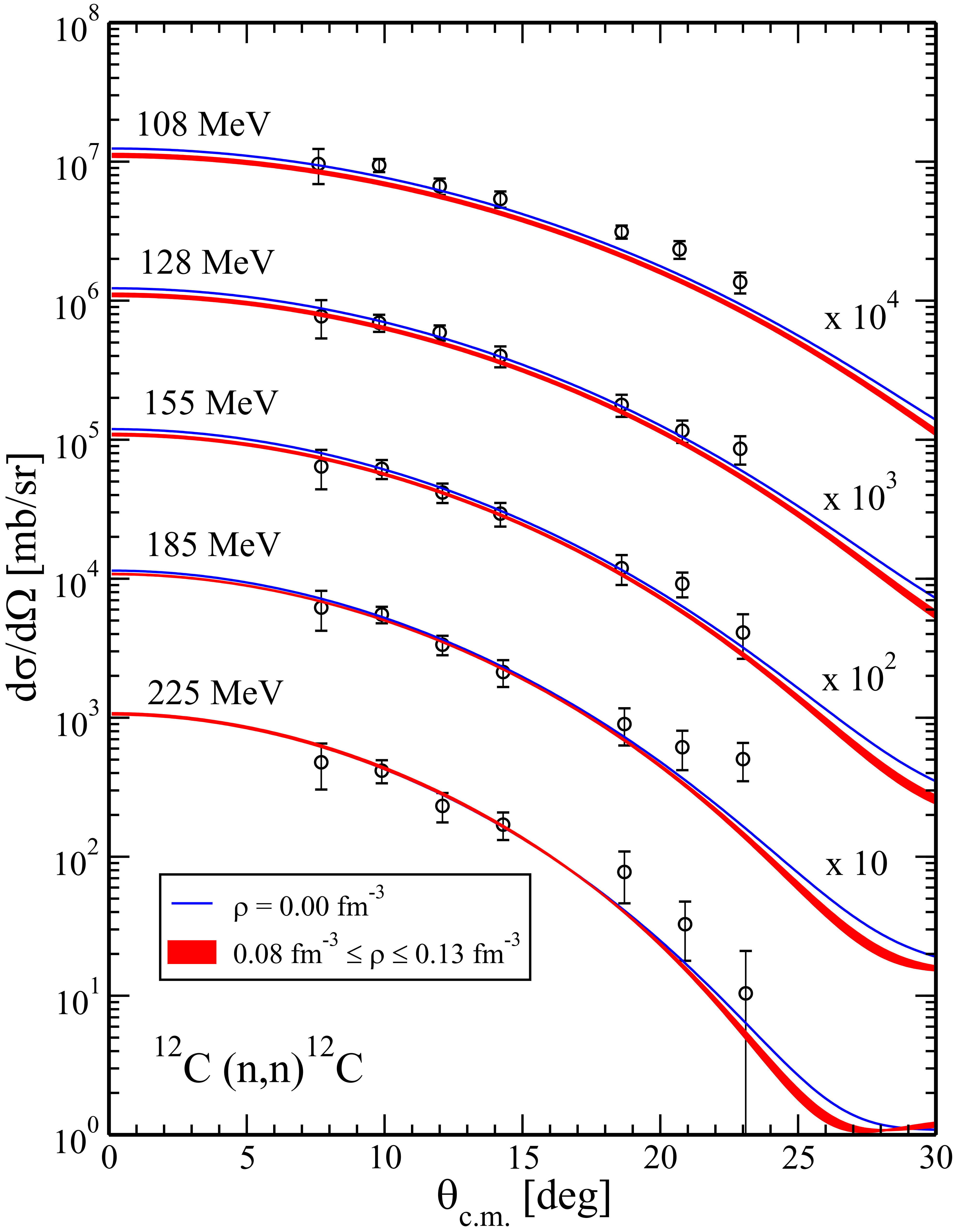

Theoretical predictions - antiprotons

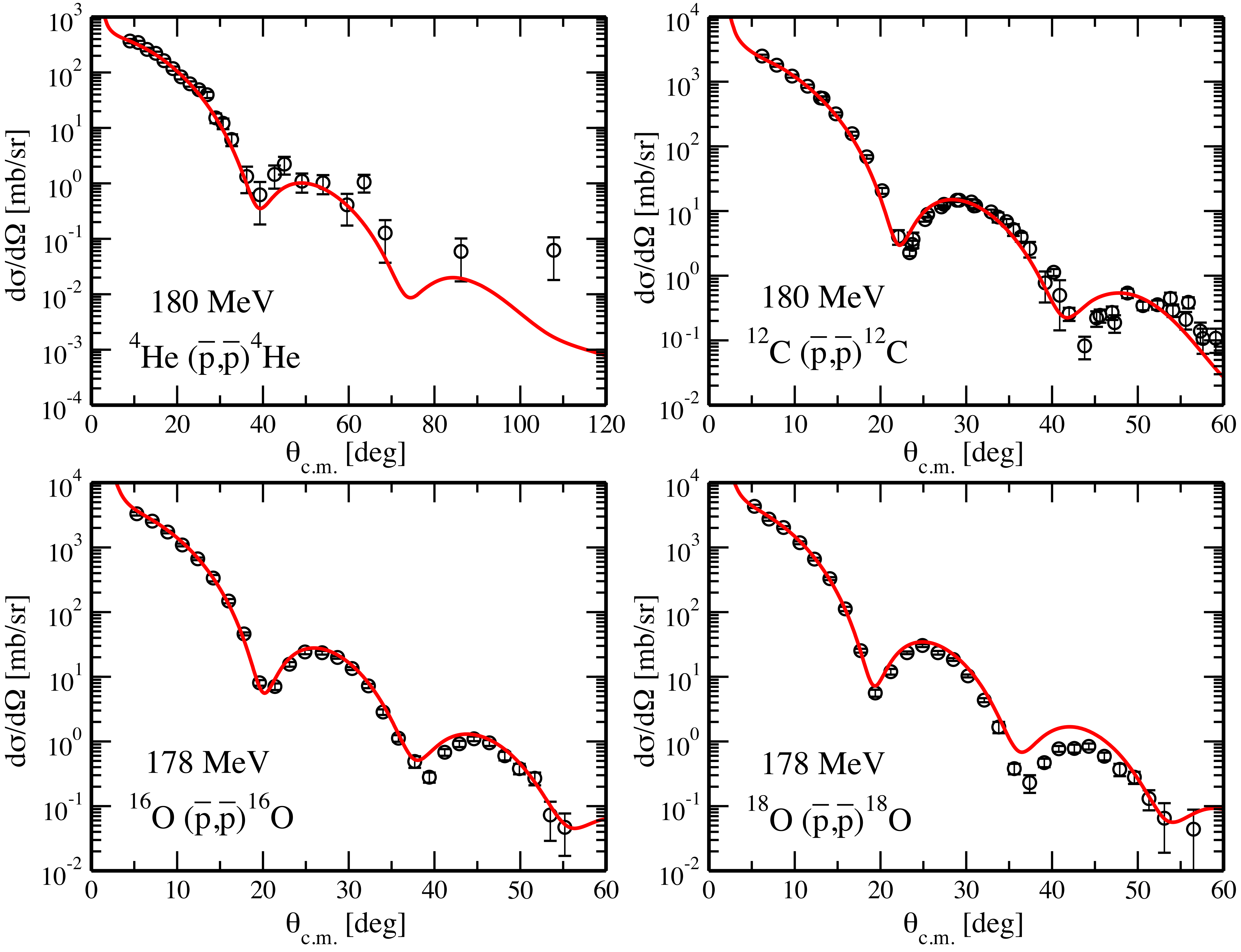

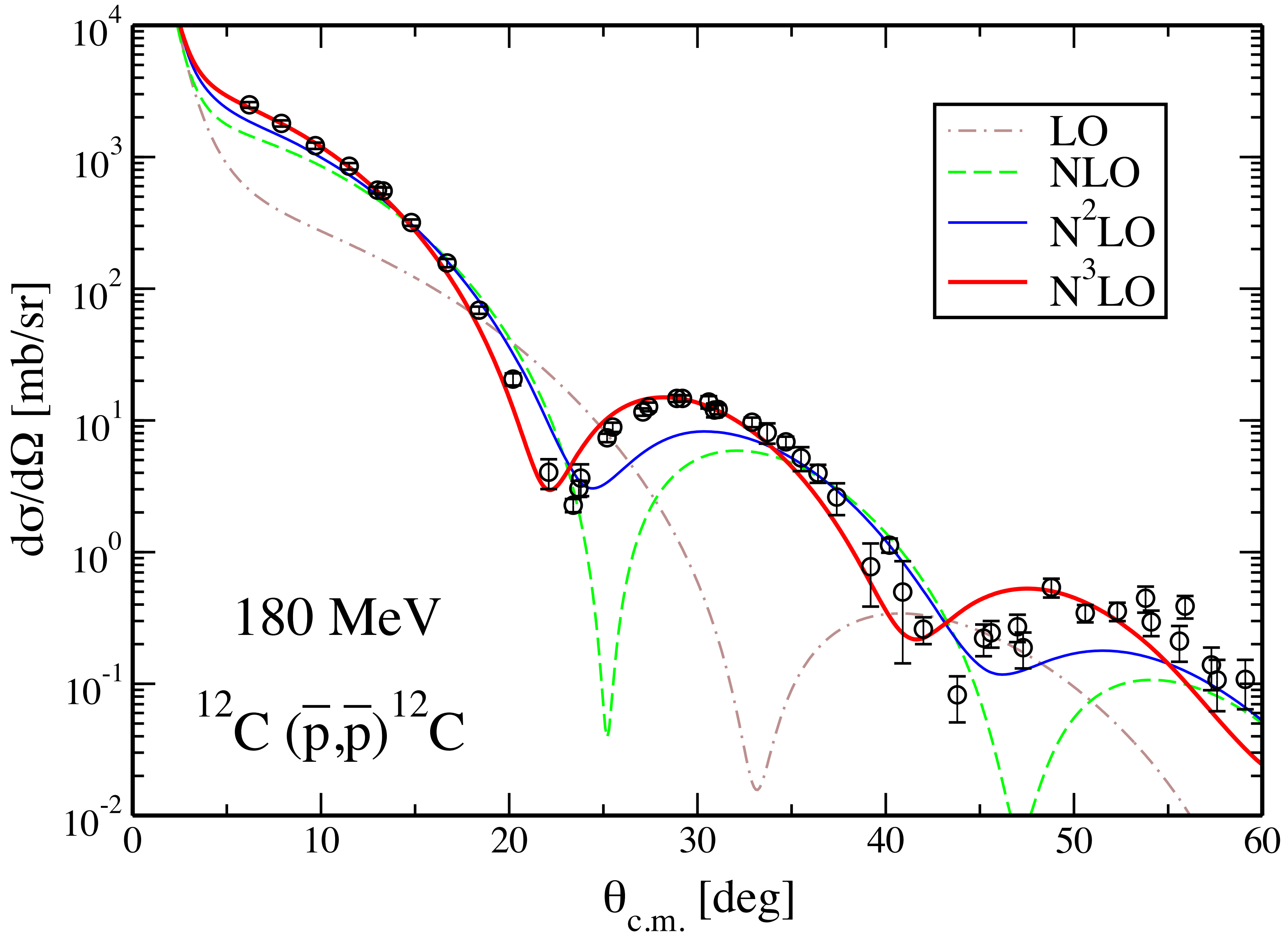

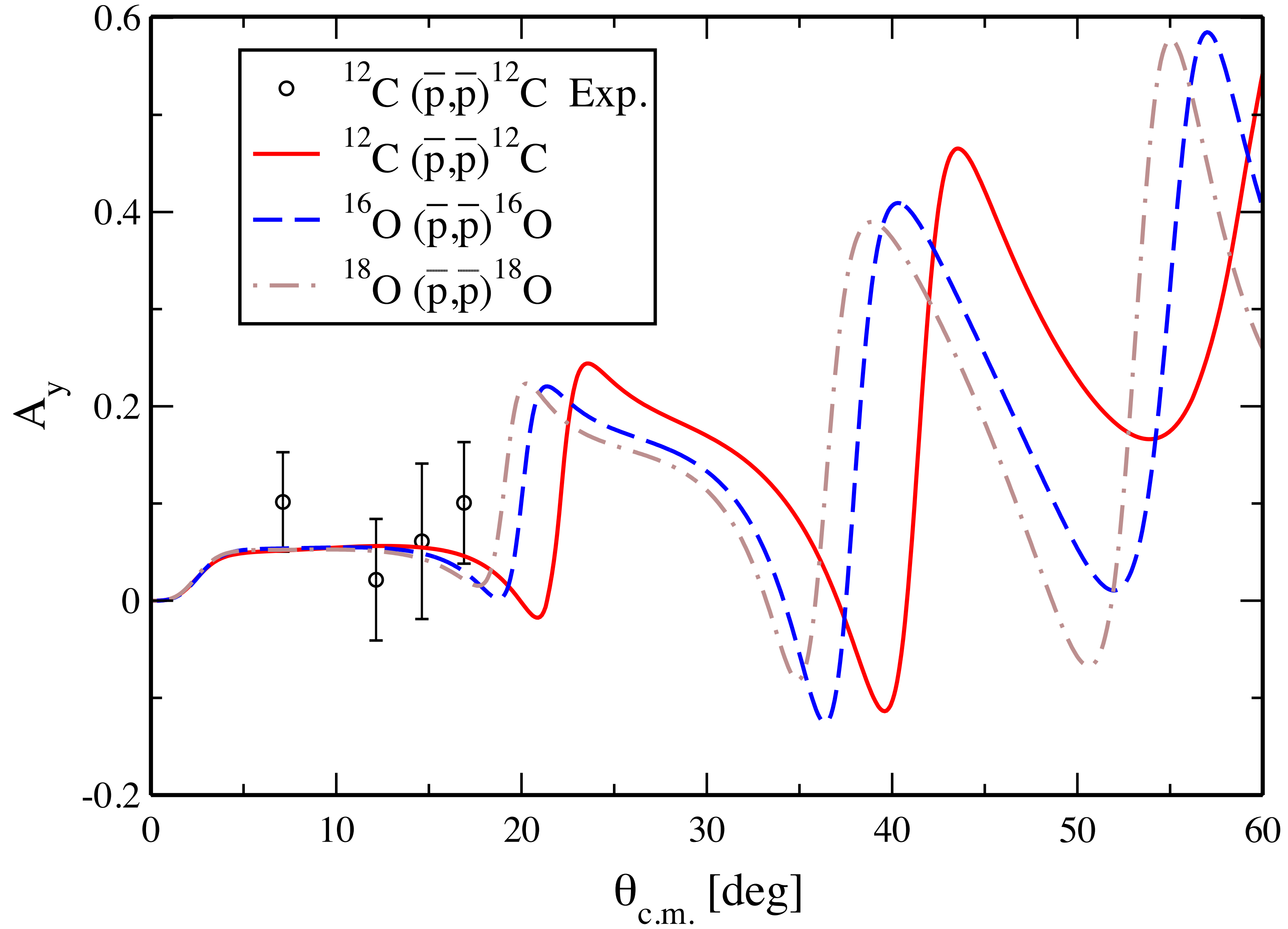

Elastic Antiproton-Nucleus Scattering from Chiral Forces

Matteo Vorabbi,[1,2] Michael Gennari,[2,3] Paolo Finelli,[4] Carlotta Giusti,[5] and Petr Navrátil[2]

PHYSICAL REVIEW LETTERS **124,** 162501 (2020)

Theoretical predictions - unsaturated spin

$$\boxed{U_{\mathbf{p}}(\boldsymbol{q},\boldsymbol{K})} = \sum_{N=p,n} \int dP\, \eta(\boldsymbol{q},\boldsymbol{K},\boldsymbol{P})\, \boxed{t_{\mathbf{p}N}(\boldsymbol{q},\boldsymbol{K},\boldsymbol{P})}\, \boxed{\rho_N(\boldsymbol{q},\boldsymbol{P})}$$

1. Spin structure of the t matrix

The t matrix is an operator in the spin space of the projectile only

$$t_{\mathbf{p}N} = \mathbf{1}\, t^{c}_{\mathbf{p}N} + i(\boldsymbol{\sigma}\cdot\hat{\mathbf{n}})\, t^{ls}_{\mathbf{p}N}$$

2. Nonlocal one-body density

Dependence on the initial and final values of the spin and its third component

$$\rho_N(\boldsymbol{q},\boldsymbol{P}) = \rho_N(\boldsymbol{q},\boldsymbol{P}; s, \sigma', \sigma)$$

3. The optical potential

- Operator in the spin space of the projectile only
- Depends on σ and σ'

Theoretical predictions - unsaturated spin

$J^\pi = 1/2^-$

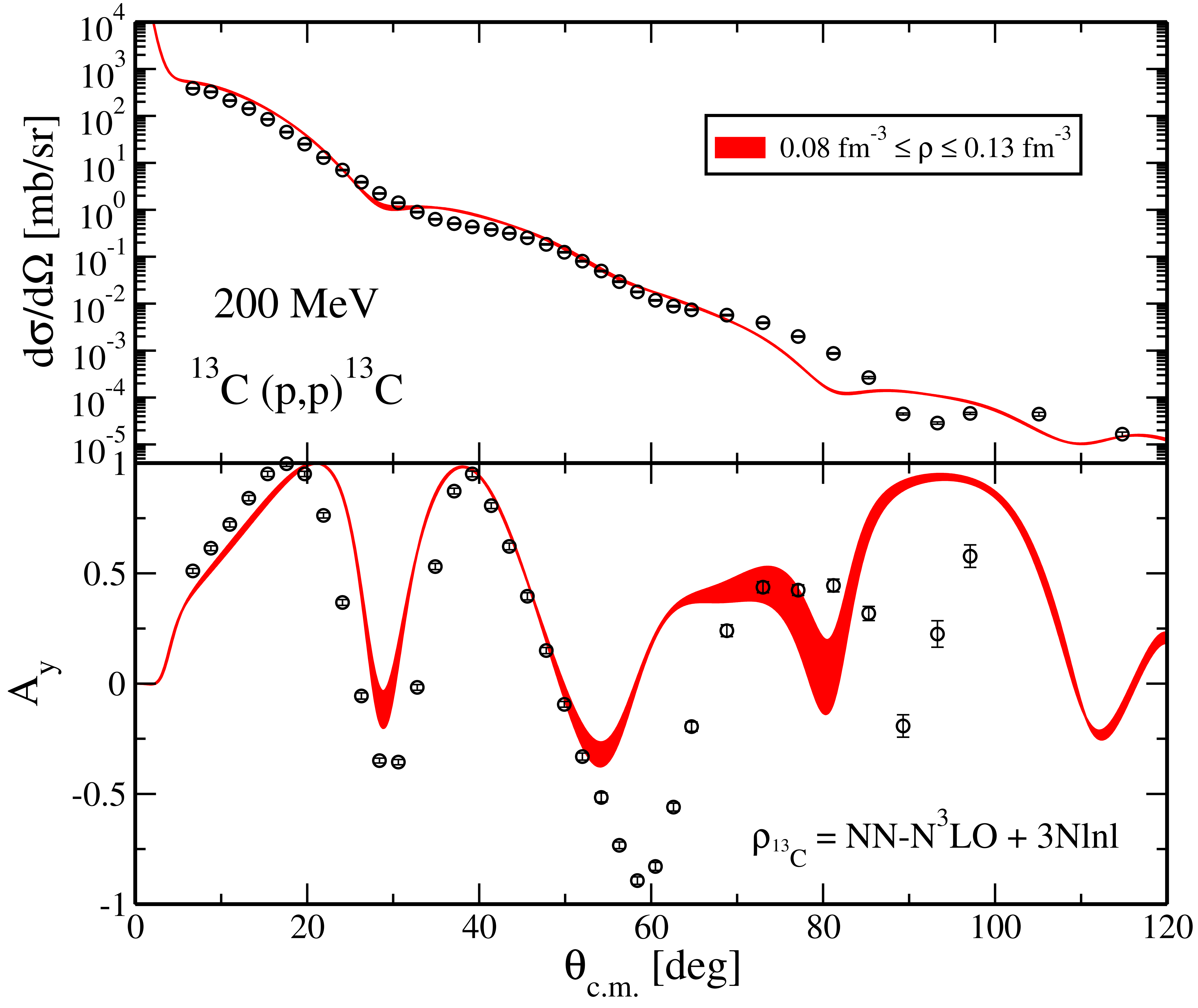

$J^\pi = 1^+$

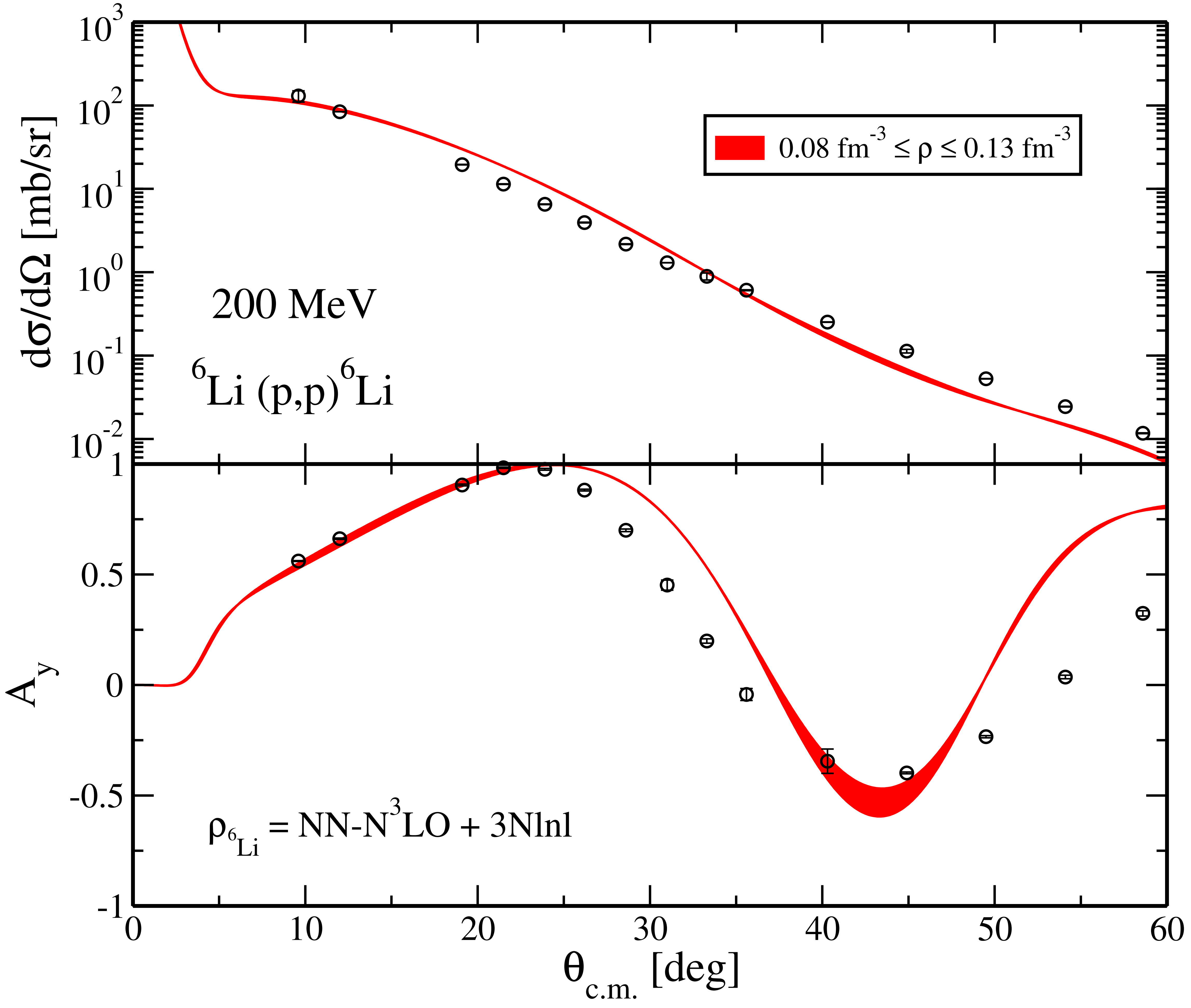

Vorabbi et al., PRC **105** (2022) 014621

Theoretical predictions - unsaturated spin

$J^\pi = 3/2^-$

$J^\pi = 3^+$

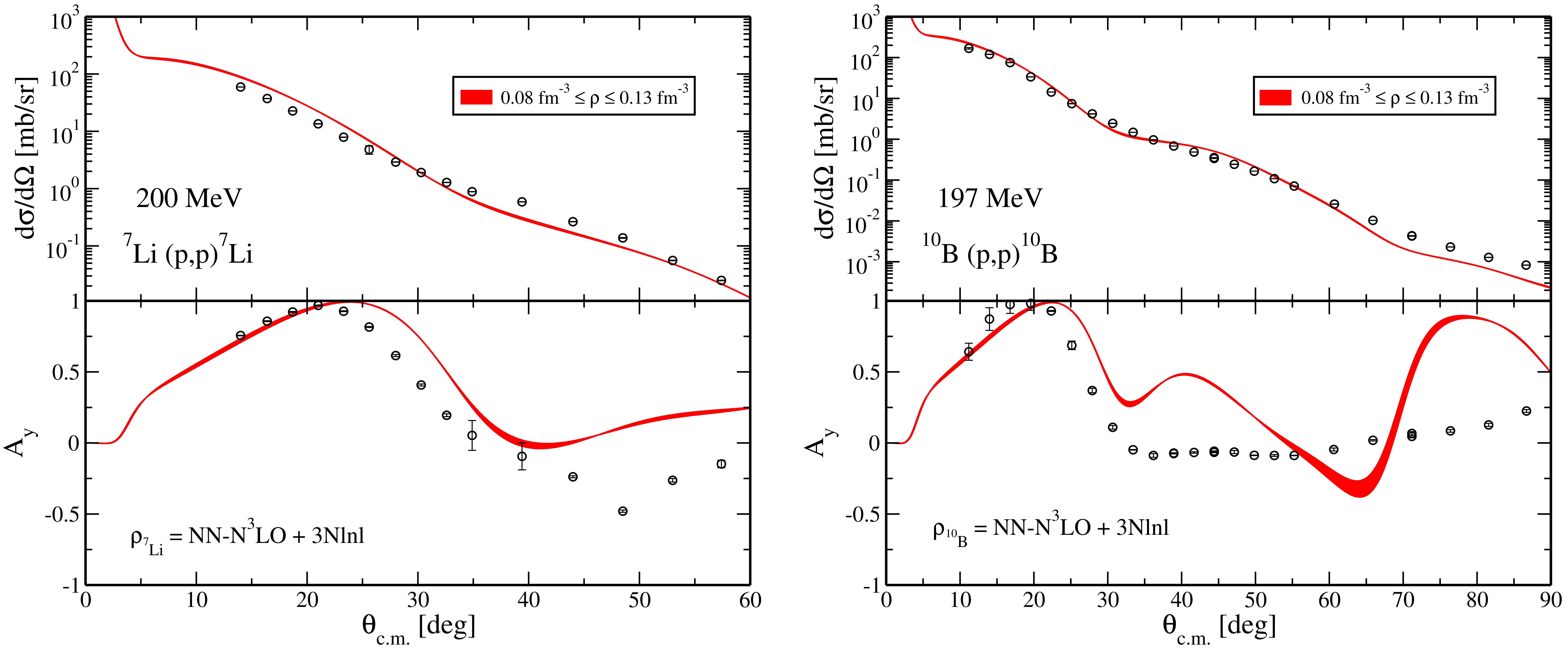

Vorabbi et al., PRC **105** (2022) 014621

Theoretical predictions - unsaturated spin

- The model reproduces the experimental data reasonably well
- The differential cross section is better reproduced
- The analyzing power is very sensitive and extremely difficult to reproduce
- The overall agreement between our results and the experimental data is of about the same quality as that obtained for spin zero targets

$J^\pi = 3/2^-$

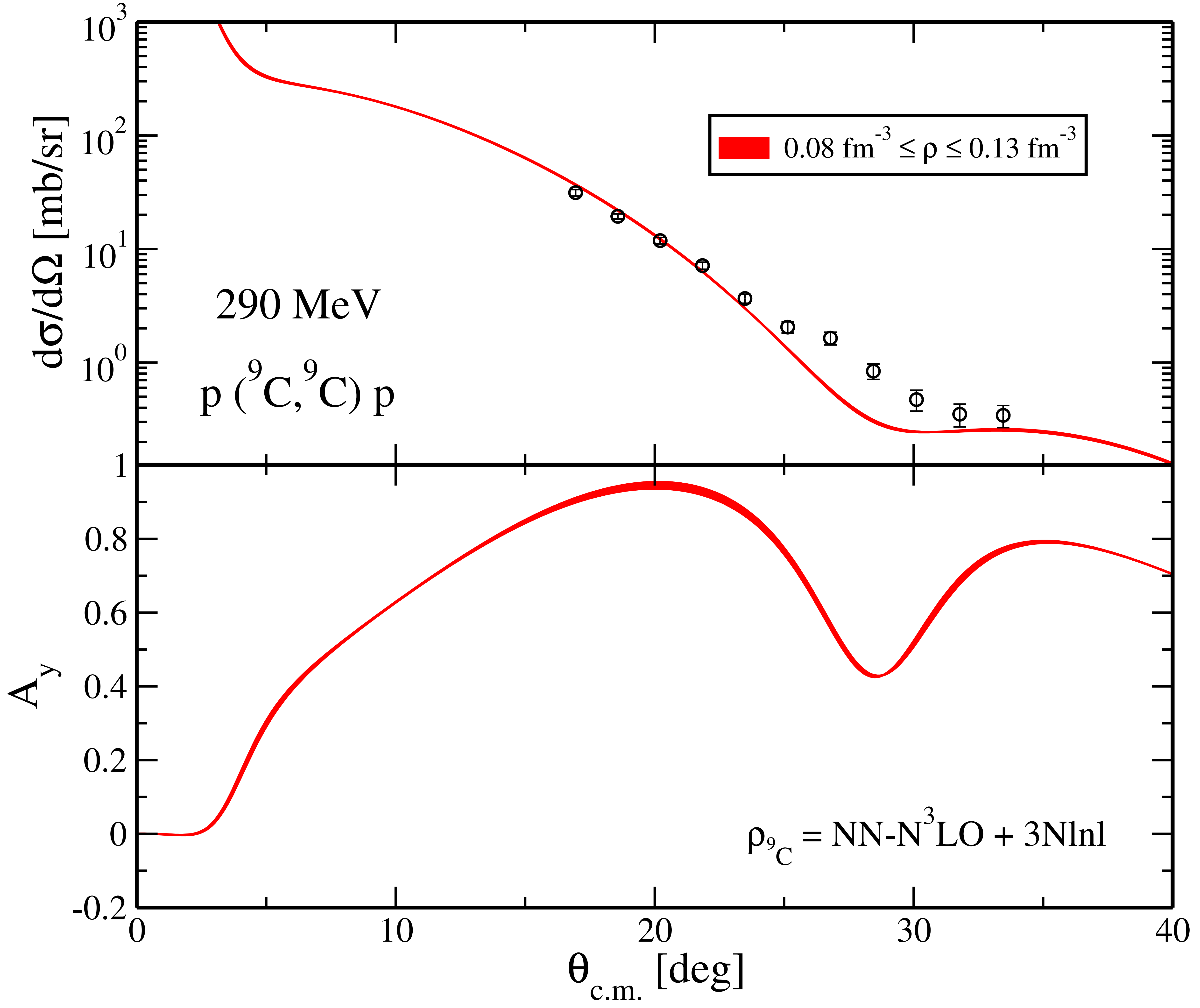

Vorabbi et al., PRC **105** (2022) 014621

Theoretical predictions - Ca and Ni isotopes

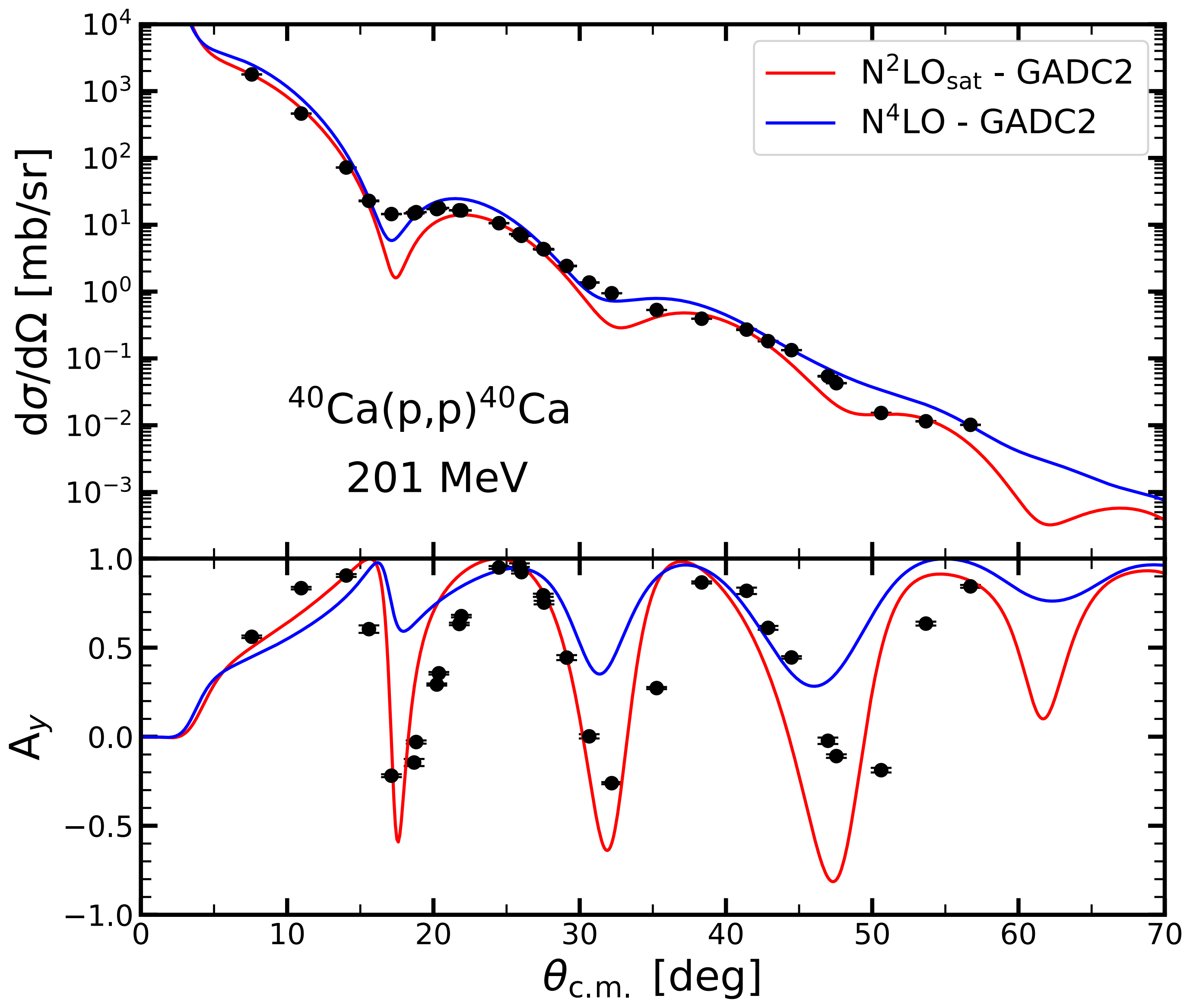

- In collaboration with Barbieri (Milano) and Somà (Paris)
- First ab-initio description of calcium and nickel isotopes
- Interesting benchmark for different realistic interactions
- Useful benchmark to test the reliability of ab-initio approaches to nuclear stricture

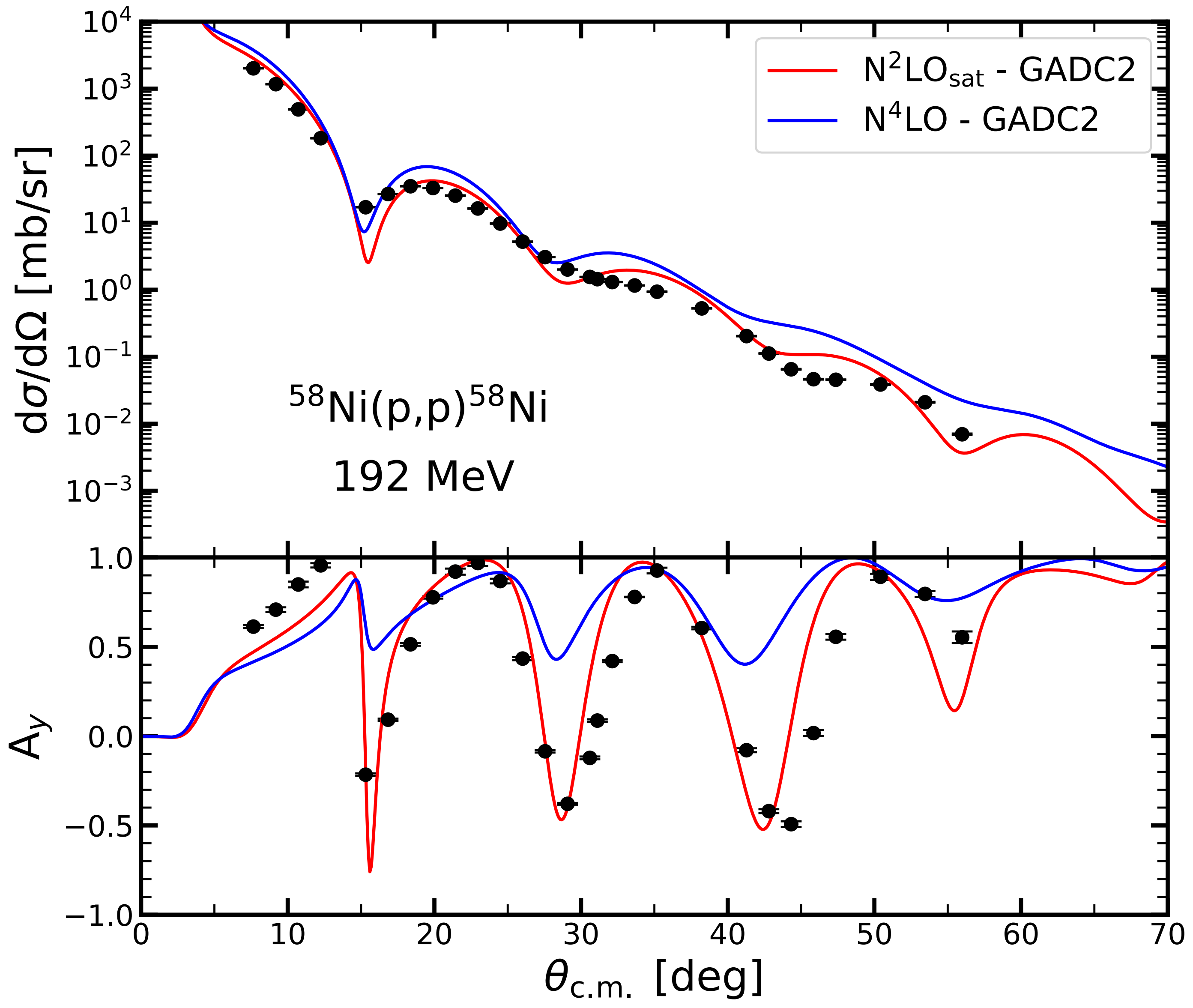

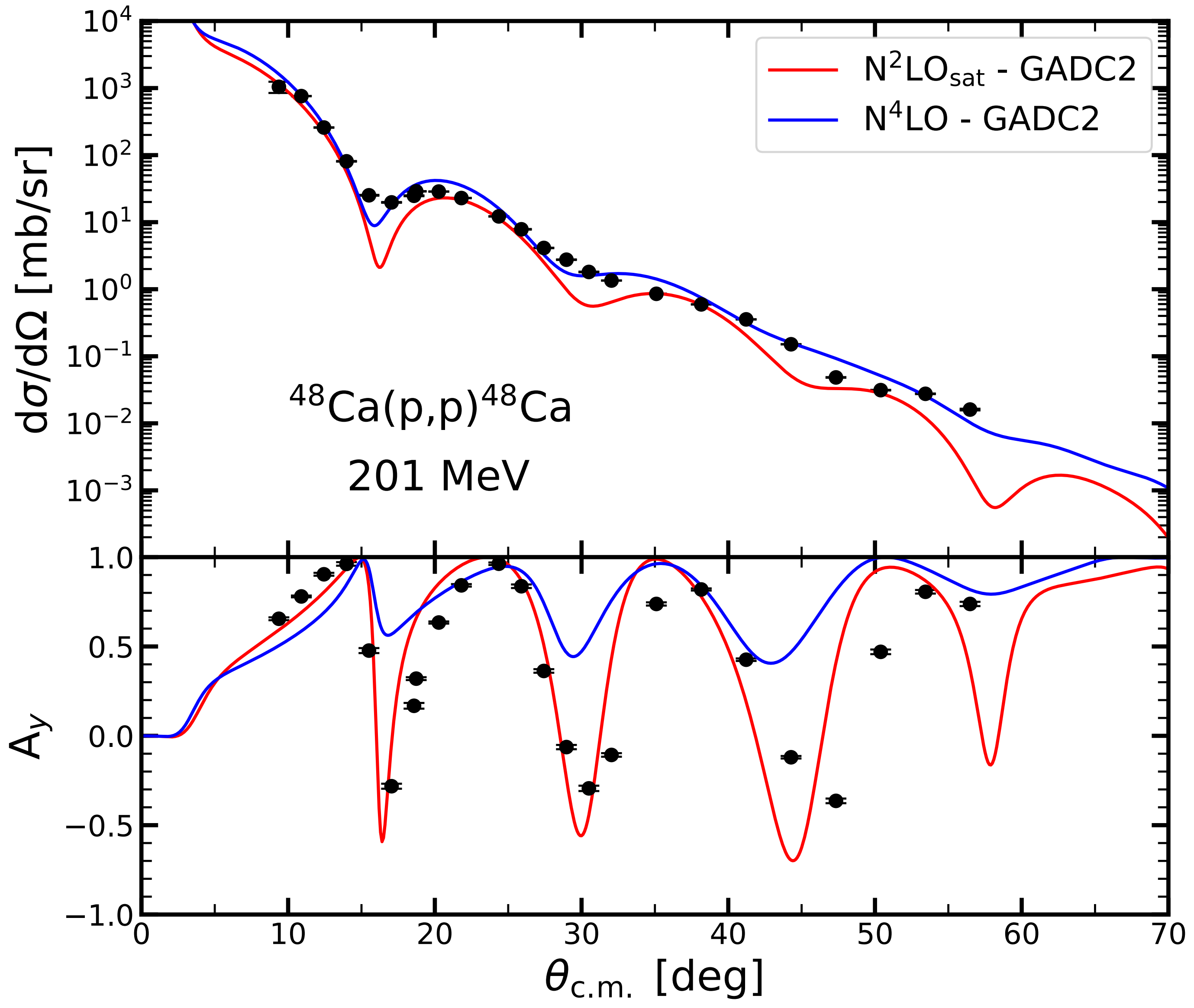

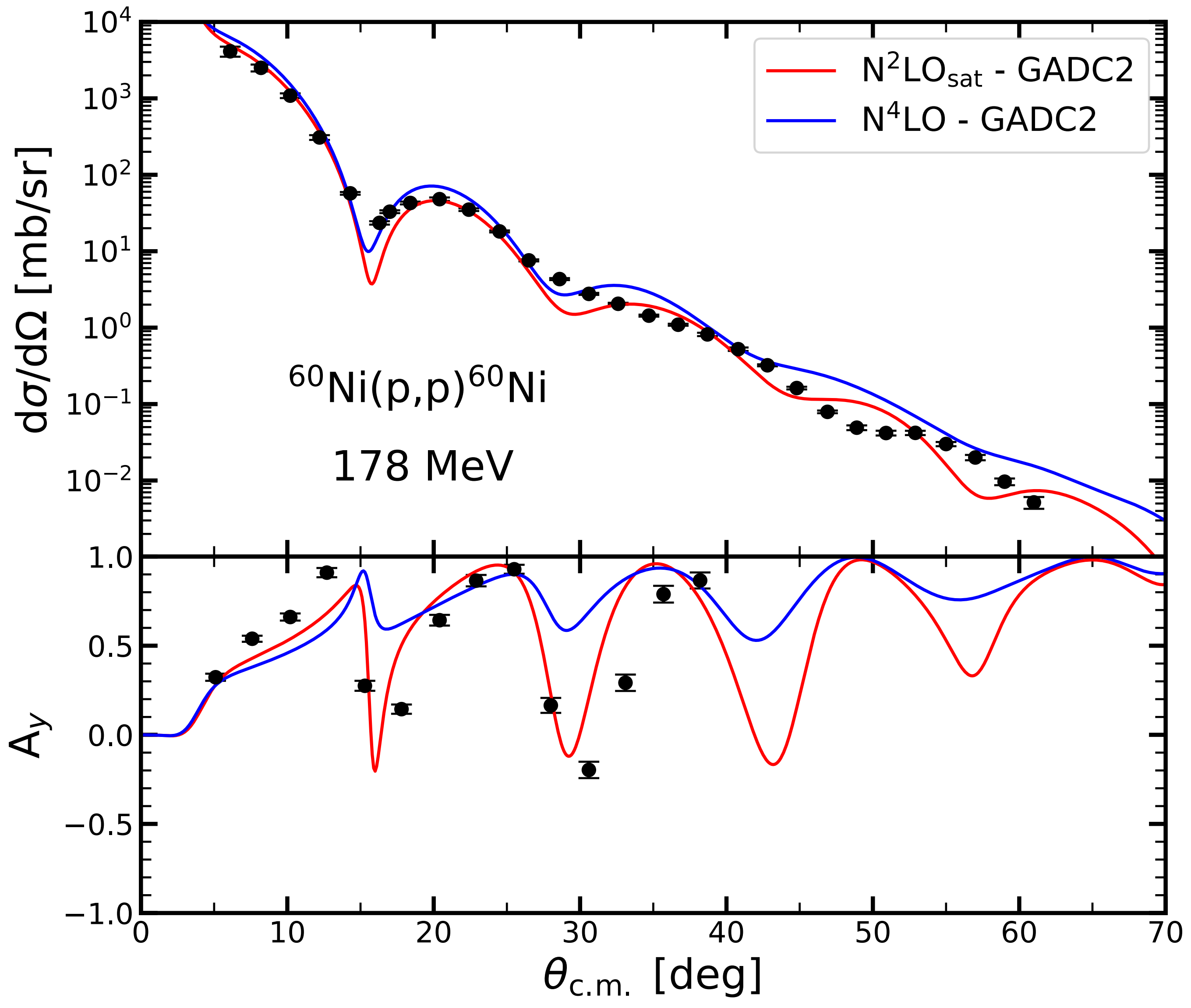

Preliminary

Ab-initio inelastic scattering

The inelastic transition amplitude

Picklesimer, Tandy, Thaler, Phys. Rev. C **25** (1982) 1215

Picklesimer, Tandy, Thaler, Phys. Rev. C **25**, (1982) 1233

$$T^{\mathrm{inel}}_{\nu' s' \sigma' \nu s \sigma}(\boldsymbol{k}_*, \boldsymbol{k}_0; E) = \int d\boldsymbol{r}' \int d\boldsymbol{r}\, \psi^\dagger_*(\boldsymbol{k}_* \nu' s' \sigma'; \boldsymbol{r}')\, U_{\mathrm{tr}}(\boldsymbol{r}', \boldsymbol{r}; s'\sigma' s\, \sigma E)\, \psi(\boldsymbol{k}_0 \nu s \sigma; \boldsymbol{r})$$

Required potentials (**DWBA**)

$$U^{\mathbf{p}}_{\mathrm{tr}}(\boldsymbol{q}, \boldsymbol{K}) = \sum_{N=p,n} \int d\boldsymbol{P}\, \eta(\boldsymbol{q}, \boldsymbol{K}, \boldsymbol{P})\, t_{\mathbf{p}N}(\boldsymbol{q}, \boldsymbol{K}, \boldsymbol{P})\, \rho^{\mathrm{tr}}_N(\boldsymbol{q}, \boldsymbol{P})$$

Requires all the *NN* amplitudes

$$U^{\mathbf{p}}_{\mathrm{gs}}(\boldsymbol{q}, \boldsymbol{K}) = \sum_{N=p,n} \int d\boldsymbol{P}\, \eta(\boldsymbol{q}, \boldsymbol{K}, \boldsymbol{P})\, t_{\mathbf{p}N}(\boldsymbol{q}, \boldsymbol{K}, \boldsymbol{P})\, \rho^{\mathrm{gs}}_N(\boldsymbol{q}, \boldsymbol{P}) \longrightarrow \psi(\boldsymbol{k}_0 \nu s \sigma; \boldsymbol{r})$$

Solve the Schrödinger equation

$$U^{\mathbf{p}}_{\mathrm{ex}}(\boldsymbol{q}, \boldsymbol{K}) = \sum_{N=p,n} \int d\boldsymbol{P}\, \eta(\boldsymbol{q}, \boldsymbol{K}, \boldsymbol{P})\, t_{\mathbf{p}N}(\boldsymbol{q}, \boldsymbol{K}, \boldsymbol{P})\, \rho^{\mathrm{ex}}_N(\boldsymbol{q}, \boldsymbol{P}) \longrightarrow \psi_*(\boldsymbol{k}_* \nu' s' \sigma'; \boldsymbol{r})$$

Ab-initio inelastic scattering

- The t matrix used to calculate the 3 potentials only contains two terms

$$A + i(\boldsymbol{\sigma} \cdot \hat{\boldsymbol{n}})C$$

- Is the transition density good enough to describe the excitation?

- Are the distorted waves sufficiently precise?

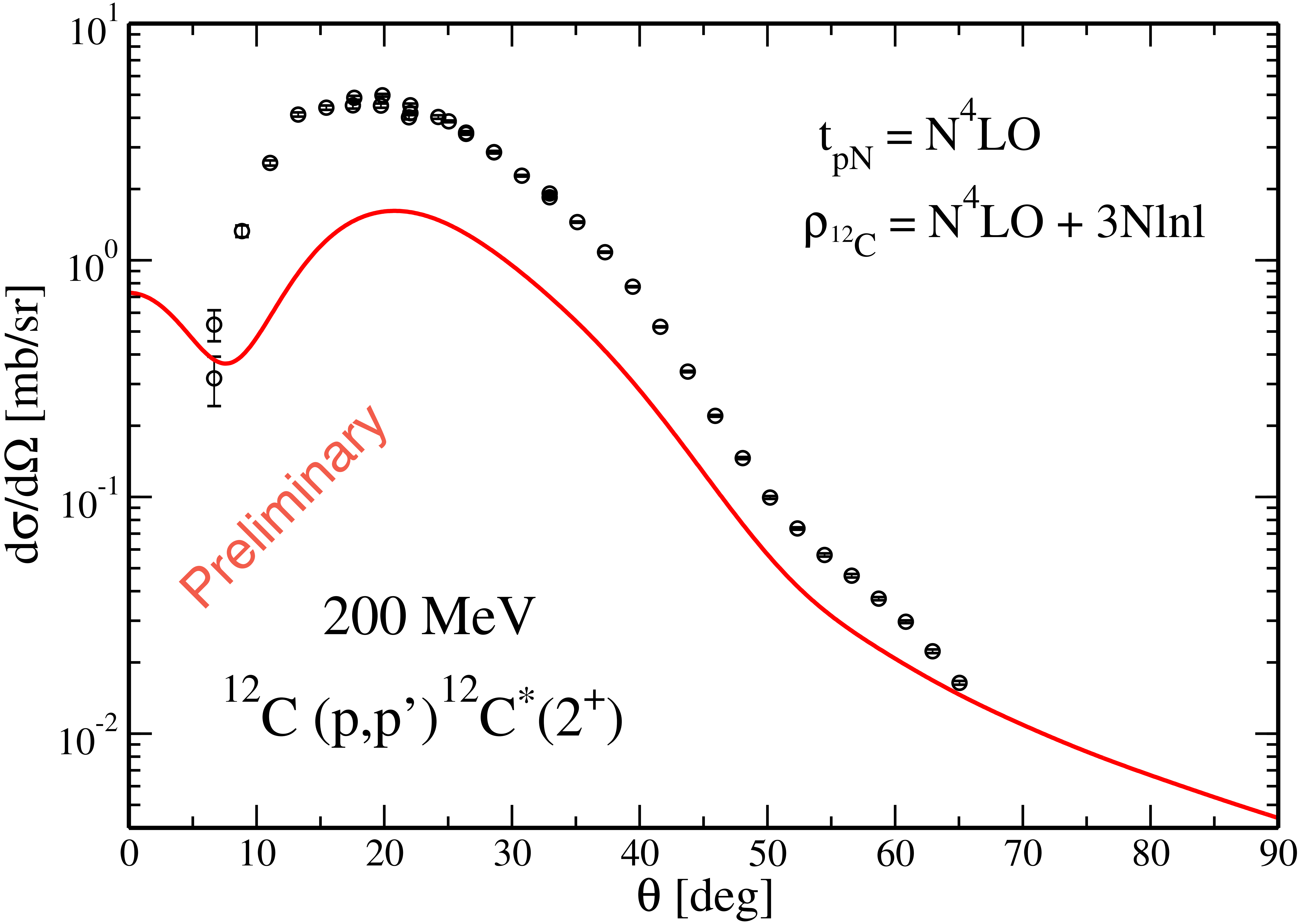

Extensions, what’s next?

1. **Higher order expansion** in the derivation of the optical potential (to describe data at lower energies)

2. Better evaluation of the **theoretical uncertainties**

3. Ab-initio description of the **single particle propagator**

4. Microscopic description of the **inelastic scattering**

5. **Charge/matter densities** from combined analysis with electron scattering calculations (unpolarised and PV)